

**SPATIAL AND TEMPORAL VARIATION IN JUVENILE
SALMON LIFE HISTORY: IMPLICATIONS OF
HABITAT ALTERATION**

A Thesis

Presented in Partial Fulfillment of the Requirements for the

Degree of Master of Science

with a

Major in Water Resources Science and Management

in the

College of Graduate Studies

University of Idaho

by

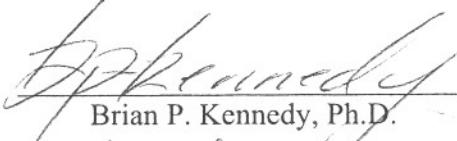
Jensen C. Hegg


April 2011

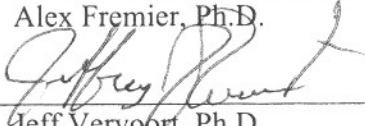
Major Professor: Brian P. Kennedy, Ph.D.

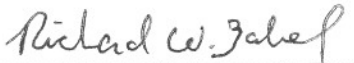
AUTHORIZATION TO SUBMIT THESIS

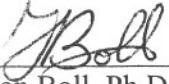
This thesis of Jensen Hegg, submitted for the degree of Master of Science with a major in Water Resources Science and Management and titled "Spatial and Temporal Variation in Juvenile Salmon Life History: implications of habitat alteration," has been reviewed in final form. Permission, as indicated by the signatures and dates given below, is now granted to submit final copies to the College of Graduate Studies for approval.

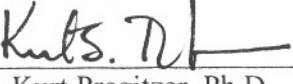
Major Professor  Date 5.15.2011
Brian P. Kennedy, Ph.D.

Committee Members  Date 5-15-11
Alex Fremier, Ph.D.


 Date 5/15/2011
Jeff Vervoort, Ph.D.

 Date 5/15/2011
Rich Zabel, Ph.D.

Department Administrator  Date 6/7/2011
Jan Boll, Ph.D.

Discipline's College Dean  Date 6/6/2011
Kurt Pregitzer, Ph.D.

Final Approval and Acceptance by the College of Graduate Studies

 Date 6/22/11
Jerry McMurtry

ABSTRACT

The unique migratory life history of salmon has evolved in dynamic riverine environments that have seen significant physical alterations during the evolution and radiation of salmon species. However, salmon in the Snake River of Idaho inhabit a river system whose hydrology has been altered relatively rapidly in the recent past. The introduction of hydropower has caused significant flow, temperature and productivity changes in salmon spawning and rearing habitats in the Snake River basin. These changes may affect individual migratory responses at major life history time points, as well as the selective pressure experienced by different migratory strategies at the population level. Snake River fall Chinook salmon (*Oncorhynchus tshawytscha*), an ESA listed species, have historically exhibited a sub-yearling juvenile out-migration strategy. In recent years, however, it has been shown that a yearling out-migration strategy may be an increasingly significant strategy within the successful spawners in the population. Yearling out-migrants remain in freshwater over the winter before out-migrating the following spring. The geographic distribution of this yearling strategy, and the resulting survival consequences for individual spawning populations in the major reaches of the basin, are unknown. We hypothesized that representation of the yearling migration strategy is non-randomly distributed within the Snake River basin, influenced by heterogeneous environmental conditions between spawning locations.

Localized environmental factors will have significant effects on individual migration success, yet current methods of study often cannot resolve important aspects of migration at both broad and fine spatial scales. Geochemical fingerprinting, through the use of isotopic and elemental variability among individuals, has been successfully used to reconstruct the migration history in salmonids using the temporal and spatial records of movement stored in salmon otoliths, or earstones. This is possible due to a close relationship between watershed geologic composition and geochemical signatures, such as strontium isotope ratios ($^{87}\text{Sr}/^{86}\text{Sr}$), and the daily preservation of distinct signatures within the otolith increments that provide a chemical record of

space use and movements. The spatial resolution of geochemical fingerprinting methods, whether isotopic or elemental, and their utility to study the source location of untagged individuals, is limited by the geographic variability of signatures from potential source sites.

We use otolith microchemistry to determine natal origin, rearing and overwintering location, and migration strategy (i.e. timing of juvenile outmigration) of returning adult fall Chinook salmon. Further, we present a method for extending the spatial extent and resolution of otolith migration studies using accurate prediction of $^{87}\text{Sr}/^{86}\text{Sr}$ from bedrock geology. Our results indicate non-random geographic distribution of yearling migratory strategy with the majority of individuals overwintering in the lower Snake River reservoirs. Juveniles are shown to overwinter in the main stem reservoirs, with outmigration continuing throughout the winter. Further, we show that fish can be accurately classified to natal origin using a method of predicting $^{87}\text{Sr}/^{86}\text{Sr}$ from bedrock geology. This method of prediction may allow greater spatial resolution or the identification of unknown source locations in isotopic studies. Accuracy of this method was limited at watershed scales significantly smaller than those used to create the predictions and at geologic diversities below a Shannon diversity score of 1. This work has implications for our understanding of the behavioral plasticity and adaptive responses of salmon to changes in their environment, and contributes to our knowledge of the timing and fate of juvenile salmon in the main stem Snake and Columbia River systems.

ACKNOWLEDGEMENTS

I would like to acknowledge the help and support of my lab group, the Center for Integrative Fish Ecology & Ecosystem Studies, for their support in developing and conducting this research. In particular I would like to thank Ellen Hamann, Jeff Reader and Sam Bourret for their help in method development, sample collection, preparation and analysis. I would also like to thank my collaborators Rich Zabel and Paul Chittarro at NOAA – Northwest Fisheries Science Center for help in development of the project objectives, sample collection and preparation, and access to additional important data. Billy Connor with the US Fish & Wildlife Service, and Bill Arnsberg with Nez Perce Tribal Fisheries helped immensely with collection of the known origin juvenile fish we used for validation. Reed Lewis with the Idaho Geological Survey was a great help in reclassifying geologic map information. The University of Idaho Statistical Consulting Center, in particular professor Michelle Weist, deserves thanks for her help developing the experimental design and refining the data analysis. My thanks also go out to NOAA for the funding that supported this work. Ultimately, this thesis would not have been possible without the support of my family, and particularly my son Berlyn, who allowed me to put in the time and effort needed to complete this project. Thanks for your support.

TABLE OF CONTENTS

TITLE PAGE	i
AUTHORIZATION TO SUBMIT THESIS	ii
ABSTRACT	iii
ACKNOWLEDGEMENTS	v
TABLE OF CONTENTS	vi
LIST OF TABLES	viii
LIST OF FIGURES	x
CHAPTER 1: SPATIAL DISTRIBUTION OF ALTERNATE MIGRATION STRATEGIES IN FALL CHINOOK SALMON (<i>ONCORHYNCHUS TSHAWYTSCHA</i>) IN THE SNAKE RIVER OF IDAHO	1
Abstract.....	2
Introduction.....	3
Methods	10
<i>Study Site</i>	10
<i>Water Chemistry</i>	11
<i>Otolith Collection</i>	12
<i>Otolith Microchemistry</i>	13
<i>Life Stage Determination</i>	15
<i>Exploratory Cluster Analysis</i>	17
<i>Outmigration Timing</i>	19
Results.....	20
<i>Water Chemistry</i>	20
<i>Life Stage Determination</i>	21
<i>Exploratory Cluster Analysis</i>	23
<i>Outmigration Timing</i>	24
Discussion.....	25
<i>Water Chemistry Variation</i>	25
<i>Life Stage Determination</i>	29
<i>Exploratory Cluster Analysis</i>	34
<i>Outmigration Timing</i>	37

<i>Effects of Environmental Change</i>	39
Tables	41
Figures.....	47
References Cited (Chapter 1)	62
CHAPTER 2: DETERMINING SALMON NATAL ORIGINS USING PREDICTIONS FROM BEDROCK GEOLOGIC DIVERSITY AND GEOCHEMICAL SIGNATURES	67
Abstract.....	68
Introduction.....	69
Methods.....	74
<i>Study site</i>	75
<i>Quantification of Geologic Diversity</i>	77
<i>Quantifying Rock Type Variability</i>	79
<i>Surface Area Calculation</i>	80
<i>Model Selection</i>	80
<i>Natal Origins Prediction</i>	81
<i>The Effects of Scale</i>	82
Results.....	84
<i>Quantification of Geologic Diversity</i>	84
<i>Model Selection</i>	85
<i>Natal Origins Prediction</i>	86
<i>Effects of Scale</i>	87
Discussion.....	88
<i>Geologic Prediction</i>	88
<i>Fish Classification</i>	89
<i>Scale and Diversity</i>	90
<i>Future Applications</i>	91
Tables	93
Figures.....	105
References Cited (Chapter 2)	115

LIST OF TABLES

TABLE 1.1	Water sample $^{87}\text{Sr}/^{86}\text{Sr}$ data for the Snake River basin 2008-2009 shows variation between tributaries and major reaches of the Snake River.	41
TABLE 1.2	Summary statistics of adult fall Chinook sampled for the study. All fish were first determined to be yearling or sub-yearling based on scale analysis. The percentage of agreement between otoliths and scale analysis is listed below. Otolith yearling determination was used for all further analysis in this study. Fish were captured between 2006 and 2008 at Lower Granite Dam and sampled as a part of hatchery spawning operations at Lyons Ferry Hatchery.	43
TABLE 1.3	Significant differences in representation of the yearling life history types are shown between natal source river groups of adult fall Chinook salmon captured at Lower Granite Dam (2006-2008). The yearling life history strategy is significantly more abundant in the Clearwater and Salmon river group. Ocean entry timing is also significantly later in the Clearwater and Salmon river group. LDFA was used to group fish to source river group based upon $^{87}/^{86}\text{Sr}$ ratio area of the otoliths corresponding to rearing. Juvenile validation samples consisted of juvenile fish of known origin (Wild=7, Hatchery=9) and were used to test the classification. Ocean entry was measured as the distance from the core of the otoliths to the onset of the global ocean signature ($^{87}\text{Sr}/^{86}\text{Sr} = 0.70918$) and characteristic spike in Sr concentration.	44
TABLE 1.4	The majority of juvenile fish rear in the Lower Snake River reservoirs. Rearing location representation between source river groups are shown for adult fall Chinook salmon captured at Lower Granite Dam (2006-2008). LDFA was used to group fish to source river group based upon $^{87}/^{86}\text{Sr}$ ratio of the area of the otoliths corresponding to rearing. Juvenile validation samples consisted of juvenile fish of known origin (Wild=7) and were used to test the classification.	45
TABLE 1.5	The majority of Snake River fall Chinook salmon juveniles overwinter in the Lower Snake River reservoirs. Overwintering location for adult fall Chinook salmon captured at Lower Granite Dam (2006-2008) is shown separated by source river groups. LDFA was used to group fish to source river group based upon $^{87}/^{86}\text{Sr}$ ratio of the area of the otolith corresponding to overwintering.	46
TABLE 2.1	Elemental and isotopic variation across major watersheds of the Snake River basin from Hegg et al. (in review) show elemental variation throughout the basin which roughly corresponds to geologic differences, including a strong correlation between Rubidium (Rb) and Potassium (K). Internal precision was measured with repeated measurement of a standard over the course of three sampling days. Coefficient of	93

variation expressed as a percentage (%CV) for each element is listed. Limits of Detection (LOD) were calculated as three times the standard deviation of a blank. External Precision was measured throughout the study through comparison to a known standard, NIST 1640. The percent deviation from the expected value is listed for each element (%Dev NIST 1640).

TABLE 2.2 95

Details of the makeup of water sampling points within the basin. The percent of each rock type upstream of the sample point was calculated using arcGIS. Predicted $^{87}\text{Sr}/^{86}\text{Sr}$ is the output of a multiple regression model using percent rock type as the independent variable. Shannon Diversity of watershed geology as well as total area (km^2) is listed for each sampled watershed. Numbers on Snake River Basin samples correspond to numbers in Figure 2.1. Observed $^{87}\text{Sr}/^{86}\text{Sr}$ values of the Snake River Basin are from Hegg et al. (in review). Big Creek watershed $^{87}\text{Sr}/^{86}\text{Sr}$ values are from Hamann (2010). Bear Valley Creek data are from Kennedy (personal communication).

TABLE 2.3 98

Reclassification of rock types from the LithClass 6.1 standard. Reclassified rock types were used to create predictive multiple regression models of $^{87}\text{Sr}/^{86}\text{Sr}$ within watersheds of the Snake River. Rocks were reclassified primarily by protolithic mafic or felsic composition. When protolith could not be determined from the listed rock type they were classified into the remaining categories. Metamorphic rocks with unknown protolith were classified separately due to the presence of very old, high $^{87}\text{Sr}/^{86}\text{Sr}$ metasedimentary rocks in the basin and their potential to influence $^{87}\text{Sr}/^{86}\text{Sr}$. Carbonate rocks were also separately classified due to their potential to influence $^{87}\text{Sr}/^{86}\text{Sr}$ signatures. Sedimentary/Other was a bucket category for rocks of unknown composition.

TABLE 2.4 102

Candidate models used for AIC model selection. The independent variables included in each model and whether variables were calculated using three-dimensional surface area or conventional map area is shown. Models with higher AICc weights are favored. A difference in AICc of >2 indicates a significant difference between models.

TABLE 2.5 103

Comparison of classification accuracy using two methods of predicting $^{87}\text{Sr}/^{86}\text{Sr}$, 5-rkm and 10-rkm, to classifications using water samples from Hegg et al (in review). Classifications were completed using discriminate functions with predicted values or water sample values as the training set. Proportions of fish classified to each source group are not significantly different between methods (Monte Carlo Chi-Square, $\alpha=0.05$) indicating that predictions of $^{87}\text{Sr}/^{86}\text{Sr}$ are capable of predicting fall Chinook Natal origins.

TABLE 2.6 104

List of candidate models generated using combined water sampling data from large and small scale watersheds in the Snake River basin. While the global model was the most parsimonious, the addition of small scale watersheds decreased the overall prediction accuracy of $^{87}\text{Sr}/^{86}\text{Sr}$.

LIST OF FIGURES

FIGURE 1.2	48
<p>The Snake River watershed is influenced by three major geologic features, the Idaho Batholith (North Central, felsic) , the Snake River Plain (South East, mafic) and the Columbia river basalts (Western, mafic). Map shows Lithology of the Snake River watershed showing rock type categories with strong impacts on $^{87}/^{86}\text{Sr}$. Rock types have been classified primarily into rocks with origins in the mantle (Mafic) and rocks of crustal origin (Felsic) which strongly influence $^{87}/^{86}\text{Sr}$ due to their differing isotopic chemistry. Metamorphic rocks of known protolith were grouped by protolith. Metamorphic rocks of unknown protolith were classified to the Metamorphic category.</p>	
FIGURE 1.3	49
<p>All analysis was performed on the dorsal section of the otoliths as shown. Laser ablation transects (A) were performed at 90° to the sulcus, recording $^{87}/^{86}\text{Sr}$ variation from the core to the rim. Ablation paths along rings (B) were used to determine more precise estimates of stable signatures. Error for A (fine dotted lines) and B expressed as ± 2 times standard error (fine dotted lines). Error bars for B are much smaller than the marker. Strontium intensity (dotted line) and convergence to the global marine signature (dashed line) were used to determine ocean entry.</p>	
FIGURE 1.4	50
<p>Strontium ratio ($^{87}\text{Sr}/^{86}\text{Sr}$) varies within the major spawning reaches of the Snake River basin. Mean and 1st quartile boxes are shown for each group of individual sample points (●).</p>	
FIGURE 1.5	51
<p>Results of natal origin LDFA classification for 120 wild adult fall Chinook Salmon (filled shapes) and 14 known origin juveniles (open shapes). Classification accuracy for known origin samples was 100%. Open squares with crosses through the center are hatchery yearlings from Lyons Ferry Hatchery. Points are jittered on the x-axis to avoid overplotting.</p>	
FIGURE 1.6	52
<p>Results of rearing location LDFA classification for 120 wild adult fall Chinook Salmon (black points) and 7 known origin juveniles (grey points) show distinct grouping between source river groups. Six known origin samples were correctly classified (86%). One juvenile captured at Lower Granite Dam during outmigration, but originally PIT tagged in the Clearwater River, was mis-classified to the Clearwater Salmon river group rather than its location of capture. Points are jittered on the x-axis to avoid overplotting.</p>	
FIGURE 1.7	53
<p>Results of overwintering location LDFA classification for 74 wild adult fall Chinook Salmon show the majority of overwintering juveniles residing in the Lower Snake River reservoirs. Points are jittered on the x-axis to avoid overplotting.</p>	
FIGURE 1.8	54

Model based cluster solution for the natal life stage shows indistinct clustering and a lack of additional chemically distinct groups beyond those of determined using LDFA. Shape indicates cluster association. Ellipses indicate cluster shape, orientation and 50% quartile for the multivariate distribution. Numbered gray circles indicate cluster centers.

FIGURE 1.955

Plot of the model based cluster solution for the rearing life stage shows additional chemically distinct clusters (#1, #3 and #4) beyond those from LDFA. Shape indicates cluster association. Ellipses indicate cluster shape, orientation and 50% quartile for the multivariate distribution. Numbered gray circles indicate cluster centers.

FIGURE 1.1056

Plot of model based cluster solution for overwintering life stage shows the possibility of chemically distinct clusters (#1 & #3) within the Lower Snake River river group determined using LDFA. Shape indicates cluster association. Ellipses indicate cluster shape, orientation and 50% quartile for the multivariate distribution. Numbered gray circles indicate cluster centers.

FIGURE 1.1157

Plot of Lower Clearwater discharge showing the increase in $^{87/86}\text{Sr}$ with increasing outflows from the North Fork Clearwater River during near baseflow (●) and subsequent drops during high spring flows (○).

FIGURE 1.1258

Plot showing the similar temporal variation of $^{87/86}\text{Sr}$ observed for both the Lower Clearwater (▲) and Salmon (●) Rivers. In contrast the Upper Clearwater (◇) shows very little variation. The increased $^{87/86}\text{Sr}$ due to the onset of flow augmentation from Dworshak reservoir can be clearly seen in the $^{87/86}\text{Sr}$ signature of the Lower Clearwater during July, 2009.

FIGURE 1.1359

Plot showing the linear relationship of Sr:Ca with $^{87}\text{Sr}/^{86}\text{Sr}$ in water and otoliths. Water data is shown as black points, otolith data as grey points. The offset between water points and otoliths points is due to the physiological regulation of calcium within the otoliths. Lines indicate best fit linear regression for the corresponding data. Otolith values follow a similar linear trend to water values, however, indicating Sr:Ca is a tracer of geographic location in this system.

FIGURE 1.1460

Kernel density plot of outmigration timing for each natal river group. Density peaks illustrate that Upper Snake River juveniles out-migrate over a short interval and at an earlier date than the other groups. In contrast, fish from the Clearwater and Salmon River group out-migrate over a longer period with a majority of yearling migrants and a smaller number of sub-yearlings. The Lower Snake River shows two outmigration peaks, however early movement or maternal $^{87}\text{Sr}/^{86}\text{Sr}$ signatures may complicate the interpretation of outmigration timing in this river group. The Tucannon, Grande Ronde and Imnaha River group is not visible due to low sample sizes.

FIGURE 1.15	61
<p>Histogram and kernel density estimates of outmigration timing for yearling and sub-yearling fall Chinook salmon from all spawning areas of the Snake River. Peaks indicate two distinct peaks of outmigration corresponding to sub-yearling and yearling outmigration, however high densities of out-migrants occur throughout, indicating that many fish out-migrate during the winter, complicating survival estimates for Snake River fall Chinook salmon.</p>	
FIGURE 2.1	105
<p>Lithology of the Snake River watershed showing rock type categories with strong impacts on $^{87}\text{Sr}/^{86}\text{Sr}$ based primarily on protolithic composition (Table 2.3). Rock types of unknown protolith were categorized into Carbonate, Metamorphic or Sedimentary/Other based on their original classification. The Snake River basin shows large variation in the geology between river basins with rivers being influenced by both felsic and mafic geologies.</p>	
FIGURE 2.2	106
<p>Map showing the location of measured and predicted $^{87}\text{Sr}/^{86}\text{Sr}$ within the Snake River basin. Each point represents the outlet of a watershed. The geologic makeup of the watershed upriver of each point was used to predict $^{87}\text{Sr}/^{86}\text{Sr}$ for that point. Numbered points represent water samplin points within the basin. Filled circles (●) represent points predicted at 5-rkm intervals upsteam and downstream of water sampling locations. Open circles (○) represent points predicted ever 10-rkm throughout the basin. Split circles represent points included in both groups.</p>	
FIGURE 2.3	107
<p>Map showing basic lithology of Big Creek, a tributary of the Middle Fork Salmon River. Rock types based on reclassified geology (Table 2.3). Big Creek is dominated by Felsic and Metamorphic rocks.</p>	
FIGURE 2.4	108
<p>Map showing basic lithology of Bear Valley Creek, a tributary of the Middle Fork Salmon River. Rock types based on reclassified geology (Table 2.3). Bear Valley Creek is dominated by Felsic and Sedimentary rocks.</p>	
FIGURE 2.5	109
<p>Map showing basic lithology of Lapwai Creek, a tributary of the Middle Fork Salmon River. Rock types based on reclassified geology (Table 2.3). Bear Valley Creek is dominated by Mafic and Sedimentary rocks.</p>	
FIGURE 2.6	110
<p>Classification to natal source location of 134 fall Chinook salmon using a discriminate function constructed using $^{87}\text{Sr}/^{86}\text{Sr}$ values predicted from geology at 5-rkm intervals. Shape indicates classification from Hegg et al. (in review) while plot location indicates where a fish was classified using the 5-rkm prediction method. Fish misclassified using the 5-rkm prediction method do not match the shape of the group in which they are located. Open shapes indicate fish of known origin.</p>	
FIGURE 2.7	111

Classification to natal source location of 134 fall Chinook salmon using a discriminate function constructed using $^{87}\text{Sr}/^{86}\text{Sr}$ values predicted from geology at 10-rkm intervals. Shape indicates classification using traditional method while plot location indicates where a fish was classified using the 10-rkm method. Fish misclassified using the 10-rkm prediction method do not match the shape of the group in which they are located. Open shapes indicate fish of known origin.

FIGURE 2.8 112

The accuracy of $^{87}\text{Sr}/^{86}\text{Sr}$ prediction based on watershed geologic composition decreases as watershed area decreases. This relationship indicates that prediction of $^{87}\text{Sr}/^{86}\text{Sr}$ in large watersheds may be limited by scale. In the Snake River basin our results indicate that prediction accuracy decreases below watershed areas of $\sim 10^3\text{km}^2$.

FIGURE 2.9 113

Accuracy of $^{87}\text{Sr}/^{86}\text{Sr}$ predictions using watershed geologic makeup increases with increasing diversity of watershed geology. The Shannon index of diversity takes into account both the richness of rock types within a basin (# of unique rock types) and the relative representation (% watershed area) of rock types in calculating the diversity index. Our results indicate that watersheds in the Snake River basin with rock type diversity below ~ 1.0 may have higher prediction error.

FIGURE 2.10 114

Watershed geologic diversity increases exponentially with increases in watershed area within the Snake River basin. The interaction of watershed area and geologic diversity indicates a lower spatial limit on prediction accuracy within the Snake River Basin. Watersheds below 8400km^2 or Shannon diversity index scores of <1 show lower $^{87}\text{Sr}/^{86}\text{Sr}$ prediction accuracy.

CHAPTER 1

SPATIAL DISTRIBUTION OF ALTERNATE MIGRATION STRATEGIES IN FALL CHINOOK SALMON (*ONCORHYNCHUS TSHAWYTSCHA*) IN THE SNAKE RIVER OF IDAHO

Abstract

Salmon in the Snake River of Idaho inhabit a river system whose hydrology has been altered significantly in the recent past. The introduction of hydropower has caused significant flow, temperature and productivity changes in salmon spawning and rearing habitats. These changes may affect individual migratory response at major life history time points, as well as the selective pressure exerted on different migratory strategies at the population level. Snake River fall Chinook salmon (*Oncorhynchus tshawytscha*), a threatened species under the Endangered Species Act (ESA), have historically exhibited a sub-yearling juvenile out-migration strategy. In recent years, however, it has been shown that an overwintering yearling out-migration strategy is an increasingly significant strategy within the population. Although these recent discoveries can be documented in the population as a whole, the geographic distribution of this migration strategy, and the resulting survival consequences for individual spawning populations are unknown. We used otolith microchemistry to determine the rearing stream, overwintering location, and migration strategy of returning adult fall Chinook salmon based upon the unique elemental and isotopic signatures of tributaries within the Snake River basin. Results indicate nonrandom spatial distribution of the yearling migratory strategy and overwintering locations predominantly represented in mainstem reservoirs. Out-migration appears to be a continuous process throughout the winter, punctuated by peaks in summer and spring.

Introduction

The evolution of migratory behavior is based on tradeoffs among relative habitat profitability, spatial variation in growth, and differences in risk of mortality (Baker 1978). Migratory movements are selected for where resources are separated in space and time across the landscape. This separation requires individuals to move in order to maintain access to resources, or to occupy habitats which are suited for particular life stage processes (Dennis et al. 2003). Migration may have arisen due to competition, predation, resource limitation, seasonal change or parasitism but likely began with simple dispersive movement to maximize fitness in response to these factors (Salewski and Bruderer 2007). Under this model, migration develops after dispersal when there is selective advantage in returning to the original habitat due to seasonal or ontogenetic resource requirements (Milá et al. 2006).

While migration is often seen as a long term evolutionary change, in some cases migratory behavior can evolve quite rapidly within a sedentary population (Able and Belthoff 1998). Rapid changes in migratory path and timing have been linked to changes in resource availability in birds (Fiedler 2003). Similarly, phenotypic differences and temporal changes in migratory life history have been observed in as few as thirty generations in salmon (Quinn et al. 2000). This evidence indicates that when environmental variables change, there is potential for rapid shifts in life history strategy and migratory behavior within the affected population.

Anadromy in salmonids fits the model of initial dispersal followed by selective advantage of return migration. Productivity differences drive the existence of anadromy in temperate fishes due to the relative growth reward of migrating to the more productive environment of the ocean (Gross et al. 1988). The cool, high oxygen, freshwater environment, however, provides optimal conditions for egg maturation and juvenile growth. Thus, there is selective advantage in returning to freshwater habitat to spawn. This growth versus spawning dichotomy selects for migratory behavior in order

maintain the advantages of both environments at each life stage. Migration is not without risk, however, and juvenile salmon must balance the risk of mortality in a changing environment with the imperative to maximize growth during their downstream migration.

For juvenile salmon the timing of downstream movement is one important factor in determining the relative costs and benefits of migration to the ocean. Based upon stage specific ontogenetic shifts in energy requirements and acquisition (Werner and Gilliam 1984) downstream movement and shifts from parr to smolt should maximize growth rates during each discrete stage. In addition, movement should be motivated by the increased growth opportunity in alternate environments. Growth of juvenile salmon is highly dependent on the temperature of their environment and the availability of energy resources (McCullough 1999), however, and river temperatures increase from the time of hatching and can reach sub-optimal or lethal temperatures during summer months. Thus, juvenile fish must pass downstream while environmental conditions allow them to maximize their growth.

The timing of downstream movement in juvenile salmon is further influenced by ontogenetic factors. The onset of migration and smoltification of juvenile salmon is likely determined by threshold body size (Brannon et al. 2004; Hutchings and Myers 1994). Size selective mortality due to natural or anthropogenic means is evidenced in salmon populations (Zabel and Williams 2008). This indicates that attaining large body size before reaching the migration threshold is selectively advantageous. With these elements in mind, the model of ontogenetic niche shifts indicates that juvenile salmon in habitats with greater growth opportunity should exhibit earlier outmigration. Those fish who attain outmigration thresholds sooner would be expected, under this model, to move into downstream environments with higher growth potential, despite the potential risks, to escape inter-specific competition (de Roos et al. 2002; Werner and Hall 1988) Additionally, the high late season water temperatures in the lower river would be expected to select for this early downstream habitat shift to decrease thermal risks of later migration. This strategy would be predicted to minimize predation risk or, perhaps more importantly, density dependent mortality in low productivity natal

habitats. Fish originating in habitats with low growth opportunity, however, might be expected to delay migration until they can achieve a more competitive size.

Physical and climactic change has likely played a large role in the diversity of salmon migration strategies throughout their range (Waples et al. 2008). The ecological changes created by the advance and retreat of ice age glaciers, favored different juvenile strategies in basins throughout the Pacific Rim. As well, smaller scale disturbances in spawning streams create selective pressure towards a resilient life history (Quinn 2005). Salmon have overcome this history of environmental disturbance through a remarkable diversity of life history strategies in concert with meta-population structure. This combination preserves locally adapted life history strategies while maintaining enough connectivity between populations to retain the ability to respond to changes in the environment. This resilience is enhanced by phenotypic plasticity which allows salmon to adapt to changing conditions (Healey 2009). Hilborn et al. (2003) have shown that geographically distinct sub-populations with locally adapted life histories have allowed Bristol Bay sockeye metapopulations to be resilient to environmental changes. Those populations best adapted to current conditions thrived, while other populations were maintained at lower levels due to local adaptation. These smaller populations ultimately became important contributors to the overall population over time as conditions changed, favoring their life history strategy over others in the population.

The ability of salmon populations to persist in dynamic environments is directly related to their diversity of life history strategies. This diversity occurred as a result of geographically heterogeneous environmental conditions over evolutionarily timescales. More recently, however, as populations have declined their life history diversity has also decreased (Burke 2004). The placement of impassable dams has restricted the range of many salmon species, presumably decreasing the geographic heterogeneity of habitat. In addition, the remaining habitat is hydrologically and thermally modified. Although salmon have historically shown the ability to adapt to major environmental changes, recent anthropogenic changes in the Northwest may exceed the adaptive plasticity of salmon in the region (Waples et al. 2009). Thus, understanding the

geographic distribution of remaining life history strategies, and the fitness advantages they confer under different environmental regimes, is crucial for developing effective conservation strategies for these species.

The Snake River of Idaho is a microcosm of the larger changes in the region. Four dams cause significant flow, temperature and productivity changes in the lower Snake River. Four dams on the Columbia River, to which the Snake is a tributary, also affect the conditions experienced by salmon migrating to and from the Snake River. Dworshak dam, on the North Fork Clearwater River, and the Hells Canyon dam complex on the upper Snake River regulate flow and temperature in the spawning areas and block upstream migration of salmon. The placement of dams in the Snake and Columbia basin has had drastic negative impacts on salmon population abundance. As a result, Snake River fall Chinook salmon are listed as threatened under the Endangered Species Act (ESA) (Waples et al. 1991).

Most Chinook populations in North America have spring and fall run populations that are closely genetically related. Fall Chinook salmon in the Snake River, however, are genetically distinct from spring-summer run stocks (Waples et al. 2004). This indicates that the outmigration life history of Snake River fall Chinook may be more closely linked to their evolutionary history, and less to adaptation within a single population, compared to other stocks from Western North America. Historically, fall Chinook salmon in the Snake River have exclusively exhibited a sub-yearling out-migration strategy in contrast to other Pacific Northwest populations which contain both yearling and sub-yearling out-migrants (Schmitt et al. 1995). Ocean migration within the first months of life presumably provided an evolutionary advantage by allowing juveniles to escape high summer water temperatures in the lower Snake and Columbia rivers. Warm temperatures in the historic spawning areas supported fast growth and subsequently enabled the sub-yearling migration strategy (Williams et al. 2008). Because fall Chinook salmon have historically spawned in the main stem of the Snake and the lower reaches of its major tributaries, this migratory strategy was supported by the relatively rapid growth available in this environment.

Recently it has been shown that a significant fraction of the population of Snake River fall Chinook salmon exhibit a yearling out-migration strategy (Connor et al. 2005). These juveniles remain in the Snake River system through the winter before leaving for the ocean the next spring rather than out-migrate during their first year. The mechanisms behind this change are not clear, however temperature differences between spawning streams may affect the timing of juvenile Snake River fall Chinook migration (Connor et al. 2002). It has been suggested that dam related environmental changes may have altered the selective pressures experienced by out-migrating fall Chinook, creating evidence for the adoption of a later, and more selectively advantageous migration strategy (Williams et al. 2008).

The environmental effects of hydropower, and its consequences for juvenile growth and outmigration, are not evenly distributed across the system. The Lower Snake River is the most affected by dam impoundment, whereas the upper range of fall Chinook salmon in Hells Canyon is comprised of highly regulated, but free flowing, water released from Hells Canyon dam. Temperatures in the lower Clearwater River are several degrees lower during high growth periods for juvenile fall Chinook relative to similar rivers in the basin due to the cold outflows from Dworshak reservoir (Connor et al. 2002). These outflows are managed to aid juvenile fall Chinook out-migration by creating cool refugia in otherwise warm downstream reservoirs (Connor et al. 2003). Land use impacts vary across the basin as well, ranging from pristine wilderness to heavy agricultural and urban impacts. The Salmon River, flowing through the largely pristine Frank Church River of No Return Wilderness, remains the only tributary of the Snake River unaffected by hydropower. This patchy distribution of environmental changes creates the possibility of locally distinct selective pressures on juvenile fall Chinook within the Snake River Basin.

Relating migration strategy to growth and environmental change requires the ability to understand fish movements on a meaningful scale. This would be difficult and expensive over a geographic area as large as the Snake River using traditional tagging techniques. Otolith microchemistry offers a resource efficient method of analyzing the movements of individual fish at a finer geographic scale than is possible with current

tagging technology. The daily growth increments of fish otoliths record the chemical signatures of the environments through which a fish passes. Naturally occurring elements and isotopes are taken up in the aragonite matrix of the otolith, resulting in a temporal and spatial record of the movements of the fish. Isotopes of strontium, as well as other period I and II elements, can substitute for calcium in the otolith matrix. These elements are incorporated into the otoliths matrix at daily intervals, making them recoverable tracers of fish movement over definable time periods. Consequently, each individual fish carries a spatially explicit record of its location, habitat use and growth over its lifetime in fresh water.

The unique structure of otoliths make them a useful structure to investigate the geographic diversity of life history of Snake River fall Chinook salmon at a spatial and temporal scale that has not been possible in the past. While the recent appearance of the yearling out-migration strategy is well documented, the details of yearling migration timing are not well understood. This lack of knowledge is due to the loss of PIT tag detection ability during winter and very early spring at Lower Granite dam due to seasonal operation of the facility (Connor et al. 2005). Further, the relationship between migration strategy, fitness and local environmental variables is difficult to unravel without a detailed spatial understanding of the movement of fish during important life history time points.

Endangered Species act listing is based in part upon metrics of diversity and spatial structure of the populations (Good 2005; Waples et al. 1991). Thus, the geographic representation and timing of movement patterns within each juvenile migration strategy of Snake River fall Chinook salmon has implications for conservation of this species. ESA recovery efforts for Snake River fall Chinook are currently predicated on a single life history, with outmigration expected in the late summer and management efforts directed toward only that population. We know that salmonid life history is often an adaptation tied to locally distinct environmental variables in a patchy landscape. Thus, the development of the yearling migration strategy in Snake River fall Chinook is likely to be geographically heterogenous rather than equally represented across the Snake River basin.

The potential geographic heterogeneity of life histories within Snake River fall Chinook salmon poses important questions for management agencies tasked with maximizing the resilience, diversity, spatial structure and fitness of the population. Is yearling migration strategy unequally represented geographically within the Snake River basin, or is it relatively homogenous across spawning habitats? This may determine whether recovery actions must be geographically tailored to maximize diversity, or applied uniformly across the basin.

The overall objective of this paper is to determine the geographic representation of the yearling out-migration strategy within Snake River fall Chinook Salmon. We examined spatial differences in yearling representation in light of geographically distinct temperature and hydrologic differences between spawning and rearing streams in the basin. We characterized the geochemical variability (temporally and spatially) of all spawning and rearing habitats for the Snake River fall Chinook population. Using strontium isotope chemistry within otoliths of individual fish we determine natal, rearing and overwintering location and the timing of juvenile entry into the ocean. This data is used to determine the geographic representation of yearling fish within each major spawning area of the population. Subsequently, we reconstruct rearing location of all fish, and overwintering location of all yearling fish. These life stages are then examined for differences in juvenile fall Chinook salmon out-migration strategy across distinct spawning populations and between yearling and sub-yearling life histories. Cluster analysis of trace elemental signatures is used to identify additional chemically distinct groups within the basin. We hypothesize that the proportion of yearling fish is higher, and outmigration timing is later, in tributaries known to have lower temperatures and later emergence timing.

Methods

Study Site

The Snake River, the largest tributary to the Columbia River on the west Coast of North America, drains an area of 280,000km² in six states. The river originates in Wyoming and flows 1,670 km to its confluence with the Columbia River in Western Washington State with the majority of the basin located in the state of Idaho (Figure 1.1). The Snake River flows through four major geologic provinces (Figure 1.2). At its source it is characterized by the Teton Range, a heterogeneous mixture of Precambrian to Paleozoic era rocks including marine origin metamorphic rock and intrusive granites. It then flows through the Snake River Canyon of Southern Idaho whose drainage is dominated by relatively recent Quaternary and Tertiary volcanic basalt and rhyolite. From Hells Canyon to its confluence, the Snake River drains two distinct geologic provinces. Tributaries to the east, including the Salmon and Clearwater Rivers, drain the very old metamorphic and granitic geology associated with the Idaho batholith. Rivers draining from the West, including the Imnaha, Grande Ronde and Tucannon, drain the more homogeneous and recent Cenozoic era Columbia River basalts. The Palouse River joins the Snake from the north as it crosses into Washington State and drains primarily Columbia River basalt.

Fall Chinook salmon runs, which once numbered as many as 500,000 returning adults per year, have been affected by the placement of dams within the basin. Upstream access to eighty percent of their historic spawning grounds was blocked by the construction of the Hells Canyon dam complex in the middle Snake River in 1959 (Figure 1.1). Four downstream dams on the Snake have impounded the river from Ice Harbor Dam near the confluence with the Columbia to the port of Lewiston, ID. Dworshak Dam, an impassable dam on the North Fork of the Clearwater River, blocks salmon migration and supplies cold, hypolimnetic water that cools the lower portion of the Clearwater river during hatching and rearing seasons. Outflows from Dworshak

Reservoir are also used to adjust temperature and flow as a part of the Columbia and Snake River salmon management plan. Based upon aerial redd surveys, it is estimated that the majority of current fall Chinook salmon spawning occurs in two locations, the Hells Canyon reach of the Snake River and the Clearwater River. Smaller runs occur in the Lower Snake, Salmon, Grande Ronde, Tucannon and Imnaha rivers (Garcia et al. 2007).

Water Chemistry

The degree of $^{87}\text{Sr}/^{86}\text{Sr}$ variation in streamwater within the Snake River basin determines our ability to determine the exact location of a fish. Greater variation between basins results in increased spatial resolution in classification of fish, while relatively homogenous signatures across a basin make classification impossible. Because the $^{87}\text{Sr}/^{86}\text{Sr}$ signature within stream water determines the $^{87}\text{Sr}/^{86}\text{Sr}$ recorded in the otoliths of resident fish without biological fractionation (Kennedy et al. 2000), water samples can be used to quantify isotopic variation and to build a training set of $^{87}\text{Sr}/^{86}\text{Sr}$ from known locations with which to classify unknown fish.

To quantify the spatial variation of $^{87}\text{Sr}/^{86}\text{Sr}$ within the Snake River basin water samples were taken from the major spawning tributaries and at sites along the main stem of the Snake River (Figure 1.1). Sampling points were determined based on the locations of significant fall Chinook spawning activity, as described in Garcia (2007) with some changes to account for addition of the impounded section of the Lower Snake River. The reaches included the Upper and Lower reaches of the Snake and Clearwater Rivers, the Salmon River, and the Imnaha, Grande Ronde, Palouse and Tucannon Rivers. The South Fork Clearwater River, as well as the Lochsa and Selway rivers, were not sampled and were assumed to be a part of the Upper Clearwater reach. The Upper Snake River and the Lower Snake River were defined separately. The Upper Snake River was defined as the free flowing river from Asotin, WA to Hells Canyon Dam. The Lower Snake River was defined as the impounded section downstream of Asotin to the

river mouth. The Palouse River was sampled but has not been included in redd surveys historically. Samples were collected from each sampling site during spring, summer and fall seasons of 2008 with duplicate fall samples collected in 2009. (Table 1.1)

All water chemistry samples were collected approximately one foot below the water surface, at or near midstream, in acid washed HDPE water sampling bottles. Clean techniques were used to minimize the possibility of contamination. Sample bottles were double bagged in a clean lab environment prior to sampling. Samples were taken in an upstream direction with gloved hands and bottles were triple rinsed in the stream before a sample was taken. Samples were subsequently centrifuged to remove particulates below 0.45 μ m, dried and digested in clean hydrofluoric and nitric acids before analysis. All samples were analyzed for $^{87}\text{Sr}/^{86}\text{Sr}$ ratios using a Finnigan MAT 262 Multi-Collector Thermal Ionization Mass Spectrometer (TIMS). We used ANOVA with pairwise Tukey's Honestly Significant Difference test ($\alpha=0.05$) to determine if signatures from sampling sites were unique.

Otolith Collection

Otoliths from returning adult fall Chinook salmon of wild origin were collected over three years (2006-2008) during spawning operations at Lyons Ferry Fish Hatchery (Lyons Ferry, WA) and prepared for growth and microchemical analysis. Both saggital otoliths were removed from unmarked, presumably wild, fish included in hatchery spawning as a part of the wild stock inclusion program. Fish were presumed to be wild if they had an intact adipose fin and contained no hatchery implanted tags. Scale samples were taken for all fish at the time of otolith removal. Scale samples were subsequently analyzed by staff at Lyons Ferry hatchery as a final estimation of hatchery or wild origin of each fish. Scale analysis was also used to determine yearling vs. sub-yearling life history. Any fish determined to be of hatchery origin through scale analysis was excluded from the study.

The otoliths from known origin juvenile fish were collected to serve as a validation sample for fish classification (Table 1.2). Wild juvenile fall Chinook salmon were captured, PIT tagged and released in 2007 as a part of ongoing cooperative juvenile survey efforts of US Fish and Wildlife, Nez Perce Tribal Fisheries and Idaho Power Company. Marked juveniles were then recaptured at Lower Granite Dam when their PIT tags were identified by a sort-by-code process at the juvenile bypass facility. For a detailed description of bypass operations and juvenile capture see Connor (2002). Otoliths from seven marked sub-yearling juveniles were processed for isotopic analysis (Clearwater, 1; Lower Snake, 3; Upper Snake, 3). These fish were used to validate subsequent natal origin classifications. Since their location of capture at Lower Granite dam provided a known signature at the time of rearing/outmigration these fish were also used to validate rearing location classifications. In addition, otoliths from nine yearling juveniles from the 2008 brood year at Lyons Ferry Hatchery were analyzed for natal origin and included in the validation sample for natal origin classification.

Left saggital otoliths were prepared for analysis using standard polishing techniques (Secor et al. 1991) to reveal daily rings associated with juvenile freshwater residence. Otoliths were mounted on glass microscope slides on a saggital plane using Crystal Bond[®] resin (<http://www.crystalbond.com/>) and subsequently polished on a lapping wheel using alumina slurries of decreasing abrasiveness to reveal their rings. Polishing was stopped when the otolith core was exposed and daily rings could be discerned from the core to the edge of the otolith. All analysis was performed on the dorsal side of the otoliths in the region perpendicular to the sulcus (Figure 1.3) as this area contained the most repeatable and clear growth rings.

Otolith Microchemistry

Prepared otoliths were analyzed for $^{87}\text{Sr}/^{86}\text{Sr}$ to reconstruct the natal origin, rearing location and overwintering location of each fish from the isotopic patterns in their otoliths. Isotopic ratio was analyzed using a Finnigan Neptune (Thermo Scientific)

multi-collector inductively coupled plasma mass spectrometer coupled with a New Wave UP-213 laser ablation sampling system (LA-MC-ICPMS). (Barnett-Johnson et al. 2005; Outridge et al. 2002; Woodhead et al. 2005) All otolith analysis were conducted at the Washington State University Geoanalytical Laboratory (Pullman, WA).

A marine shell standard, which was assumed to be in equilibrium with the global marine value of $^{87}\text{Sr}/^{86}\text{Sr}$ (0.70918), was used to evaluate measurement error. The average marine shell value over the length of the study was 0.709214 ± 0.000010 (1 SE), slightly higher than expected. A correction factor was calculated for each analysis day based upon the average deviation of the shell standard from the marine value and otolith $^{87}\text{Sr}/^{86}\text{Sr}$ values were adjusted accordingly.

Two methods were combined to recover the isotopic patterns in otoliths (Figure 1.3). First, a transect was analyzed from the otoliths edge to its core at 90° from the sulcus on the dorsal side. If clear rings were not present in that region the analysis was shifted to the nearest location with more distinct rings. The laser was set to ablate the sample at a constant speed ($30\mu\text{m}/\text{second}$, $40\mu\text{m}$ laser spot size, .262 integration time). This scan recorded changes in $^{87}\text{Sr}/^{86}\text{Sr}$ across the otoliths with excellent temporal resolution but lower precision (± 0.00028 , 2 SE). To capture more precise estimates of $^{87}\text{Sr}/^{86}\text{Sr}$, transect ablations were followed by analyses, which determined precise values for stable signatures within the natal, rearing and overwintering regions of the otoliths. These longitudinal analyses ablated a curved path along individual rings of the otolith at points of stable signature ($10\mu\text{m}/\text{second}$, $30\mu\text{m}$ laser spot size, .262 integration time, 100 integrations). This method provides very precise measures of isotopic chemistry (± 0.00012 , 2 SE) at specific life history points. In cases where a more precise scan was not completed, signatures were determined using the transect scan. This was done by calculating the mean of the corrected $^{87}\text{Sr}/^{86}\text{Sr}$ integration points within a region of stable $^{87}\text{Sr}/^{86}\text{Sr}$ corresponding to the life stage being analyzed.

In addition to $^{87}\text{Sr}/^{86}\text{Sr}$ all otoliths were analyzed for trace elemental concentrations using a Finnigan Element-2 ICP-MS. Samples were laser ablated using the same New Wave laser system used for $^{87}\text{Sr}/^{86}\text{Sr}$ analysis above. Elemental concentrations (mmol/mol) of Sr, Mg, Mn, Ba were determined using a laser transect

located immediately adjacent to the ablation transect used for $^{87}\text{Sr}/^{86}\text{Sr}$ analysis. Transects were ablated at a constant speed (11 $\mu\text{m}/\text{s}$ scan speed, 30 μm spot size) and counts for each element were recorded for each second of the run. Counts per second (cps) were converted to concentrations (ppm) and then converted to elemental ratios with calcium (mmol/mol).

Limits of detection for each element were calculated as three times the standard deviation of a blank run multiple times throughout the run. Limits of detection were below measured levels for all elements included in analysis; Sr (LOD = 0.0010mmol/mol), Mg (LOD = 0.0410 mmol/mol), Mn (LOD = 0.0567mm/mole), Ba (LOD = 0.0002). Analysis of a prepared standard was used to estimate within run error and percent coefficient of variation (%COV) was reported for each element; Sr (2.36% COV), Mg (3.37% COV), Mn (1.98% COV), Ba (3.50% COV). Laser ablation results of a NIST610 solid standard were used to estimate external precision and error was reported as percent deviation (%DEV) of the mean from the expected value; Sr (2.66% DEV), Mg (7.87% DEV), Mn (9.69% DEV), Ba (7.03% DEV). Transects were ablated at a constant speed (11 $\mu\text{m}/\text{s}$ scan speed, 30 μm spot size) and counts for each element were recorded for each second of the run. Counts per second (cps) were converted to elemental ratios of Sr:Ca, Mg:Ca, Mn:Ca, Ba:Ca.

No longitudinal scans were performed for elemental data. If a longitudinal scan was performed during $^{87}\text{Sr}/^{86}\text{Sr}$ analysis, a 100 μm range of the element data, centered on the distance from the core of the longitudinal scan, was averaged to create the corresponding element values. If no longitudinal scan was performed during $^{87}\text{Sr}/^{86}\text{Sr}$ analysis, then the same range of μm from the otoliths core which was used to calculate the $^{87}\text{Sr}/^{86}\text{Sr}$ signature was used to calculate the elemental values for the same otolith.

Life Stage Determination

We examined three stages of outmigration within the juvenile section of each adult otolith in the study, natal origin, rearing, and overwintering. In all cases $^{87}\text{Sr}/^{86}\text{Sr}$

was used as the primary microchemical signature for determination of each life stage. The first stable signature beyond 110 μm and within 250 μm from the otolith core on the dorsal side was considered to be the natal origin signature. If no stable signature was detected, the first peak or valley in $^{87}\text{Sr}/^{86}\text{Sr}$ was used as the natal signature. This range was used in order to most closely approximate the natal location, before migration to downstream rearing habitat but outside the area of maternal influence on the signature.

The justification for this measurement came from several sources. In a separate study, 110 μm corresponded to the mean distance of the hatch check from the otolith core of juvenile fish captured at Lower Granite dam during outmigration ($n=19$, st. dev.=13 μm) (Zabel and Chittaro 2011). 250 μm represented a conservative estimate of the beginning of downstream migration to rearing habitat based on the location of exogenous feeding checks reported in California Central Valley fall Chinook salmon (Barnett-Johnson et al. 2005). The geometry of our adult otoliths made it difficult to repeatably determine daily rings on the ventral side of the otolith as that study did, and we were unable to consistently determine the exogenous feeding check in adult otoliths. The smaller geometry of the dorsal side of the otoliths, or differences in growth between the two river systems, may contribute to any discrepancy in natal signature determination in our study.

Rearing signature was considered to be the first stable, freshwater signature between 250 μm and 800 μm . An overwintering signature was considered to be the first stable signature or peak beyond 800 μm from the otolith core. This distance was based on calculations of otolith size at length for fall Chinook juveniles (Zabel and Chittaro, personal communication) which indicated that 800 μm exceeded the expected size for a fish outmigrating past Lower Granite dam in October, when bypass captures are terminated for the year and sub-yearling fall Chinook outmigration has ended. These results were checked against scale analysis to confirm similarity in determination of yearling life history (78% similarity, see Table 1.1). Any fish exhibiting a freshwater signature beyond 800 μm from the otoliths core was considered a yearling fish for subsequent analysis.

I. Discriminant Function Classification

Adult fish were classified to their natal, rearing and overwintering location using linear discriminate function analysis (LDFA) with equal prior probability and jackknife re-sampling. $^{87}\text{Sr}/^{86}\text{Sr}$ signatures for all water sampling points within the basin were used as the training set to develop the LDFA. Water sampling points were grouped into river groups based on chemical similarity, determined by the results of ANOVA with Tukeys HSD ($\alpha = 0.05$). Elemental data was excluded from the LDFA analysis because we lacked baseline elemental signatures from representative resident fish within the basin. Without this training set we were unable to account for the physiological, temporal and spatial interactions responsible for trace elemental differences. Instead, elemental data was included in subsequent cluster analysis (see next sub-section). Overwintering was determined using otolith ocean entry signature ($>800\mu\text{m} =$ yearling) and no attempt was made to reconcile scale and otolith yearling determinations. Known origin juvenile otoliths were included in the classification to provide validation of our ability to correctly classify fish.

We tested the hypothesis that expression of the yearling juvenile life history is non-randomly distributed within the basin using Fishers exact test of proportions. We compared the proportion of yearling fish originating from each of the classification groups to the pooled proportion for the other rivers within the basin, to determine statistically significant differences in each river ($\alpha=0.05$).

Exploratory Cluster Analysis

Trace elements provide additional location information as they are recorded in otolith rings. Concentrations of these elements within the otoliths, however, can be biologically or thermally regulated within the fish, so the molar ratios within otoliths do not directly relate to that of the ambient water chemistry. Without a training set of

known origin otoliths, these trace elements could not be used as part of the LDFA classification. To identify possible chemically distinct groups that were not captured by the LDFA, trace elemental ratios and $^{87}\text{Sr}/^{86}\text{Sr}$ results were used to further examine the clustering structure within the data. Clustering was begun under the a-priori assumption that any clustering algorithm used should be optimized for elliptical clusters. Elliptical clusters were expected due to the relationship between $^{87}\text{Sr}/^{86}\text{Sr}$, which should exhibit very low within stream variation in resident fish, and elemental data, which may exhibit wider variation. This wide variation in trace element data is due to the physiological regulation of elemental concentrations, local environmental conditions and seasonal fluctuations in elemental deposition in the otolith, each of which influence the elemental ratio with calcium. Data was not scaled in order to preserve possible clustering information contained in this variance relationship.

Principal Component Analysis (PCA) and model based variable selection were used as a guide for selecting variables which contributed to clear clustering of the data. Horn's procedure of bootstrapped eigenvalues was used to determine the most meaningful principle components, and the most highly weighted variables within these were retained. Model based variable selection was also performed using the CLUSTVARSEL package for R as a competing variable selection technique. CLUSTVARSEL is a companion package to the MCLUST package based upon model based variable selection techniques from Raferty (2006). This package uses iterative BIC selection to determine the variables within a set which contribute most to the clustering within a dataset over a range of cluster solutions from 2 to a maximum defined by the user.

Model based clustering was performed using the MCLUST package for R (<http://www.stat.washington.edu/mclust/>) due to its ability to easily incorporate elliptical cluster solutions while objectively determining the best cluster model for the data. The Mclust algorithm is based upon work by Fraley and Rafferty (2007) using hierarchical, model based clustering and model selection using Bayesian Information Criterion (BIC). BIC is a model selection tool similar to Akaike's Information Criterion (AIC). These selection criterion are used to evaluate model fit and parsimony between

candidate models, in this case cluster solutions created by MClust. BIC more heavily penalizes for inclusion of model elements than does AIC and is thus a more stringent test for parsimony. A difference in BIC of greater than two is considered to be indicative of significant improvement in the model. Mclust cluster models may be comprised of spherical, diagonal or ellipsoidal distributions; equal or variable volume clusters; elliptical or circular clusters; and with coordinate, equal or variable cluster axes. BIC is used to determine the most parsimonious combination of these cluster elements given the data supplied.

Outmigration Timing

Ocean entry timing was used as a test of geographic differences in life history expression. Specifically, under our hypothesis we would expect that natal source locations with high representation of the yearling life history would, on average, enter the ocean later. Ocean entry timing for each natal river group was tested using ANOVA ($\alpha=0.05$) to determine if mean ocean entry timing was significantly different between natal river groups. Tukey's HSD test ($\alpha=0.05$) was used to test for pairwise differences between groups.

Ocean entry was determined using MC-ICPMS by a characteristic, sudden increase in the intensity of the Sr signal in the otoliths, followed closely by a stable signature approaching 0.70918, the global marine signature (Figure 1.3). This characteristic pattern is due to the great increase in Sr concentration in the ocean compared to fresh water. This concentration change causes intensity of the strontium signal to increase as a fish moves from ocean to river. As $^{87}\text{Sr}/^{86}\text{Sr}$ in the fish comes to equilibrium with the marine environment the signature moves to the global marine value. Ocean entry was measured as the distance between the core and the point of inflection of the Sr intensity increase. This value was recorded for all otoliths to determine the relative timing of ocean entry for each fish.

Juvenile growth rate follows a discontinuous pattern and no growth model exists for the entirety of the freshwater phase for fall Chinook salmon. Thus, ocean entry measurements cannot be easily converted into age but function as a relative measure of freshwater residence time. Unpublished growth data (Zabel and Chittaro, personal communication) from sub-yearling juvenile fall Chinook captured at Lower Granite dam indicate an average relationship between otolith size and juvenile fork length of $5.37\mu\text{m}/\text{mm}$. realizing that this is a very rough estimate of fish size, all outmigration measurements in this study are converted to fork length (FL) to aid in interpretation of otolith data.

Results

Water Chemistry

Water $^{87}\text{Sr}/^{86}\text{Sr}$ signatures vary substantially in the major reaches of the Snake River basin (Figure 1.4) with significant differences between reaches (ANOVA, $F=99.4$, $p<0.001$). Pairwise comparison (ANOVA, Tukey's HSD). indicated four major groups of distinguishable signatures in the basin. These groups were combined into a reduced model for the purpose of fish classification. The Tucannon, Grande Ronde, and Imnaha rivers (TGI) were grouped based upon similar isotopic signatures. The Clearwater and Salmon Rivers (CWS) were grouped into a second group. Lyons Ferry Hatchery and the Lower Snake River made up a third group (LSK). The Upper Snake River (USK) made up a fourth group. All comparisons were significant in this reduced model (ANOVA, Tukey's HSD, $F=268.8$, $p<0.001$). (Table 1.1)

The $^{87}\text{Sr}/^{86}\text{Sr}$ values for samples from the TGI, CWS, LSK and USK river groups were used as a training set to create a linear discriminate function (LDFA) for subsequent fish classification. Cross-validation was used to estimate the true classification error rate and prior probability of group membership was assumed to be

equal. The cross validation error rate for this model was 0%. This LDFA was subsequently used to classify fish to location at discrete juvenile life history stages.

The Palouse River was not included in the LDFA training set. The Palouse River was sampled at a location near the confluence with the Snake River that is affected by the impoundment of water behind Lower Monumental dam. Although samples were taken at mid-flow it is likely that mixing of signatures from the Lower Snake river resulted in the high variability in the signature. Although the 10 km stretch of the Palouse River downstream of the impassable Palouse Falls is open to spawning, no redd surveys are done in the Palouse (Garcia et al. 2007) and little to no spawning is thought to occur within the reach. For this reason the Palouse River was removed from the dataset in order to better determine differences between the Upper and Lower Snake Rivers, which are important spawning grounds for fall Chinook.

Life Stage Determination

I. Natal Origin Classification

We classified all adult otoliths (n=120), as well as known origin juveniles (n=14), to natal origin based on the $^{87}\text{Sr}/^{86}\text{Sr}$ signature recovered from the natal section of their otoliths (100-250 μm) using the previously developed LDFA model (Table 1.3). The LSK claimed the largest share of natal fish (58 fish, 48%). The second largest group was the CWS (44 fish, 37%). The USK group contained 16 fish (13%) and the TGI classification contained only 2 fish (2%). Classification was successful for 100% of the known origin juveniles (Figure 1.5).

To compare the occurrence of the yearling life history between natal locations, the percentage of yearling fish (ocean entry >800 μm from otoliths core) was calculated for each group from the LDFA (Table 1.3). The CWS contained the largest percentage of yearling fish (77%, 74% female). The LSK was comprised of 62% yearling fish (55% female) and the USK group contained only 13% yearling fish (37% female). 50% of the

TGI group was made up of yearling fish (100% female), however the sample size was small (2 fish).

The proportion of yearling fish in the CWS group was significantly higher than the pooled proportion in the rest of the basin (Fishers exact test, $p=0.01$, $\alpha=0.05$). In contrast the USK group contained a significantly lower proportion of yearling fish than the rest of the basin using the same test ($p>0.001$, $\alpha=0.05$). The LSK group was not significantly different. The TGI group was not significantly different, however sample sizes were low and statistical power was not sufficient to draw a conclusion.

II. Rearing Location Classification

All adult otoliths ($n=120$), as well as wild tagged, known origin juveniles ($n=7$), were classified to rearing location based on the $^{87}\text{Sr}/^{86}\text{Sr}$ rearing signature from their otoliths (250-800 μm) using the LDFA model (Table 1.4). The LSK group contained 78 fish (66%). The CWS group contained 37 fish (31%). The USK group contained 2 fish (2%) and the TGI group contained only 1 fish (1%).

To compare the occurrence of the yearling life history between rearing locations, the percentage of yearling fish (ocean entry $>800\mu\text{m}$ from otoliths core) was calculated for each group from the LDFA (Table 1.4). Yearling representation varied between rearing locations. The LSK group contained 58% yearling fish (71% female). The CWS group contained 76% yearling fish (61% female). The TGI group and USK groups contained no yearling fish.

Classification of known origin juveniles was successful for 6 of the seven samples (Figure 1.6). All fish were known to have been captured at Lower Granite Dam, however one sample was misclassified to the CWS group as a result of possible use of CWS as rearing habitat either before tagging or between recapture events.

III. Overwintering Location

All adult otoliths determined to be yearling based upon a saltwater entry signature greater than 800 μm from the otoliths core (n=74) were classified to overwintering location (Figure 1.7) based upon the $^{87}\text{Sr}/^{86}\text{Sr}$ signature in the overwintering portion of their otoliths (>800 μm) (Table 1.5). The LSK group contained 72 fish (97%). The CWS group contained 2 fish (3%). The TGI and USK groups did not contain any fish.

The LSK group was comprised of 68% female fish. The CWS group contained 50% female fish.

Exploratory Cluster Analysis

Cluster analysis based upon the full suite of isotopic and elemental variables resulted in cluster solutions with poor separation of clusters and little relationship to the LDFA groupings. Six-cluster solutions were found for the natal (Diagonal distribution, variable volume, equal shape, coordinate axes) and rearing (Diagonal distribution, variable volume, equal shape, coordinate axes) datasets. A three-cluster solution was selected for the overwintering dataset (Diagonal distribution, equal volume, variable shape, coordinate axes) with separation of the expected LSK and CWS groups and a third group comprising four outlying points. Overall, the global cluster model was unsatisfactory and variable selection was needed to provide relevant cluster solutions.

Variable selection was performed for all life stages with limited success. Horn's procedure selected the first principle component (PC) in the natal dataset. Principle component directions 1 and 2 were selected in the rearing dataset. In the overwintering dataset Horn's procedure was inconclusive, failing to select a PC direction with variance larger than the bootstrapped data and thus failing to eliminate any variables. This was likely due to the tight grouping of fish within the Lower Snake River, leading to

relatively equal variance within the data. In the natal and rearing datasets the three most heavily weighted variables within the selected PC's were Sr:Ca, Ba:Ca and $^{87}\text{Sr}/^{86}\text{Sr}$ respectively. Model based variable selection using CLUSTVARSEL failed to eliminate any variables using a maximum number of clusters between 5 (one larger than the number of LDFA groups) and 10.

Sr:Ca and Ba:Ca were highly correlated in both natal (corr = 0.61) and rearing (corr = .82) datasets. Sr:Ca showed greater variance, illustrated by its higher PC loadings, and thus was more likely to contribute to clustering. For this reason Ba:Ca was removed from the cluster analysis for these datasets. BIC indicated the best fit cluster model for the reduced natal dataset (Figure 1.8) was a two-cluster model with diagonal distribution, variable cluster volume, variable cluster shape and coordinate cluster axes. A five-cluster model was selected for the rearing dataset (Figure 1.9) with diagonal distribution, equal volume, equal shape and coordinate axes. In the absence of a compelling variable selection result for the overwintering dataset, $^{87}\text{Sr}/^{86}\text{Sr}$ and Sr:Ca were used to cluster this data as well. This resulted in a three-cluster model for the overwintering dataset (Figure 1.10) with diagonal distribution, variable volume, variable shape and coordinate axes.

Outmigration Timing

Significant differences were found in timing of ocean entry between natal origin groups (ANOVA, $F=4.14$, $p=0.007$, $\alpha=0.05$). Minimum freshwater entry was $482\mu\text{m}$ (89mm FL) with the latest out-migrant entering saltwater at $1280\mu\text{m}$ (238mm FL). The USK and LSK groups exhibited significantly different ocean entry timing (Tukey's HSD, $p=0.02$, $\alpha=0.05$) with fish from USK entering the ocean $160\mu\text{m}$ (29mm FL) earlier than those from LSK. CWS was also found to be significantly different from USK (Tukey's HSD, $p=0.005$, $\alpha=0.05$) with individuals from CWS entering the ocean $188\mu\text{m}$ (35mm FL) later on average than USK.

Yearling fish outmigrated on average $305.5\mu\text{m}$ (57mm FL) later than subyearling fish. The mean distance from the otoliths core for subyearling ocean entry was $693.8\mu\text{m} \pm 212\mu\text{m}$ (129mm FL $\pm 39\text{mm}$). Yearling fish entered the ocean at a mean otolith distance of $998.3\mu\text{m} \pm 102\mu\text{m}$ (186mm FL $\pm 35\text{mm}$).

Discussion

Water Chemistry Variation

Strontium isotopic chemistry in streamwater is controlled by the weathering of underlying watershed lithology. These differences are based upon the unique distribution of rubidium and strontium between the crust and mantle of the earth (Faure 1977). ^{87}Sr is a radiogenic isotope and a decay product of ^{87}Rb (half life 4.5billion years) while ^{86}Sr is stable. Rb is particularly enriched in silicate minerals forming the crust (felsic minerals) while largely absent from minerals derived from the mantle (mafic minerals). The decay of ^{87}Rb to ^{87}Sr over time results in much higher $^{87}\text{Sr}/^{86}\text{Sr}$ values in rocks of felsic composition compared to mafic rocks with the effect being more pronounced in older rocks.

Due to the isotopic differences between rock types, surface water $^{87}\text{Sr}/^{86}\text{Sr}$ generally follows the isotopic composition of the geologic formations that underlie the watershed. Strontium concentration, isotope ratio and weathering rates combine to control strontium ratio based upon a mixing model (Palmer and Edmond 1992). Strontium ratios have been shown to be relatively temporally invariant (Bain and Bacon 1994; Kennedy et al. 2000). Clow et al. (1997), however, reports evidence for seasonal variation in $^{87}\text{Sr}/^{86}\text{Sr}$ driven by the $^{87}\text{Sr}/^{86}\text{Sr}$ differences between snowmelt and baseflow. The effects of dam storage and outflow on downstream $^{87}\text{Sr}/^{86}\text{Sr}$ is unknown, however Kennedy (personal communication) reports significant changes in

$^{87}\text{Sr}/^{86}\text{Sr}$ based upon water withdrawal and dam outflow effects in the Henry's Fork River of Idaho.

The Snake River basin is a snowmelt-dominated system with watersheds flowing through diverse geologic regions. Our data on aqueous chemistry demonstrated significant differences between sampling points, with differences corresponding generally to differences in the mafic/felsic composition of rocks underlying the watershed. The Clearwater and Salmon Rivers contain large areas of felsic granites, as well as much older metamorphic rocks. As predicted based on their composition, these rivers have the highest $^{87}\text{Sr}/^{86}\text{Sr}$ values within the basin. The Imnaha, Tucannon, and Grande Ronde flow over nearly homogenous deposits of basalt, a rock of mafic origin. As predicted these rivers exhibit lower $^{87}\text{Sr}/^{86}\text{Sr}$ signatures consistent with their mafic origin.

We expected $^{87}\text{Sr}/^{86}\text{Sr}$ signatures to remain relatively temporally stable as reported in the literature. This was the case in the majority of sampled reaches, however the Clearwater, Salmon and Palouse rivers showed high variation inconsistent with the reported literature (Figure 1.4). The reasons for this are unknown, however the data indicate that seasonal snowmelt effects, as well as seasonally controlled dam outflows, may be a driver of $^{87}\text{Sr}/^{86}\text{Sr}$ variation in the Clearwater and Salmon Rivers.

Dworshak Dam impounds the North Fork Clearwater River near its confluence with the mainstem Clearwater River. Outflows from the dam are managed seasonally to provide cooler reservoir temperatures for outmigrating fall Chinook salmon in Lower Granite Reservoir (Connor et al. 2003). For this reason outflows are low in the winter and spring but are increased in early to mid-July, augmenting flows in the Lower Clearwater river. These seasonally controlled releases from the Dworshak Reservoir on the North Fork Clearwater River are likely to be responsible for significant $^{87}\text{Sr}/^{86}\text{Sr}$ variation in the Lower Clearwater River, though our sampling was not at a scale to resolve this definitively.

Surface water $^{87}\text{Sr}/^{86}\text{Sr}$ data is not available for this region, however, the North Fork Clearwater is expected to have a significant influence on $^{87}\text{Sr}/^{86}\text{Sr}$ signature due to the presence of several sources of rock with high strontium concentration and high

$^{87}\text{Sr}/^{86}\text{Sr}$ in the watershed. Mesoproterozoic Belt Supergroup metasedimentary and carbonate rocks ($^{87}\text{Sr}/^{86}\text{Sr} = 0.714\text{-}0.925$, Sr conc. = 47-95ppm) are one source of high strontium signatures (Fleck et al. 2002). Granitic plutons of the Idaho Batholith ($^{87}\text{Sr}/^{86}\text{Sr} = 0.707\text{-}0.715$, Sr conc. = 242-895ppm) also contain very high $^{87}\text{Sr}/^{86}\text{Sr}$ and significant strontium concentrations (King et al. 2007). Both are likely to contribute high strontium ratios to outflows from Dworshak dam, creating a strong reservoir outflow effect on $^{87}\text{Sr}/^{86}\text{Sr}$ in the Lower Clearwater River.

This reservoir outflow effect may be visible in our data from the Lower Clearwater sampling site directly below the North Fork confluence (Figure 1.11). When the fall sample was taken on October 17, 2009 (0.713782 $^{87}\text{Sr}/^{86}\text{Sr}$) no water was being released from the spillways at Dworshak Dam and total flow in the Lower Clearwater River at the USGS gauging station (Peck, ID) just downstream was $3,280\text{ft}^3\text{s}^{-1}$. The summer sample had a much higher signature and was taken on July 10, 2009 (0.714726 $^{87}\text{Sr}/^{86}\text{Sr}$) when the spillways were full and flow augmentation had begun. The flow on this date was $15,400\text{ft}^3\text{s}^{-1}$ at the Peck gauging station at the time of the July sample. This pattern continues with the Summer and Fall samples from the Lower Clearwater at Lapwai Creek. At these times the river is at, or near, base flows and the effect of increased flows from the North Fork would be greatest. This pattern is not evident for the Spring 2009 sample, leaving open the possibility of other explanations of $^{87}\text{Sr}/^{86}\text{Sr}$ variation. During the Spring sampling period, flows in the main stem Clearwater River were at springtime highs ($39,900\text{ft}^3\text{s}^{-1}$ on June 8, 2009) yet $^{87}\text{Sr}/^{86}\text{Sr}$ for the lower Clearwater was at its lowest. At this time outflows from Dworshak reservoir would have been minimal as the reservoir filled with Spring runoff. Also, extremely high flows from the mainstem Clearwater would likely overwhelm the North Fork Clearwater signature, resulting in lower $^{87}\text{Sr}/^{86}\text{Sr}$ values. (Figure 1.11)

Unexpectedly high variation in the Salmon River indicates that dam outflows cannot explain all the seasonal variation in $^{87}\text{Sr}/^{86}\text{Sr}$ within the basin. Because the Salmon River is free flowing, and flows largely through wilderness areas, human impacts are not likely the cause of this variation. Natural disturbances are one possible source of the observed $^{87}\text{Sr}/^{86}\text{Sr}$ variation. Evidence suggests, however, that fire may

decrease bulk dissolved strontium in streamwater (Hough 1981) but should not affect $^{87}\text{Sr}/^{86}\text{Sr}$. The effect of other natural disturbances on $^{87}\text{Sr}/^{86}\text{Sr}$ are not reported in the literature. This indicates that other processes are responsible for the variation in $^{87}\text{Sr}/^{86}\text{Sr}$ in the Salmon River.

The Salmon and Lower Clearwater Rivers each follow a similar temporal trend in $^{87}\text{Sr}/^{86}\text{Sr}$ (Figure 1.12). Both rivers exhibit higher $^{87}\text{Sr}/^{86}\text{Sr}$ during the fall season and lower levels in the spring and summer, with the exception of the Lower Clearwater samples in July which, as previously discussed, are likely increased due to flow augmentation from the North Fork Clearwater. The Upper Clearwater reach, however, sampled 4 miles upstream of the North Fork confluence, and above possible dam effects, maintains a steady signature throughout the seasons with very little variation (Figure 1.12, Table 1.1). This indicates that signature variation in the Lower Clearwater likely occurs due to outflows from the North Fork Clearwater River. The North Fork Clearwater River is the only major tributary joining the main stem below the Upper Clearwater sampling location and prior to the confluence with the Snake River (Figure 1.1).

Clow et al. (1997) report a possible explanation for the anomalous seasonal variation in $^{87}\text{Sr}/^{86}\text{Sr}$ in the Clearwater and Salmon rivers. Clow et al. found that $^{87}\text{Sr}/^{86}\text{Sr}$ was depressed during spring and summer due to the effect of snowmelt in alpine streams dominated by snowmelt, and flowing over granitic geology with high $^{87}\text{Sr}/^{86}\text{Sr}$. The depression in $^{87}\text{Sr}/^{86}\text{Sr}$ was due to snowmelt dominated streamflow with low $^{87}\text{Sr}/^{86}\text{Sr}$ driven by windblown carbonates captured in the snowpack. The large volume of snowmelt diluted the higher strontium ratios of the underlying granitic geology, depressing $^{87}\text{Sr}/^{86}\text{Sr}$ during non-baseflow periods.

While the size of watersheds is much different, the basic geology of the Salmon and Clearwater rivers is similar to the geology studied by Clow et al. Both are snowmelt dominated systems flowing over areas of granitic geology containing with high $^{87}\text{Sr}/^{86}\text{Sr}$. It is possible that a similar snowmelt interaction is responsible for the variability of $^{87}\text{Sr}/^{86}\text{Sr}$ in the Lower Clearwater and Salmon, with flow augmentation from Dworshak reservoir artificially increasing $^{87}\text{Sr}/^{86}\text{Sr}$ during the late summer

months. Stable isotopic signatures in the Upper Clearwater are anomalous under this interpretation, however, and further study is needed to confirm the causes of $^{87}\text{Sr}/^{86}\text{Sr}$ variation in the Clearwater and Salmon Rivers. It is also possible that spatio-temporal differences in snowmelt within such a large geographic area due to altitude, rainfall, or other factors may play a role in the observed $^{87}\text{Sr}/^{86}\text{Sr}$ variation.

The Palouse River also shows high variation and unexpectedly exhibits a signature similar to the Snake River. It flows primarily over mafic basalts similar in age and composition to the Imnaha, Tucannon and Grande Ronde and would be expected to exhibit a similar signature. Water samples were taken from the Palouse near the confluence with the Snake River, in a location inundated by the reservoir created behind Lower Monumental Dam but below the impassable Palouse Falls. Although samples were taken at midflow, uneven mixing of water from the Snake River is the likely cause of the anomalous signature and high variation in the Palouse River samples.

Life Stage Determination

The Snake River presents a unique opportunity to determine the location of migrating salmon within the basin during key points in their lives. The diversity of $^{87}\text{Sr}/^{86}\text{Sr}$ signatures makes possible discrimination of source locations and movement patterns of fish based upon the recorded $^{87}\text{Sr}/^{86}\text{Sr}$ signatures in their otoliths. Not all $^{87}\text{Sr}/^{86}\text{Sr}$ signatures were unique however, and some aggregation of river reaches was needed to successfully classify fish to location using LDFA.

Aggregation of watersheds to river groups with similar $^{87}\text{Sr}/^{86}\text{Sr}$ signatures results in a decrease in the spatial resolution to which a fish's location can be determined. If aggregation combines populations of interest within the same river group it could result in the inability to draw concrete conclusions about the distribution of fish within the basin. This was not the case within the Snake River, however, due to favorable geographic distribution of spawning areas within the basin as shown by studies of redd counts.

The results of redd surveys in the Snake River basin indicate that we have captured the majority of distinct population groups within the basin with our LDFA river group classifications. The majority of fall Chinook salmon spawning occurs in the Upper Snake River and the Lower Clearwater River (Garcia et al. 2007), which are captured in separate LDFA classifications in our study. In 2007, 1,117 fall Chinook salmon redds were counted in the Upper Snake River. In the same period 718 redds were counted in the Lower Clearwater River, with less than 10 redds counted per year above the confluence of the North Fork Clearwater in the Upper Clearwater River. Only 18 redds were counted in the Salmon river during the 2007 season. This indicates that the Salmon river would contribute less than 1% to the CWS river group. Thus, redd surveys show that the major spawning populations in the basin are separated within our LDFA.

The Tucannon, Grande Ronde and Imnaha populations are geographically separated and likely distinct, yet our LDFA groups them together. The low redd counts in these tributaries make it unlikely, however, that large sample sizes would be collected from returning adults in any case. Garcia et al (2007) report 81 redds were observed in the Grande Ronde River and 17 redds in the Imnaha River. In the Tucannon river 127 redds were counted in 2006 (Milks et al. 2009). The Lower Snake River reservoirs are not considered a spawning area due to low flows, deep water and high temperatures.

Classification accuracy of the LDFA was high for known origin fish, giving us confidence in our LDFA results. 100% of known origin juveniles were classified correctly to natal origin. Of the known origin fish classified to rearing area, 86% were classified correctly with 1 misclassification. The misclassified fish was a wild caught juvenile originating from the Clearwater River, subsequently PIT tagged, and recaptured using sort-by-code at Lower Granite Dam as a subyearling outmigrant. Its natal signature exhibited higher than expected $^{87}\text{Sr}/^{86}\text{Sr}$ when captured at Lower Granite dam, leading to misclassification.

This misclassification may be due to migration speed. If fish movement downstream is faster than the speed of Sr equilibration within its tissues then the

signature may be closer to that of a location upstream than the actual location of the fish. Bath et al. (2000) showed stable strontium signatures in marine fish within one week in controlled experiments, however juvenile salmon move quickly over large distances during periods of downstream dispersal and may not reach $^{87}\text{Sr}/^{86}\text{Sr}$ equilibrium with the waters they pass through. Despite this, the high degree of classification success in our study indicates that fish from the major spawning reaches of the Snake Basin can be successfully classified based on $^{87}\text{Sr}/^{86}\text{Sr}$ ratios within their otoliths at various life history time points.

Our results did not appear to show a yearling bias in one sex over the other. Our sample consisted of a higher proportion of female fish than males (Table 1.2), however the percentage of yearling females was approximately equal to the percentage overall for both sexes. This higher number of females is likely due to the exclusion of jack males in the spawning operations at Lyons Ferry hatchery, not to differential survival of female fish. Interestingly, Connor et al. showed a higher percentage of yearling males returning as jacks or mini-jacks as compared to subyearling males. If this were the case, the culling of jacks during spawning operations would result in a higher percentage of yearling females compared to the population as a whole. Our data does not indicate that this is the case (Table 1.2).

I. Natal Origins

Despite historically being considered solely a sub-yearling outmigrating population, a portion of the population of Snake River fall Chinook salmon have recently adopted a yearling life history and remain in freshwater over the winter before migrating to the ocean in the Spring (Connor et al. 2002; 2005). Later emergence in the cooler tributaries of the Snake is thought to create separate but overlapping outmigration groups, with the Upper Snake River producing earlier migrants and the Clearwater River the latest. Based on juvenile sampling Connor et al. (2005) concluded that adoption of the yearling life history was correlated with temperature and was likely the result of geographically distinct growth opportunity among spawning areas.

Their findings suggest that 2% of juveniles from the warmest spawning area (Upper Snake River) adopted a yearling life history compared to 53% of fish from the coolest spawning area (Lower Clearwater River). In the same study 41% of wild spawning individuals exhibited a yearling growth pattern based upon scale analysis, however the natal origin of these fish was not determined.

Our results support previous results by Connor et al. (2005) that significant differences exist in the distribution of the yearling migration strategy between spawning areas in the Snake River Basin. The results of natal origin classification indicate that the proportion of yearling juveniles in the Clearwater River is significantly higher than for the rest of the basin (Table 1.3), with 77% of Clearwater River juveniles adopting a yearling migration strategy. In contrast with Connor et al. we found 13% of juveniles from the Upper Snake River, the second important spawning area in the basin, adopted a yearling strategy.

The fact that a large number of fish were classified to Lower Snake River natal origin is somewhat surprising. It is unlikely that this represents a spawning population since reservoir habitat does not contain the elements needed for successful salmon spawning. This result is more likely due to downstream movement of fish prior to the location of analysis on the otolith, or error due to the unique biology of the otoliths core. Several studies point to the existence of a maternal strontium signature in the otolith core, however the extent of maternal influence and ontogenetic factors on microchemical signatures is debated (Bacon et al. 2004; Ruttenberg et al. 2005; Volk et al. 2000). While we attempted to exclude maternal influence by limiting analysis to 100 μ m from the otoliths core, the extent of natal influence is unknown. Some otoliths did not have a stable signature starting at 100 μ m and a later signature had to be used. A fish could be unknowingly misclassified in either of these situations, if it moved downstream prior to attaining a stable natal signature or if there was maternal influence on the signature. Further, the transition between the Upper and Lower Snake River is not abrupt, but instead is likely a gradual transition. Any fish residing in an area near the transition between the Upper and Lower Snake rivers might be mis-classified to the Lower Snake River under our classification system.

Our data indicate that the yearling migration strategy is not limited exclusively to the Clearwater River. This migration strategy was found in fish originating from all river groups in significant percentages, albeit to a lesser degree, in contrast to the much lower estimates of Connor et al. The proportion of yearling fish was highest in the coolest and latest emerging habitat (Clearwater) and lowest where emergence is earliest and temperatures are highest (Upper Snake). This supports the observations of Connor et al., that early emergence, temperature or growth opportunity seem to play a part in determining yearling behavior. Because our study was limited to returning adult fish it is possible that the representation of yearlings may be more pronounced if a higher probability of survival exists for yearling fish. The potential for this increased survival has been proposed (Williams et al. 2008), however, yearling survival is currently unknown due to difficulties in counting PIT tagged juveniles leaving the system during the winter months.

II. Rearing Location

Our ability to distinguish the Lower Snake River reservoirs from the natal tributaries allows us to understand Snake River fall Chinook salmon juvenile migration patterns with a resolution that has not previously been accomplished. Extensive tagging studies in the basin have allowed the study of fish movement on the large scale, however PIT tag detectors are located primarily at dams or in scattered low order streams within the basin. This has presented difficulties in studying smaller scale movement patterns out of the natal stream and into rearing and overwintering habitat.

Our results generally support the idea that fish move downstream to the Lower Snake River for (LSK) for rearing (Table 1.4). All upriver groups decreased in numbers, while the LSK group increased, showing 66% of the population rearing in the Lower Snake River based on LDFA classification. Fish from the Clearwater and Salmon (CWS) river group were less likely to move downstream to rear than those from the Upper Snake River (USK) with 33% of the CWS group remaining in their natal stream. This

may, however, be a result of later emergence timing rather than a sign of rearing within the Clearwater or Salmon rivers.

III. Overwintering Location

Connor et al. (2005) assumes overwintering location to be Lower Granite Reservoir on the Lower Snake River, however, the location of overwintering habitat had not been previously confirmed. Our results indicate that the majority of fall Chinook juveniles in the Snake River overwinter in the reservoirs of the lower Snake River (Table 1.5, Figure 1.7). In our study 97% of overwintering fish were classified to the Lower Snake River group based on LDFA, supporting the findings of Connor et al.

Exploratory Cluster Analysis

LDFA maintained a high classification accuracy using the sampled watersheds as a training set, however, there is the possibility that additional important groupings exist among juvenile fish in the basin. By including elemental data in a subsequent cluster analysis we attempted to explore the possibility that additional groupings exist within the data. The ratio of strontium to calcium (Sr:Ca), as well as ratios of other elemental metals, act as tracers of geographic location, with strontium substituting into the otolith matrix proportionally to local concentrations (Figure 1.13). These ratios are also under biological regulation and incorporate differences in concentration due to growth and temperature (Martin et al. 2004). The effect of temperature is of particular interest in this study due to its possible effect on Clearwater juvenile migration timing.

I. Natal Origins

Clustering of the natal life stage does not reveal additional grouping beyond that of the $^{87}\text{Sr}/^{86}\text{Sr}$ LDFA. This is likely due to the large degree of scatter within this dataset related to early movement of fish to rearing locations or maternal influence. Two large

clusters generally divide the data above and below $^{87}\text{Sr}/^{86}\text{Sr} = 0.710$ (Figure 1.10). Cluster #1 generally corresponds to the LSK and USK groups. Cluster #2 corresponds approximately to the CWS group. However, correspondence between these clusters and LDFA groupings is low. This lack of correspondence and defined clustering indicates a lack of further groupings beyond those of the LDFA analysis.

II. Rearing Location

The rearing life stage shows much tighter grouping of fish consistent with more precise location of this life stage on the otoliths (Figure 1.11). Two of the clusters correspond well to the LDFA results for this life stage, while three do not. Cluster #2 corresponds to a combination of the USK and LSK values, cluster #5 corresponds to the single fish classified to the TGI group. Clusters #1, #3, and #4 do not correspond and are of particular interest as possibly distinct rearing groups.

Cluster #3 represents a well-defined cluster which falls between the LSK and CWS groups (mean $^{87}\text{Sr}/^{86}\text{Sr} = 0.71143$). This group does, however, contain as one of its members a known origin juvenile fish from the Clearwater river (Figure 1.11). This indicates that there may be a distinct rearing area within the Clearwater River that was not included in our water sampling plans. The lower section of the Clearwater River, at the confluence with the Lower Snake River, transitions from a free-flowing river to reservoir habitat. The mixing of cooler water from the Clearwater River and warmer water from the Snake River may provide a balance of temperature regulation and feeding opportunity. Fish inhabiting this transition might be expected to exhibit a transitional chemical signature between the Clearwater and Lower Snake River, similar to cluster #3.

Clusters #1 and #4 in the rearing data are also of particular interest. These clusters contain most of the fish classified to the CWS group and split the CWS group into two smaller groups (Figure 1.11). Cluster #1 (Mean $^{87}\text{Sr}/^{86}\text{Sr} = 0.71413$, mean Sr:Ca = 1.08mmol/mol), corresponds well to the range of the Lower Clearwater River signature (Figure 1.4). Cluster #4 (Mean $^{87}\text{Sr}/^{86}\text{Sr} = 0.71299$, mean Sr:Ca =

1.43mmol/mol), also fits within the range of the Lower Clearwater signature. We might expect ontogenetic or temperature differences, perhaps correlated with out-migration timing, to create clusters based on Sr:Ca. The percentage of yearling juveniles within each cluster, however, is not significantly different between clusters #1 and #4 (Fishers exact test, $P=0.26$). Cluster #1 contains 85% yearling juveniles ($n=20$) and cluster #4 contains 65% yearling juveniles ($n=13$).

While clusters #1 and #4 do not show differences in the expression of the yearling life history, the clusters may be evidence of distinct rearing areas. The differences in Sr:Ca between the clusters could be due to locally distinct Sr concentrations, differences in growth, or other metabolic regulators of calcium concentration within these juvenile fish. Because temperature differences are one driver of Sr:Ca differences between populations it is possible that these clusters may correspond to fish exposed to different temperature regimes within the Clearwater river. If so, Sr:Ca may be useful in understanding the environmental effects of life history among fall Chinook Juveniles in future studies.

III. Overwintering Location

The clustering results of overwintering location show potentially interesting patterns in Sr:Ca in fish which were classified to the LSK group using LDFA . While the majority of these fish remained tightly clustered within cluster #1 (Figure 1.10) three fish show wider variation in Sr:Ca and were classified within cluster #3. With so few datapoints it is possible that these fish simply represent scatter within the data. If, however, distinct signatures exist within the Lower Snake River reservoirs this would be of particular interest. Further investigation is needed to determine whether differences in Sr:Ca could be used to classify overwintering location within the reservoir system.

IV. Further investigation

The results of our cluster analysis seem to indicate avenues for future investigation of rearing and overwintering behavior within the Snake River basin. In particular, determining whether clusters #1, #3 & #4 within the rearing dataset represent legitimate groups within the Clearwater or Salmon river populations offers the possibility of enhancing the spatial resolution of future studies. It is possible that these groups are geographically based, however, it is equally probable that group differences due to Sr:Ca are due to environmental or physiological differences. If the differences are environmentally driven, it may offer a link between environmental conditions and Clearwater juvenile life history, an important next step in tying migration strategy to the effects of selection. This also applies to determining the validity and provenance of cluster #3 within the overwintering dataset.

Validating the existence of these clusters within the population will require the creation of a spatially explicit baseline dataset of elemental values across the basin. This can be accomplished through sampling of juveniles within the target tributaries. The use of known origin fish as a training set would allow elemental data to be used within a multivariate LDFA analysis that may provide greater discriminatory power.

Outmigration Timing

The timing of juvenile ocean entry varied significantly between the natal tributaries of the Snake River (Table 1.2). Upper Snake River (USK) juveniles outmigrate in a strong sub-yearling pulse, at a significantly earlier time than the majority of fish from the CWS river group (Figure 1.14) according to kernel density estimates. Fish in the CWS, in contrast, appear to have two outmigration peaks, one smaller outmigration corresponding to sub-yearling ocean entry and a second, larger peak corresponding to yearling outmigration. The Lower Snake River exhibited peaks for both yearling and sub-yearling outmigration. If the LSK group is indeed made up

primarily of fish who move to rearing habitats early (between 0 μ m and 250 μ m) this would indicate yearling migration timing is not limited to late emerging populations.

Interestingly, outmigration overall did not take place in discrete events, with one peak in late summer and another the following spring, as expected. (Figure 1.15) Outmigration continued through the winter months at a somewhat lower level, with the highest density of outmigrants occurring in two periods presumably corresponding to late summer and spring. The estimated mean ocean entry size of yearlings (186mm FL \pm 35mm) corresponds roughly with the sizes (222mm-224mm) reported at Lower Granite dam in Spring (Connor et al. 2005), indicating that the second density peak of outmigrants corresponds to a spring outmigration pulse. Similarly, the estimate of subyearling outmigration size (129mm FL \pm 39mm) corresponds well to fork length from the Connor study (112mm-139mm). Still, the second highest ocean entry density (Figure 1.15) occurred near 900 μ m (168mm FL), approximately halfway between the subyearling and yearling outmigration pulses. This indicates larger numbers of juveniles may be out-migrating during the winter than has been previously thought.

The movement of smolts to the ocean during winter months poses problems for estimating survival within the population. Estimates of the percentage of smolts surviving to return as adults is based on the number of out-migrating juveniles passing through the juvenile bypass system at Lower Granite dam each year. This facility closes in October (Connor et al. 2005) and winter passage of fish is not counted, resulting in error in survival estimates for the population. Our study indicates that a large proportion of yearling fish may be passing downstream during the winter months. If this is the case then a robust method of determining winter juvenile outmigration is required before survival estimates can be considered reliable for the Snake River fall Chinook population.

Effects of Environmental Change

Pacific Salmon have survived and thrived in a dynamic and changing environment for much of their history (Waples et al. 2008). Population declines due to anthropogenic changes, however, may indicate that salmon do not have the evolutionary plasticity to overcome these recent changes. Waples et al. (2009) suggest that restoration efforts should seek to shape current anthropogenic disturbance regimes in ways which more closely mimic those experienced historically by salmon. The case of fall Chinook Salmon, however, showcases the complexity of attempting to manage disturbance.

fall Chinook have been relegated to a small fraction of their former range, including areas that are cooler than their historic spawning areas. Cool outflows from Dworshak Reservoir, used to provide temperature refugia in the downstream reservoirs and increase smolt survival, further cool the Lower Clearwater River spawning area. This study, however, confirms previous findings indicating that the cooler temperatures and later hatch dates in the Clearwater may have resulted in changes to the out-migration strategy of the population. Absolute estimates of survival differences are currently unknown, however Williams et al (2008) indicates that survival may be greater for yearling migrants. If this is the case it would indicate a wider ability to adapt to the environmental changes of hydropower than has been observed previously in Pacific Salmon populations, complicating the conclusions of Waples et al. (2009) for Snake River fall Chinook Salmon.

Understanding the causes of the recent population shift in juvenile Snake River fall Chinook salmon is dependent on a better understanding of the timing and growth of juveniles as they complete their seaward migration. This study shows that $^{87}\text{Sr}/^{86}\text{Sr}$ microchemistry and the temporally explicit growth of otoliths can be used to examine differences in timing of key migration stages with temporal and spatial accuracy. Using this technique we have confirmed the geographic and temporal differences in migration timing shown earlier by Connor et al. We have also shown that the majority of fish overwinter in the Lower Snake River reservoirs as predicted.

Increased spatial and temporal precision of otolith microchemical investigations may be possible using $^{87}\text{Sr}/^{86}\text{Sr}$ in combination with other elemental signatures within the otolith, or with improved baseline sampling of water signatures. Further progress, however, hinges on a greater understanding of temporally explicit growth of juvenile fish and better estimates of their survival.

Juvenile salmon grow at different rates during different periods of their life. Without a detailed understanding growth rate and otolith ring deposition across life stages, otolith measurements from adult fish cannot be placed explicitly in time. By understanding their growth rate, linked with their location and migration timing, we can begin to make specific predictions about selective pressures experienced by juveniles in different spawning reaches of this or other river systems. Finally, better estimates of juvenile survival are needed. To understand the benefits of the yearling migration strategy, and its effect on the Snake River fall Chinook population as a whole, the robust methods to estimate the survival of yearling juveniles must be developed.

Tables

Table 1.1

Water sample $^{87}\text{Sr}/^{86}\text{Sr}$ data for the Snake River basin 2008-2009 shows variation between tributaries and major reaches of the Snake River.

River Group	Standard Site Name And Map Number	Sample #	Sampling Period	$^{87}\text{Sr}/^{86}\text{Sr}$	Site Average	River Group Average
USK	1. U. Snake (Pittsburg Landing)	BK-2008-34	Fall 2008	0.708585±12	0.708685±12	0.708685±12
		BK-2009-28	Spring 2009	0.708704±10		
		BK-2009-47	Summer 2009	0.708810±12		
		BK-2009-33	Fall 2009	0.708639±12		
CWS	2. Salmon River	BK-2008-35	Fall 2008	0.713765±14	0.713318±14	0.713308±14
		BK-2009-24	Spring 2009	0.712534±12		
		BK-2009-48	Summer 2009	0.712928±14		
		BK-2009-35	Fall 2009	0.713682±16		
		BK-2009-35*	Fall 2009	0.713682±16		
3. L. Clearwater (Below North Fork)	3. L. Clearwater (Below North Fork)	BK-2009-41	Summer 2009	0.714726±14	0.713809±14	
		BK-2009-38	Fall 2009	0.713782±14		
4. L. Clearwater (Lapwai Creek)	4. L. Clearwater (Lapwai Creek)	BK-2008-37	Fall 2008	0.713338±14		
		BK-2009-25	Spring 2009	0.712713±12		
		BK-2009-46	Summer 2009	0.714723±16		
		BK-2009-30	Fall 2009	0.713570±12		
5. U. Clearwater (Orofino)	5. U. Clearwater (Orofino)	BK-2008-36	Fall 2008	0.712266±14	0.712292±13	
		BK-2009-50	Summer 2009	0.712315±14		
		BK-2009-37	Fall 2009	0.712294±12		
LSK	6. L. Snake (Lewiston)	BK-2008-39	Fall 2008	0.709651±12	0.709677±12	0.709699±12
		BK-2009-29	Fall 2009	0.709703±12		
	7. L. Snake (Chief Timothy)	7. L. Snake (Chief Timothy)	BK-2008-38	Fall 2008	0.709746±14	0.709781±12
BK-2009-27			Spring 2009	0.709655±10		
BK-2009-49			Summer 2009	0.709874±12		

		Bk-2009-31	Fall 2009	0.709849±12		

	8. Lyons Ferry					
	Hatchery	BK-2008-44	Fall 2008	0.709659±14	0.709659±14	

	9. L. Snake	BK-2008-43	Fall 2008	0.709701±12	0.709576±12	
	(Lyons Ferry)	Bk-2009-32	Fall 2009	0.709450±12		

**	10. Palouse	BK-2008-41	Fall 2008	0.709684±12	0.709225±12	0.709225±12
		BK-2009-23	Spring 2009	0.708836±10		
		BK-2009-53	Summer 2009	0.709023±14		
		BK-2009-40	Fall 2009	0.709357±12		

TGI	11. Grand Ronde	BK-2008-40	Fall 2008	0.706588±12	0.706488±15	0.70681±13
		BK-2009-51	Summer 2009	0.706300±20		
		BK-2009-34	Fall 2009	0.706575±12		

	12. Imnaha	BK-2009-36	Fall 2009	0.707136±10	0.707204±12	
	(Cow Creek)	BK-2009-36*	Fall 2009	0.707137±14		
	13. Imnaha (Imnaha, OR)	BK-2009-45	Fall 2009	0.707340±12		

	14. Tucannon	BK-2008-42	Fall 2008	0.706845±12	0.706756±14	
		BK-2009-26	Spring 2009	0.706565±12		
		BK-2009-52	Summer 2009	0.706782±16		
		BK-2009-39	Fall 2009	0.706833±14		

Error is expressed as ± 2 SE from the mean, based upon 150-200 TIMS ratios.

Bold lines enclose sample points which were not significantly different (ANOVA, Tukey's HSD, $\alpha=0.05$)

Dotted Lines enclose major reaches

* Indicates duplicate TIMS analysis.

** The Palouse River was excluded from final LDFA analysis.

Table 1.2

Summary statistics of adult fall Chinook sampled for the study. All fish were first determined to be yearling or sub-yearling based on scale analysis. The percentage of agreement between otoliths and scale analysis is listed below. Otolith yearling determination was used for all further analysis in this study. Fish were captured between 2006 and 2008 at Lower Granite Dam and sampled as a part of hatchery spawning operations at Lyons Ferry Hatchery.

Summary Statistics

Year	Sample Size	Mean Age	% Female	%	%	%
				Yearling Female	Yearling	Otolith/Scale Agree
2006	15	4.3	100	67	67	87
2007	38	3.7	42	63	66	80
2008	67	4.0	72	60	57	75
Overall	120	4.0	66	62	62	78

Table 1.3

Significant differences in representation of the yearling life history types are shown between natal source river groups of adult fall Chinook salmon captured at Lower Granite Dam (2006-2008). The yearling life history strategy is significantly more abundant in the Clearwater and Salmon river group. Ocean entry timing is also significantly later in the Clearwater and Salmon river group. LDFA was used to group fish to source river group based upon $^{87}/^{86}\text{Sr}$ ratio area of the otoliths corresponding to rearing. Juvenile validation samples consisted of juvenile fish of known origin (Wild=7, Hatchery=9) and were used to test the classification. Ocean entry was measured as the distance from the core of the otoliths to the onset of the global ocean signature ($^{87}\text{Sr}/^{86}\text{Sr} = 0.70918$) and characteristic spike in Sr concentration.

Natal Origin

Source River Groupings	Natal Origin (%)	Sub-Yearling	Yearling (%)	Juvenile		% Yearling Female	Ocean Entry μm
				Validation Samples	% Female		
Grande Ronde, Imnaha, Tucannon	2 (2)	1	1 (50)	0	100	100	986
Clearwater, Salmon	44 (37)	10	34 (77) [◇]	1 [*]	71	74	915 [†]
Lower Snake	58 (48)	22	36 (62)	10 [*]	55	58	888 [‡]
Upper Snake	16 (13)	12	2 (13) ^{◇**}	3 [*]	37	100	727 ^{†,‡}
Total Sample Size	120	45	71 (61)	14			879

** Yearling signatures for two fish were unrecoverable and were excluded from yearling analysis.

* indicates successful classification to known source river group.

†,‡ indicates groups are significantly different (ANOVA, Tukey's HSD, $\alpha=0.05$)

◇ indicates yearling proportion is significantly different from the rest of the basin (Fishers Exact Test, $\alpha=0.05$)

Table 1.4

The majority of juvenile fish rear in the Lower Snake River reservoirs. Rearing location representation between source river groups are shown for adult fall Chinook salmon captured at Lower Granite Dam (2006-2008). LDFA was used to group fish to source river group based upon $^{87/86}\text{Sr}$ ratio of the area of the otoliths corresponding to rearing. Juvenile validation samples consisted of juvenile fish of known origin (Wild=7) and were used to test the classification.

Rearing Location

Source River Groupings	Rearing			Juvenile		%
	Location (%)	Sub-Yearling	Yearling (%)	Validation Samples	% Female	Yearling Female
Grande Ronde, Imnaha, Tucannon	1 (1)	1	0	0	0	0
Clearwater, Salmon	37 (31)	9	28 (76)	1	61	61
Lower Snake	78 (66)	33	45 (58)**	6*	65	71
Upper Snake	2 (2)	2	0	0	-	-
Total Sample Size	120	45	73 (62)	7		

** Yearling signatures for two samples were unrecoverable and were excluded from yearling analysis

* indicates successful classification to known source river group.

Table 1.5

The majority of Snake River fall Chinook salmon juveniles overwinter in the Lower Snake River reservoirs. Overwintering location for adult fall Chinook salmon captured at Lower Granite Dam (2006-2008) is shown separated by source river groups. LDFA was used to group fish to source river group based upon $^{87}/^{86}\text{Sr}$ ratio of the area of the otolith corresponding to overwintering.

Overwintering Location

Source River Groupings	Overwintering	
	Location (%)	% Female
Grande Ronde, Imnaha, Tucannon	0	-
Clearwater, Salmon	2 (3)	50
Lower Snake	72 (97)	68
Upper Snake	0	-
Total Sample Size	74	

Figures

Figure 1.1

The range of fall Chinook salmon in the Snake river extends from the mouth of the Snake River to Hells Canyon Dam, with spawning occurring in the upper reaches and major tributaries. Gray highlighting indicates the extent of fall Chinook Salmon spawning in the basin. Diamonds represent locations of hydropower dams. Crosshatching indicates watershed above the impassable Hells Canyon Dam on the Snake River. Numbered circles indicate locations of baseline water samples. The full extent of the Snake River watershed is shown in gray (inset)

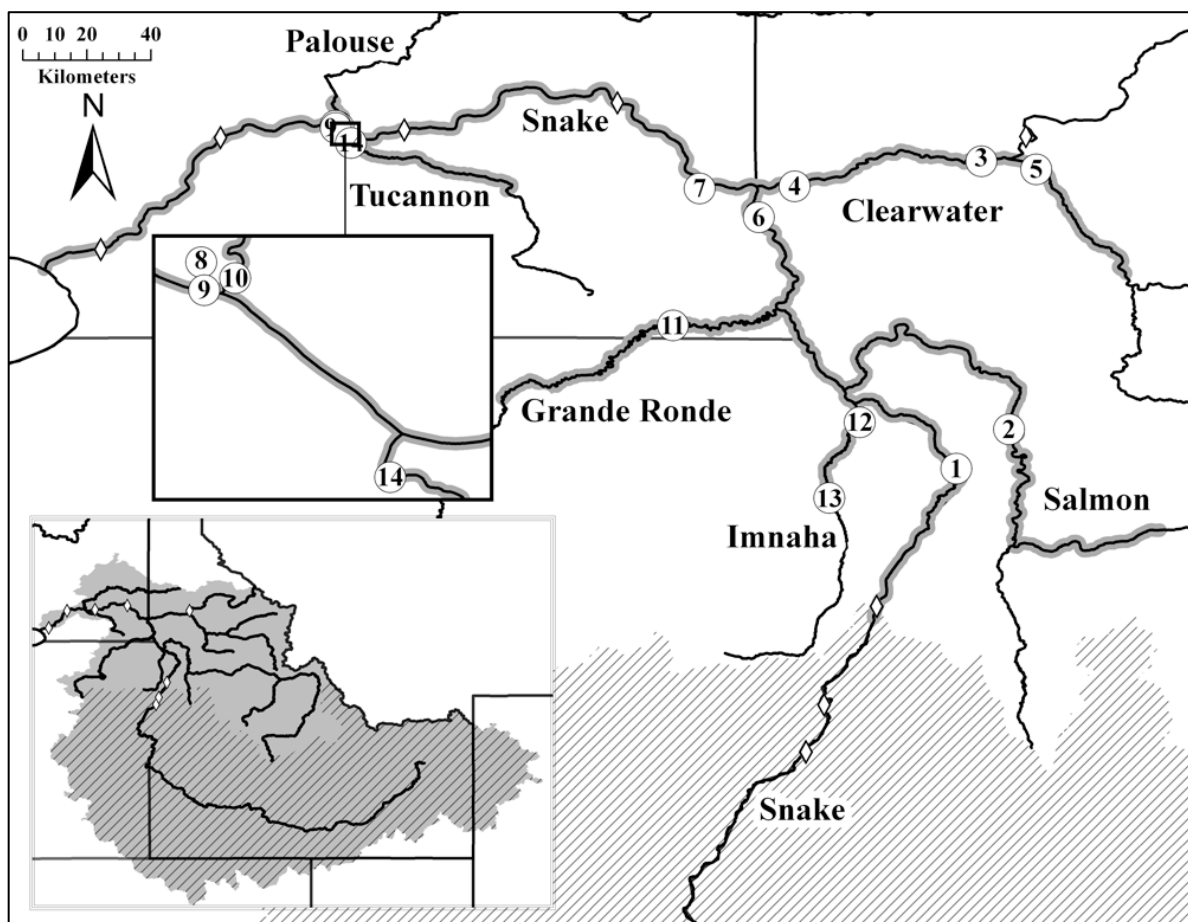


Figure 1.2

The Snake River watershed is influenced by three major geologic features, the Idaho Batholith (North Central, felsic), the Snake River Plain (South East, mafic) and the Columbia river basalts (Western, mafic). Map shows Lithology of the Snake River watershed showing rock type categories with strong impacts on $^{87}/^{86}\text{Sr}$. Rock types have been classified primarily into rocks with origins in the mantle (Mafic) and rocks of crustal origin (Felsic) which strongly influence $^{87}/^{86}\text{Sr}$ due to their differing isotopic chemistry. Metamorphic rocks of known protolith were grouped by protolith. Metamorphic rocks of unknown protolith were classified to the Metamorphic category.

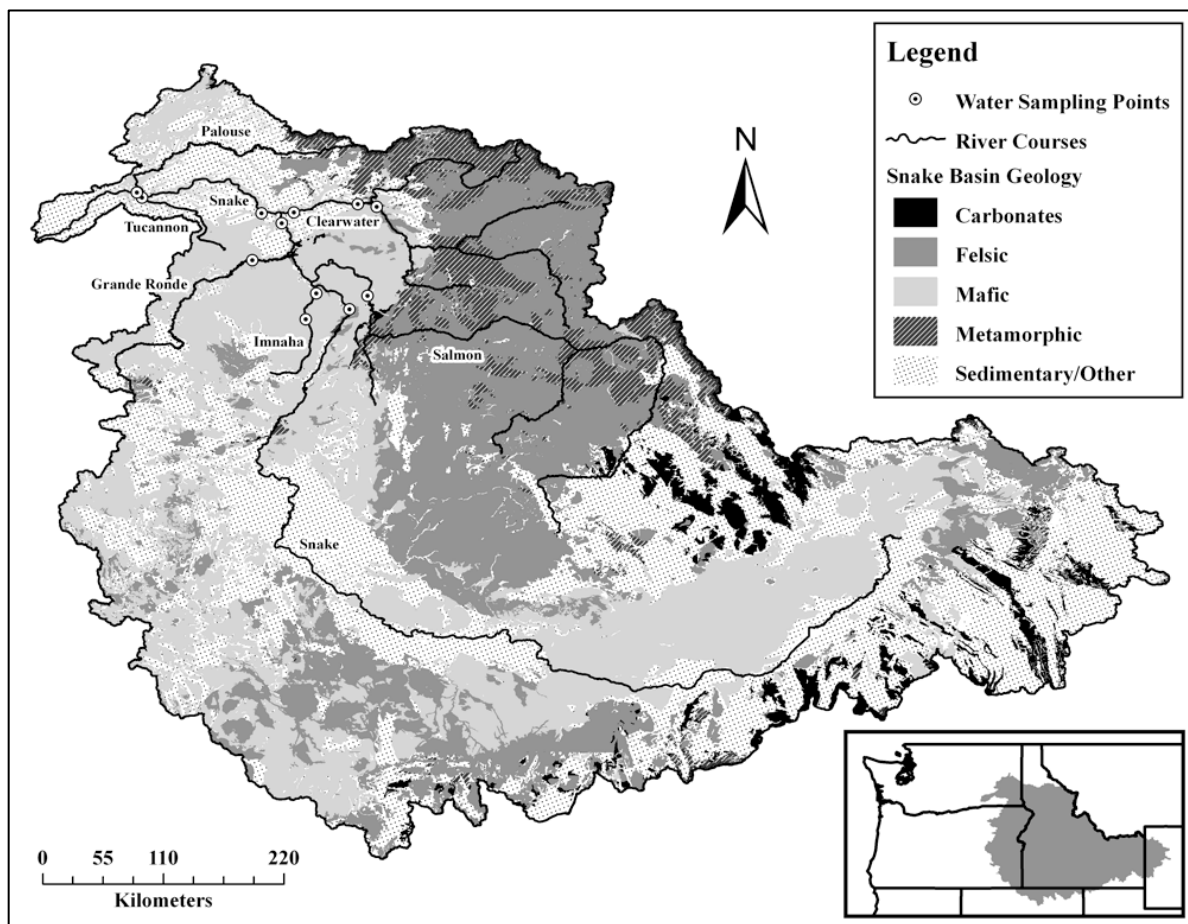


Figure 1.3

All analysis was performed on the dorsal section of the otoliths as shown. Laser ablation transects (**A**) were performed at 90° to the sulcus, recording $^{87}/^{86}\text{Sr}$ variation from the core to the rim. Ablation paths along rings (**B**) were used to determine more precise estimates of stable signatures. Error for **A** (fine dotted lines) and **B** expressed as ± 2 times standard error (fine dotted lines). Error bars for **B** are much smaller than the marker. Strontium intensity (dotted line) and convergence to the global marine signature (dashed line) were used to determine ocean entry.

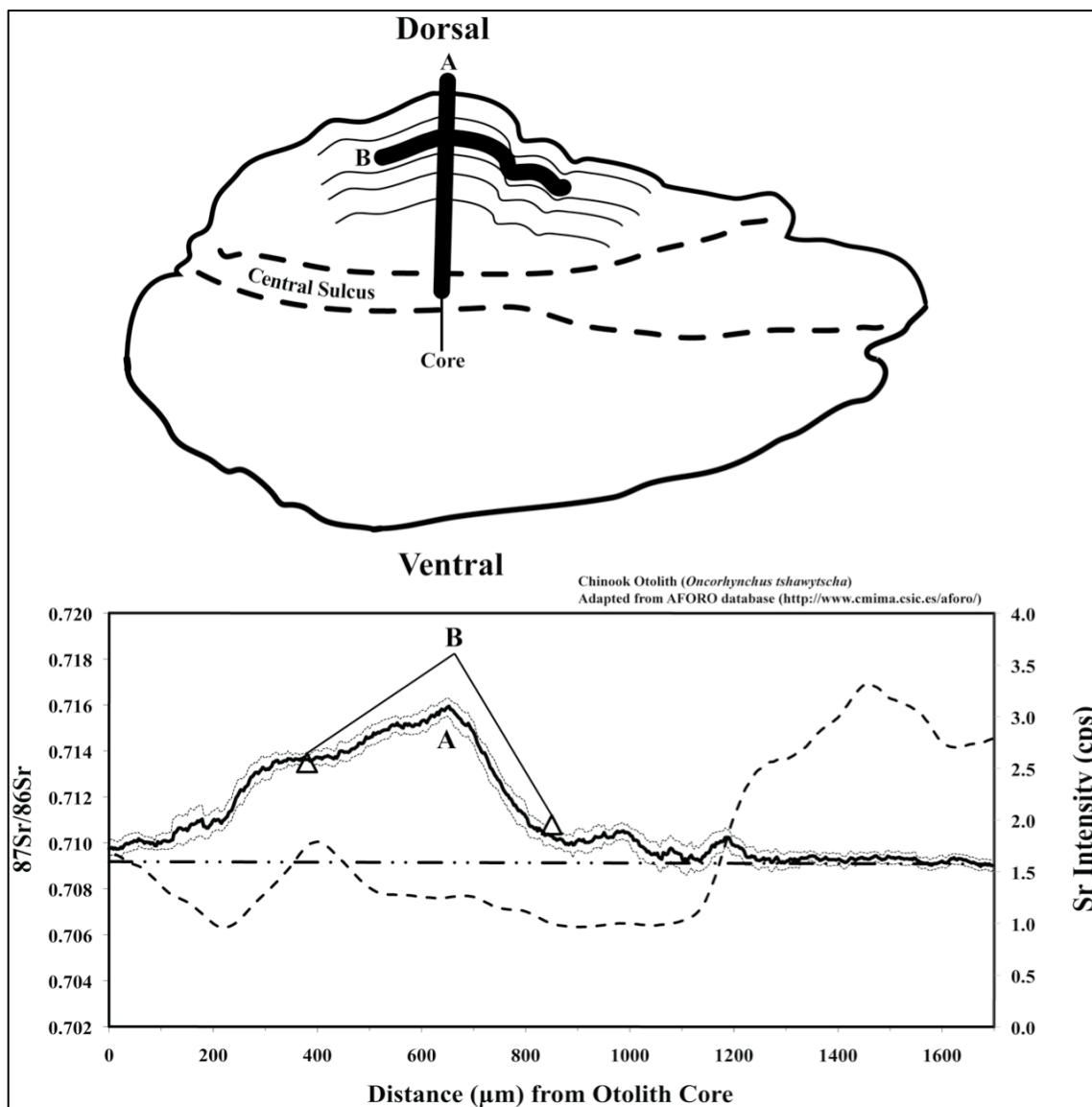


Figure 1.4

Strontium ratio ($^{87}\text{Sr}/^{86}\text{Sr}$) varies within the major spawning reaches of the Snake River basin. Mean and 1st quartile boxes are shown for each group of individual sample points (●).

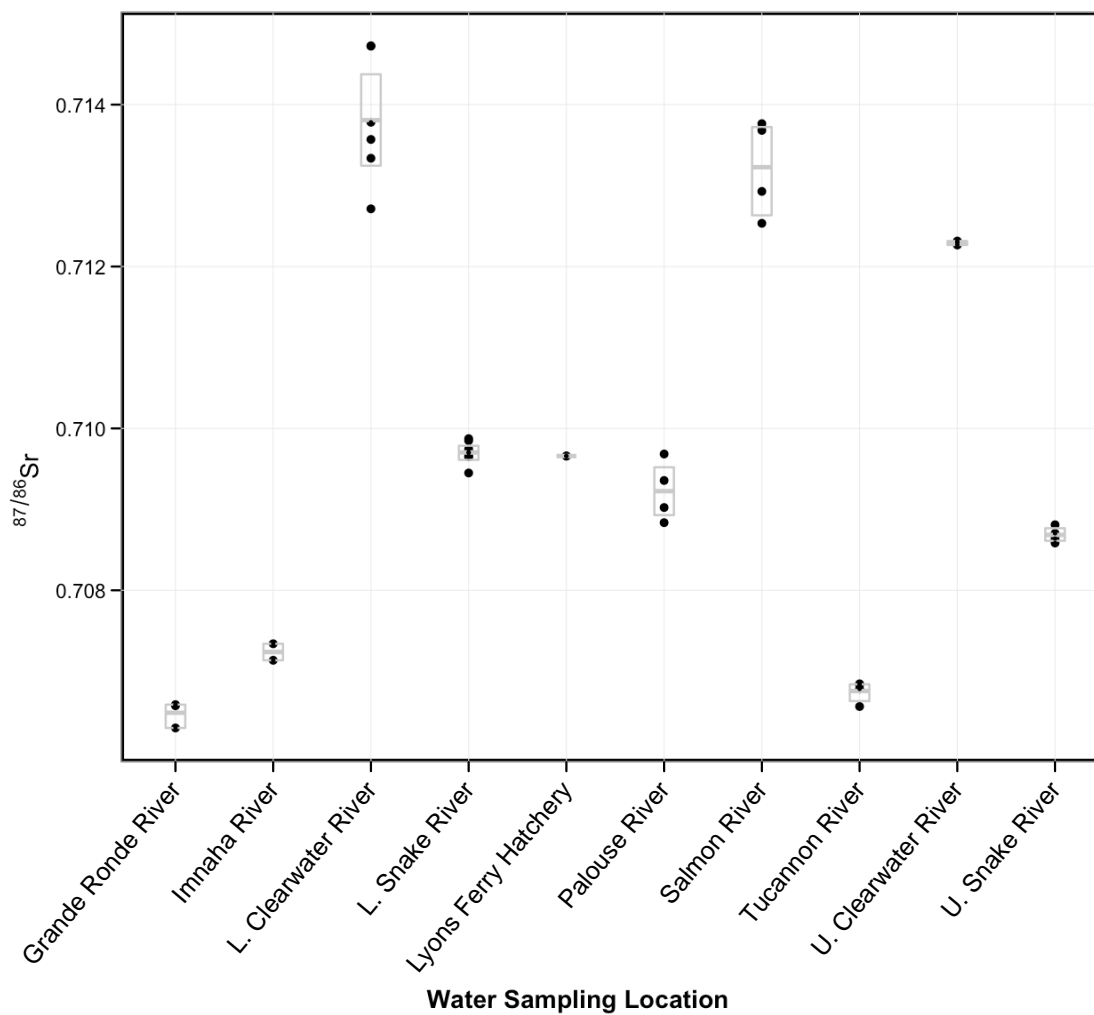


Figure 1.5

Results of natal origin LDA classification for 120 wild adult fall Chinook Salmon (filled shapes) and 14 known origin juveniles (open shapes). Classification accuracy for known origin samples was 100%. Open squares with crosses through the center are hatchery yearlings from Lyons Ferry Hatchery. Points are jittered on the x-axis to avoid overplotting.

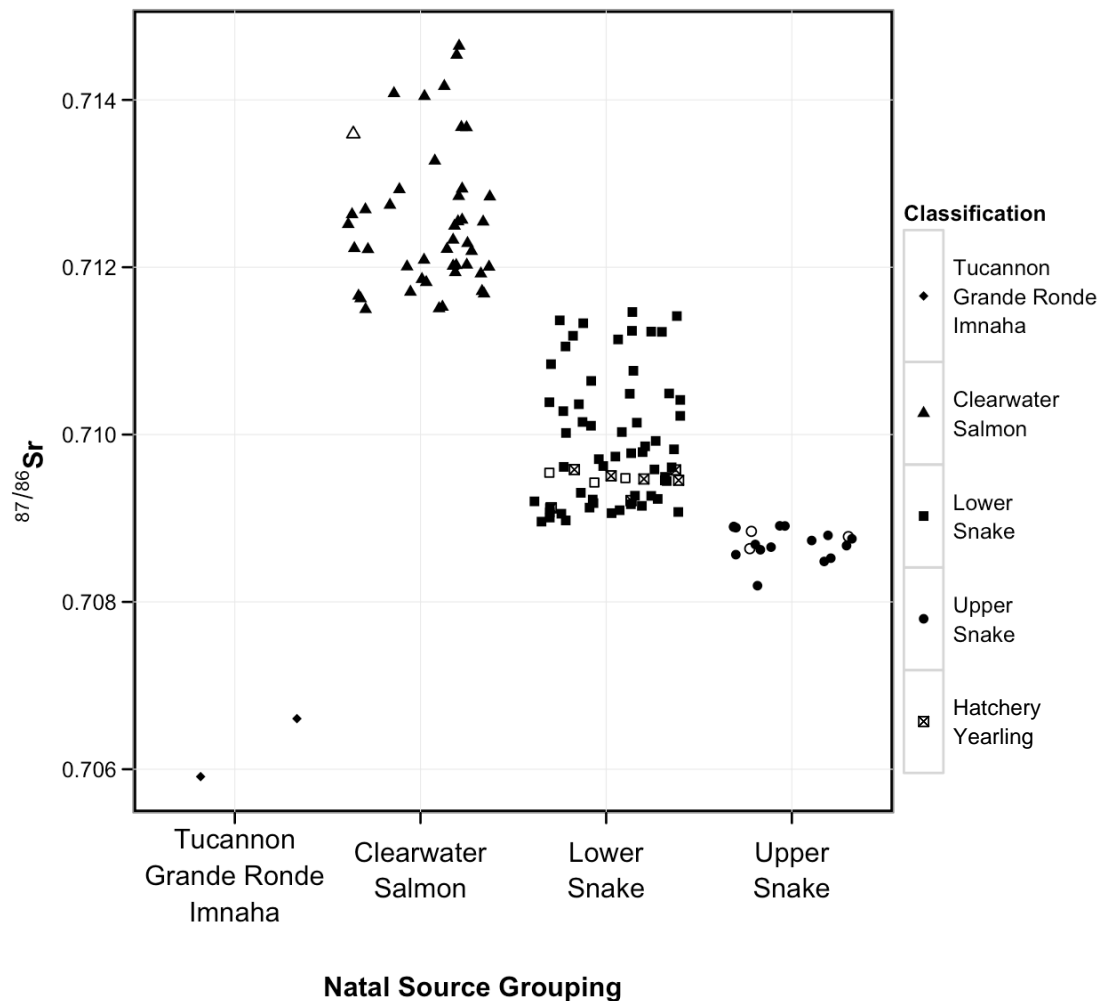


Figure 1.6

Results of rearing location LDA classification for 120 wild adult fall Chinook Salmon (black points) and 7 known origin juveniles (grey points) show distinct grouping between source river groups. Six known origin samples were correctly classified (86%). One juvenile captured at Lower Granite Dam during outmigration, but originally PIT tagged in the Clearwater River, was mis-classified to the Clearwater Salmon river group rather than its location of capture. Points are jittered on the x-axis to avoid overplotting.

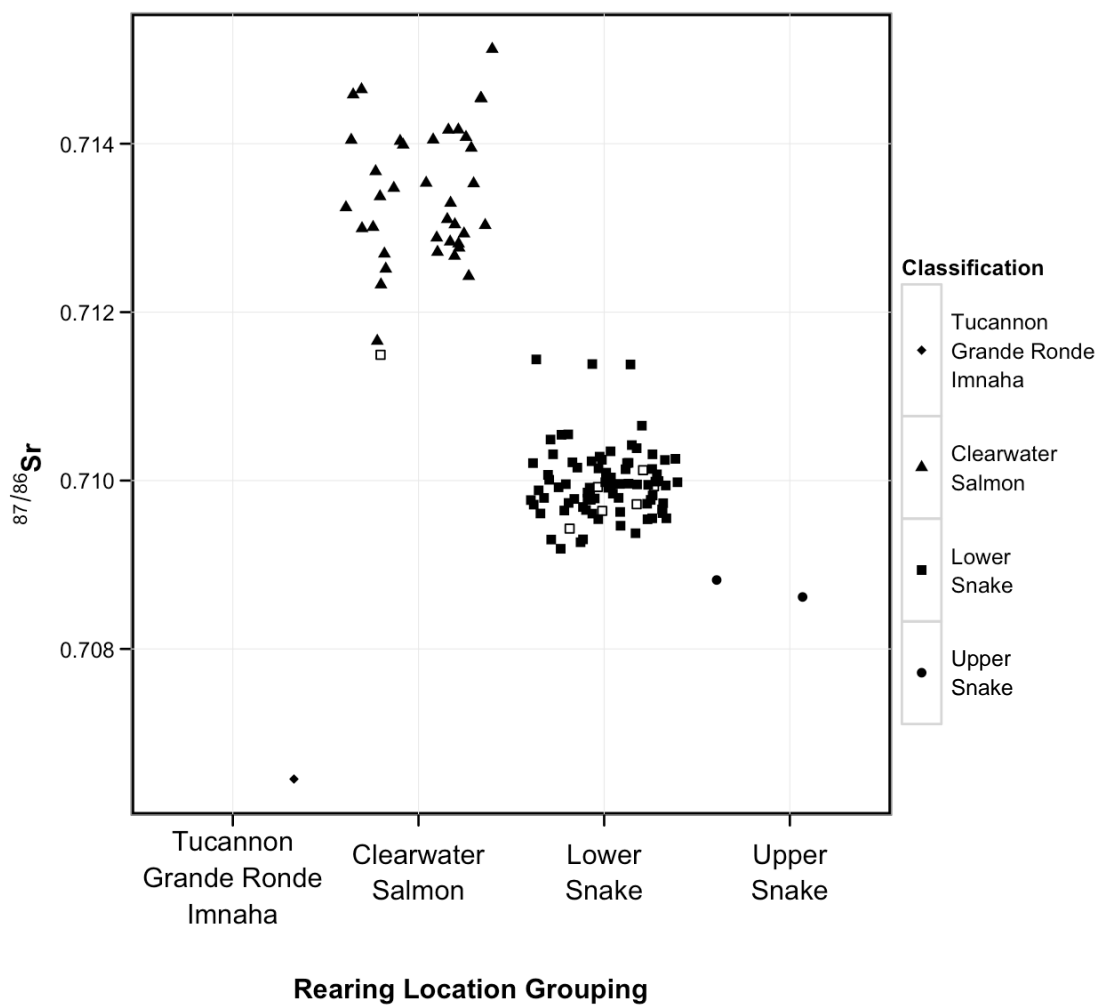


Figure 1.7

Results of overwintering location LDA classification for 74 wild adult fall Chinook Salmon show the majority of overwintering juveniles residing in the Lower Snake River reservoirs. Points are jittered on the x-axis to avoid overplotting.

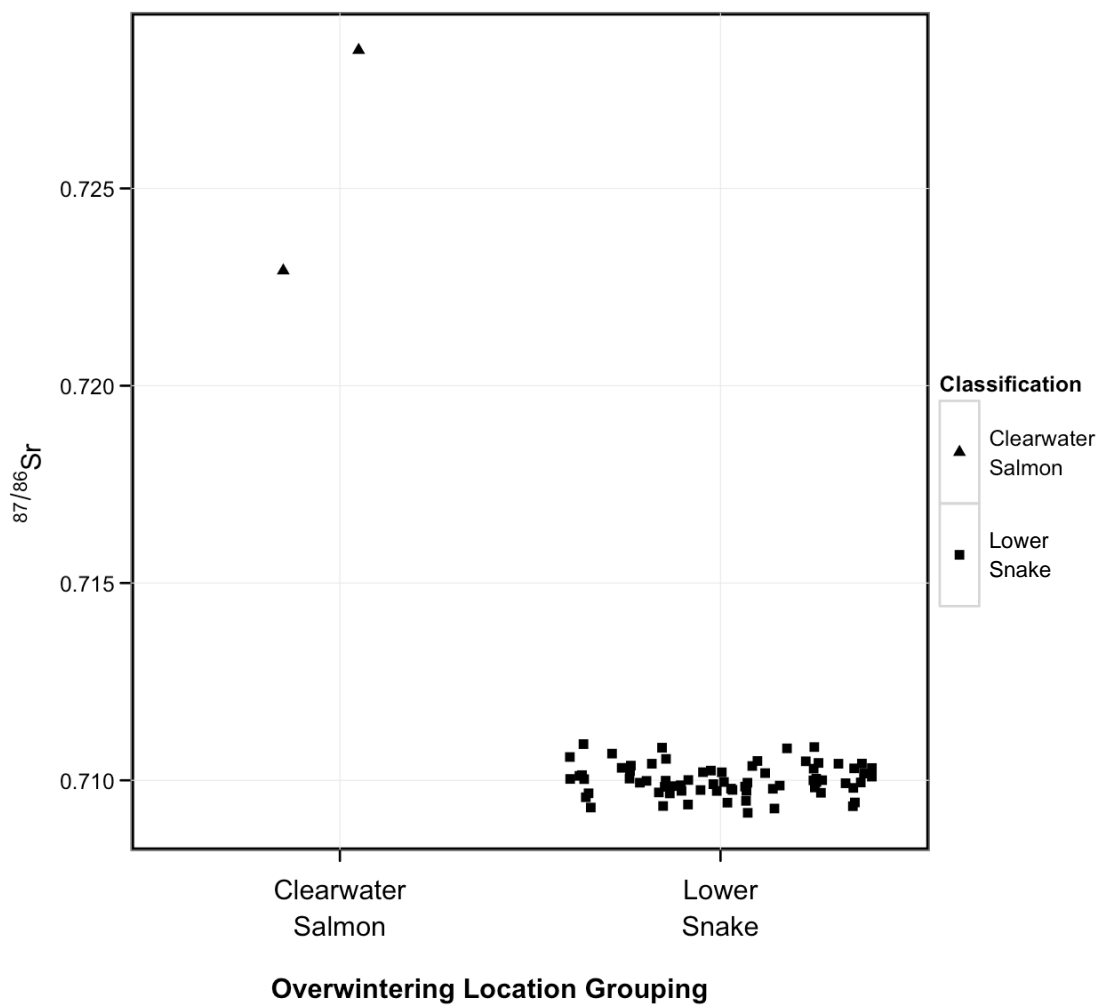


Figure 1.8

Model based cluster solution for the natal life stage shows indistinct clustering and a lack of additional chemically distinct groups beyond those of determined using LDFA. Shape indicates cluster association. Ellipses indicate cluster shape, orientation and 50% quartile for the multivariate distribution. Numbered gray circles indicate cluster centers.

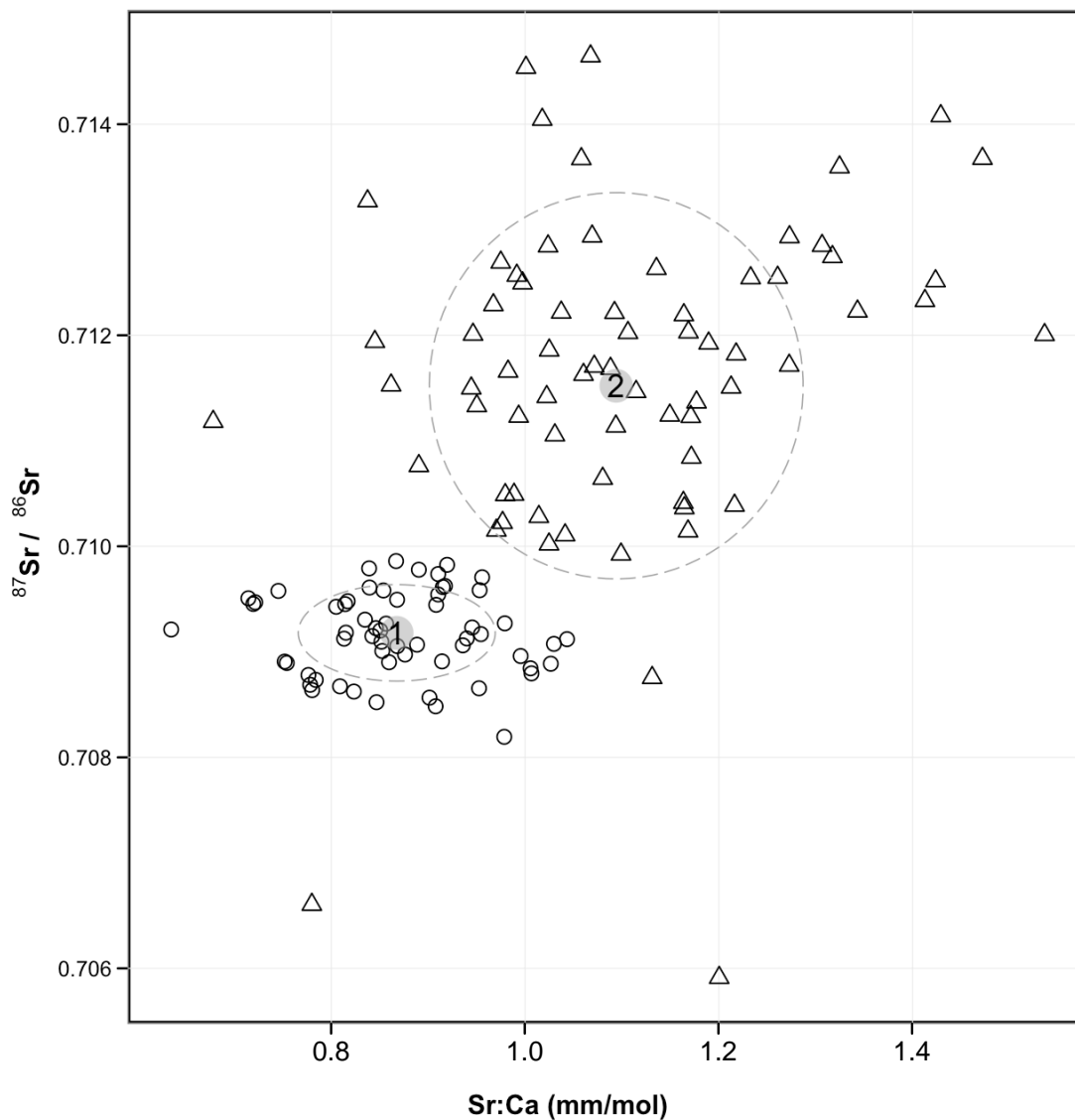


Figure 1.9

Plot of the model based cluster solution for the rearing life stage shows additional chemically distinct clusters (#1, #3 and #4) beyond those from LDFA. Shape indicates cluster association. Ellipses indicate cluster shape, orientation and 50% quartile for the multivariate distribution. Numbered gray circles indicate cluster centers.

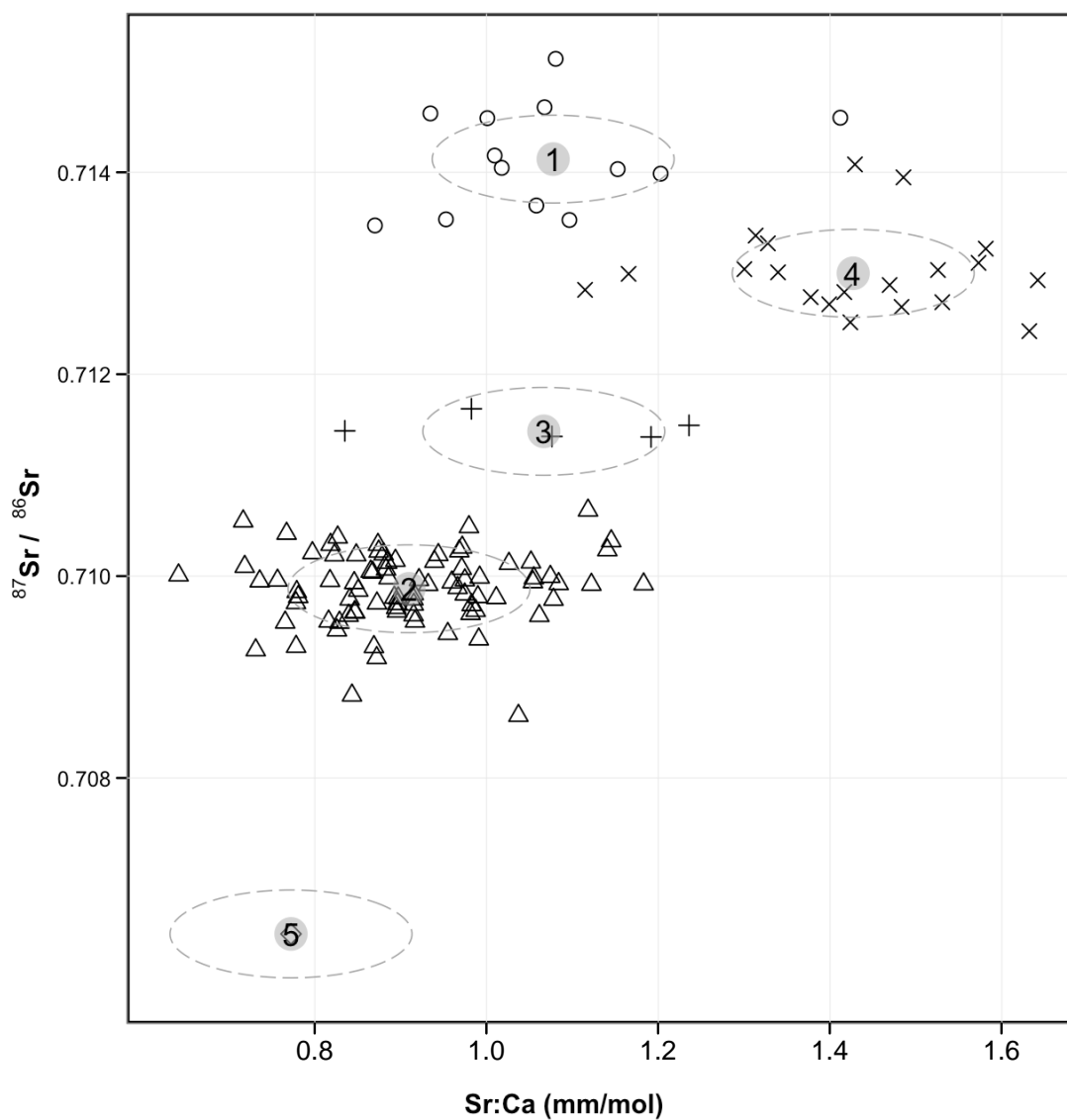


Figure 1.10

Plot of model based cluster solution for overwintering life stage shows the possibility of chemically distinct clusters (#1 & #3) within the Lower Snake River river group determined using LDFA. Shape indicates cluster association. Ellipses indicate cluster shape, orientation and 50% quartile for the multivariate distribution. Numbered gray circles indicate cluster centers.

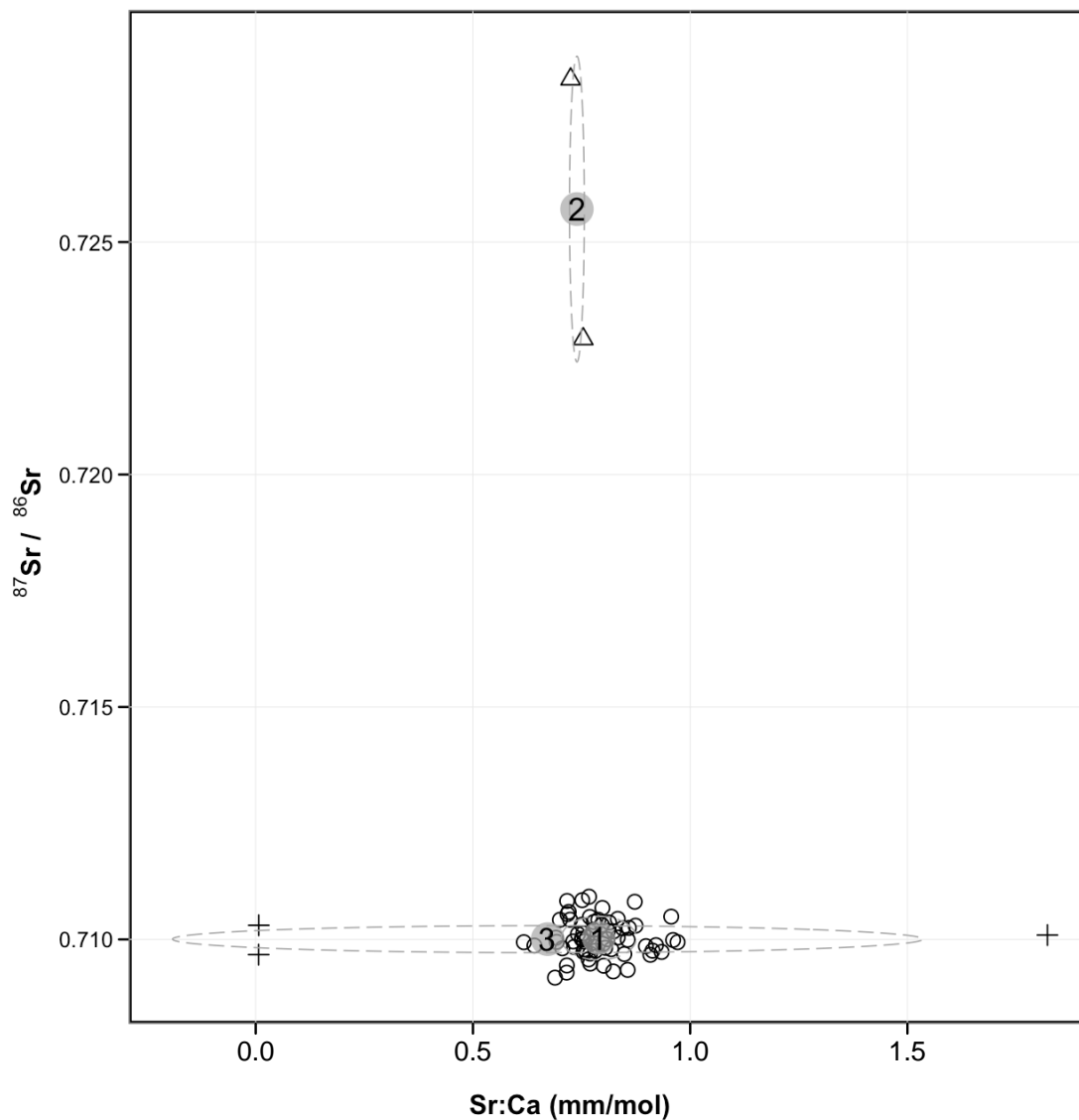


Figure 1.11

Plot of Lower Clearwater discharge showing the increase in $^{87}/^{86}\text{Sr}$ with increasing outflows from the North Fork Clearwater River during near baseflow (●) and subsequent drops during high spring flows (○).

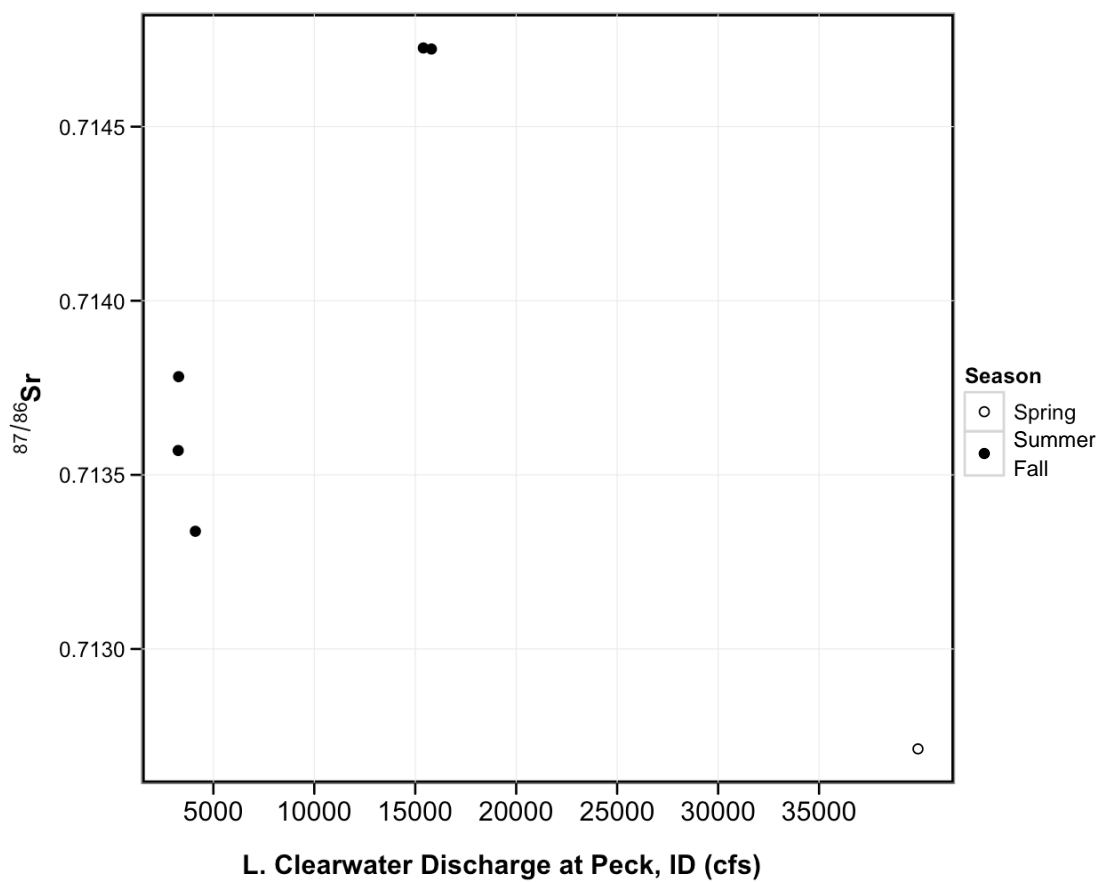


Figure 1.12

Plot showing the similar temporal variation of $^{87/86}\text{Sr}$ observed for both the Lower Clearwater (\blacktriangle) and Salmon (\bullet) Rivers. In contrast the Upper Clearwater (\diamond) shows very little variation. The increased $^{87/86}\text{Sr}$ due to the onset of flow augmentation from Dworshak reservoir can be clearly seen in the $^{87/86}\text{Sr}$ signature of the Lower Clearwater during July, 2009.

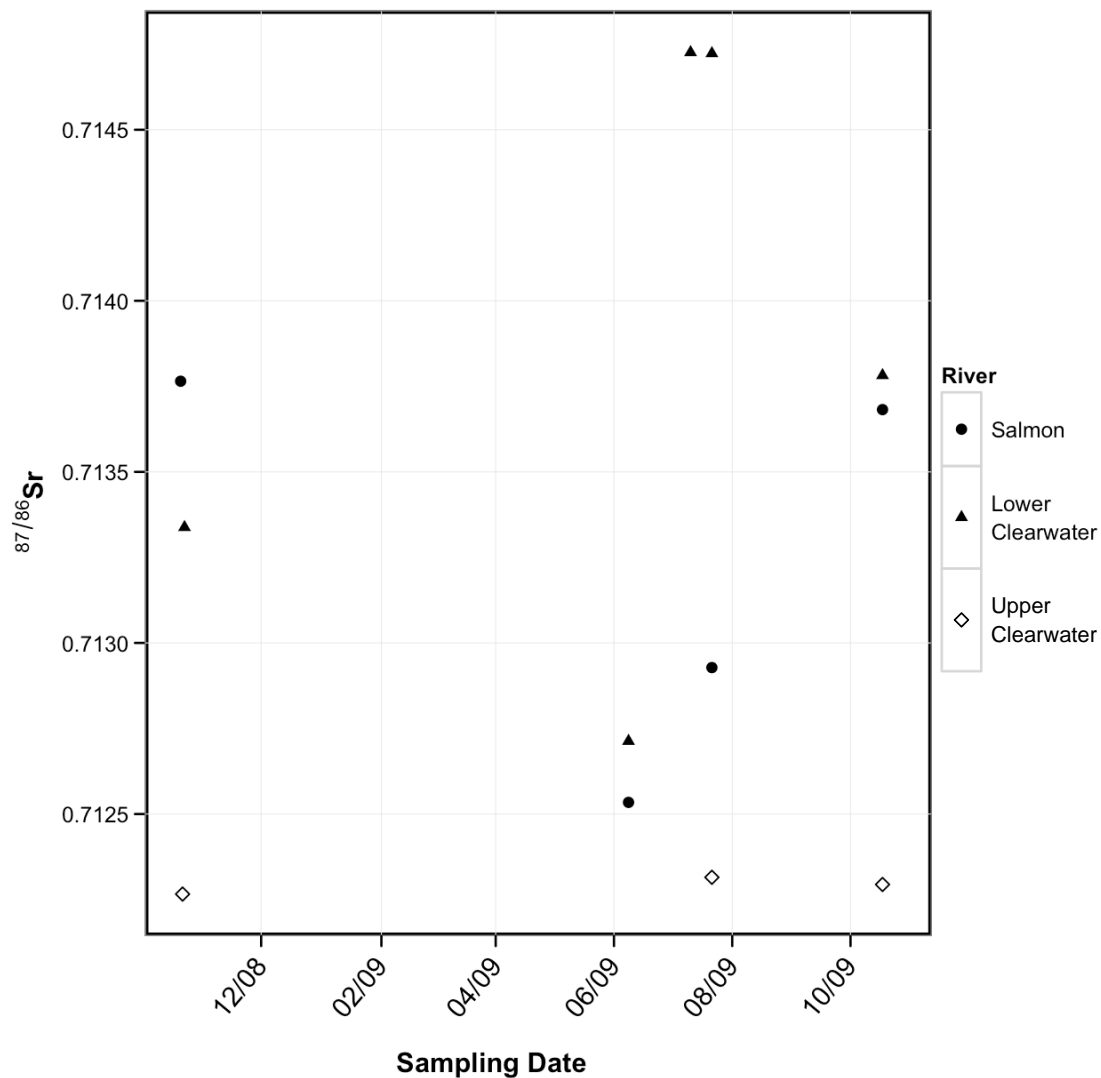


Figure 1.13

Plot showing the linear relationship of Sr:Ca with $^{87}\text{Sr}/^{86}\text{Sr}$ in water and otoliths. Water data is shown as black points, otolith data as grey points. The offset between water points and otoliths points is due to the physiological regulation of calcium within the otoliths. Lines indicate best fit linear regression for the corresponding data. Otolith values follow a similar linear trend to water values, however, indicating Sr:Ca is a tracer of geographic location in this system.

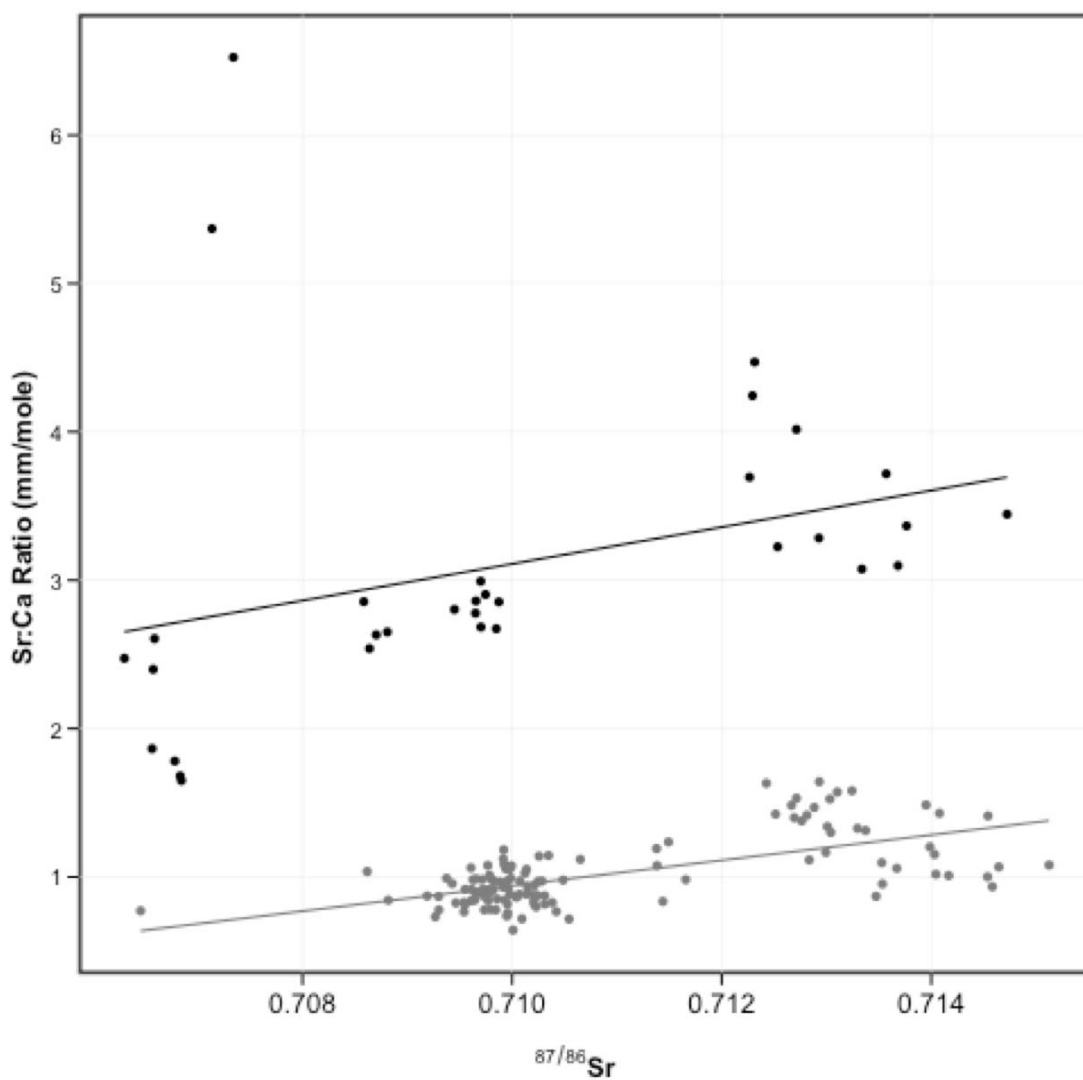


Figure 1.14

Kernel density plot of outmigration timing for each natal river group. Density peaks illustrate that Upper Snake River juveniles out-migrate over a short interval and at an earlier date than the other groups. In contrast, fish from the Clearwater and Salmon River group out-migrate over a longer period with a majority of yearling migrants and a smaller number of sub-yearlings. The Lower Snake River shows two outmigration peaks, however early movement or maternal $^{87}\text{Sr}/^{86}\text{Sr}$ signatures may complicate the interpretation of outmigration timing in this river group. The Tucannon, Grande Ronde and Imnaha River group is not visible due to low sample sizes.

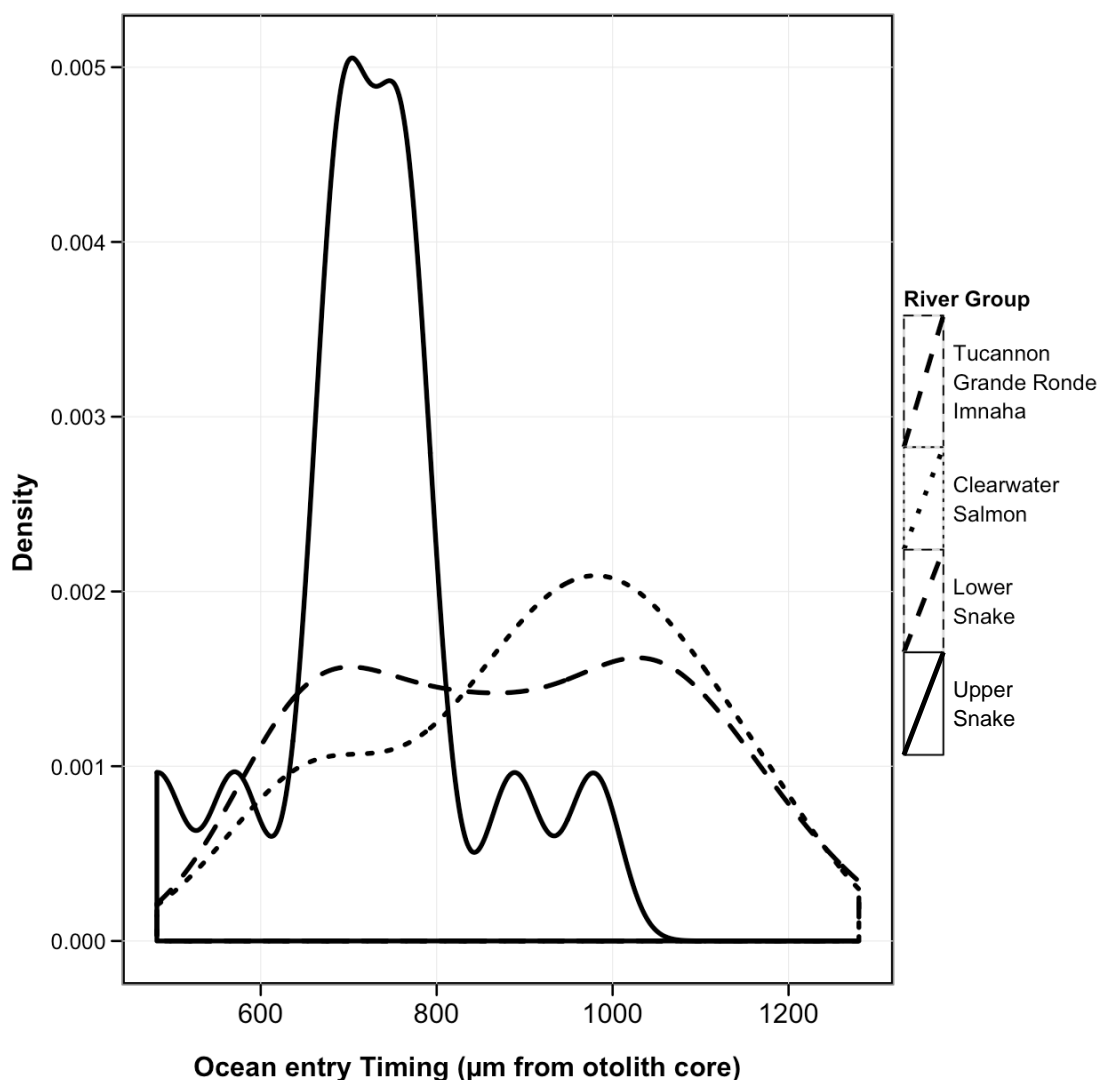
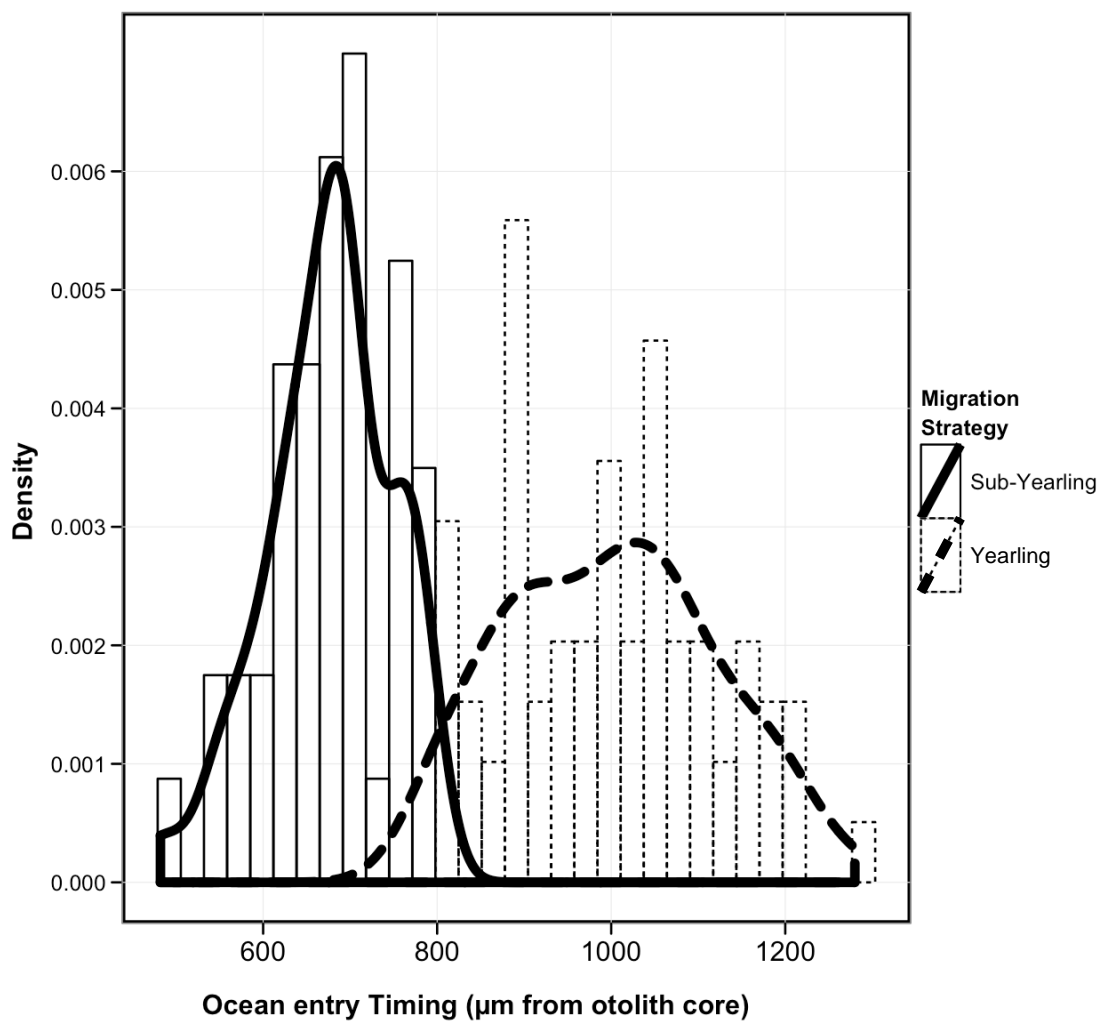


Figure 1.15

Histogram and kernel density estimates of outmigration timing for yearling and sub-yearling fall Chinook salmon from all spawning areas of the Snake River. Peaks indicate two distinct peaks of outmigration corresponding to sub-yearling and yearling outmigration, however high densities of out-migrants occur throughout, indicating that many fish out-migrate during the winter, complicating survival estimates for Snake River fall Chinook salmon.



References Cited (Chapter 1)

- Able KP, Belthoff JR (1998) Rapid evolution of migratory behaviour in the introduced house finch of eastern North America. *Proceedings of the Royal Society of London. Series B: Biological Sciences* 265:2063
- Bacon C, Weber P, Larsen K, Reisenbichler R, Fitzpatrick J, Wooden J (2004) Migration and rearing histories of chinook salmon (*Oncorhynchus tshawytscha*) determined by ion microprobe Sr isotope and Sr/Ca transects of otoliths. *Canadian Journal of Fisheries and Aquatic Sciences* 61:2425-2439
- Bain D, Bacon J (1994) Strontium isotopes as indicators of mineral weathering in catchments. *Catena* 22:201-214
- Baker RR (1978) The evolutionary ecology of animal migration
- Barnett-Johnson R, Ramos F, Grimes C, MacFarlane R (2005) Validation of Sr isotopes in otoliths by laser ablation multicollector inductively coupled plasma mass spectrometry (LA-MC-ICPMS): opening avenues in fisheries science applications. *Canadian Journal of Fisheries and Aquatic Sciences* 62:2425-2430
- Bath G, Thorrold S, Jones C, Campana S, McLaren J, Lam J (2000) Strontium and barium uptake in aragonitic otoliths of marine fish. *Geochimica et Cosmochimica Acta* 64:1705-1714
- Brannon E, Powell M, Quinn T, Talbot A (2004) Population structure of Columbia River Basin Chinook salmon and steelhead trout. *Reviews in Fisheries Science* 12:99-232
- Burke JL (2004) Life histories of juvenile chinook salmon in the Columbia River estuary: 1916 to the present.
- Clow D, Mast M, Bullen T, Turk J (1997) Strontium 87/strontium 86 as a tracer of mineral weathering reactions and calcium sources in an alpine/subalpine watershed, Loch Vale, Colorado. *Water Resources Research* 33:1335-1351

- Connor W, Burge H, Waite R, Bjornn T (2002) Juvenile life history of wild fall Chinook salmon in the Snake and Clearwater rivers. *North American Journal of Fisheries Management* 22:703-712
- Connor W, Burge H, Yearsley J, Bjornn T (2003) Influence of flow and temperature on survival of wild subyearling fall Chinook salmon in the Snake River. *North American Journal of Fisheries Management* 23:362-375
- Connor W, Sneva J, Tiffan K, Steinhorst R, Ross D (2005) Two alternative juvenile life history types for fall Chinook salmon in the Snake River basin. *Transactions of the American Fisheries Society* 134:291-304
- de Roos AM, Leonardsson K, Persson L, Mittelbach GG (2002) Ontogenetic niche shifts and flexible behavior in size-structured populations. *Ecological monographs* 72:271-292
- Dennis RLH, Shreeve TG, Van Dyck H (2003) Towards a functional resource-based concept for habitat: a butterfly biology viewpoint. *Oikos*:417-426
- Faure G (1977) *Principles of isotope geology*
- Fiedler W (2003) Recent changes in migratory behaviour of birds: a compilation of field observations and ringing data. *Avian migration*:21-38
- Fleck RJ, Criss RE, Eaton GF, Cleland RW, Wavra CS, Bond WD (2002) Age and Origin of Base and Precious Metal Veins of the Coeur D'Alene Mining District, Idaho. *Economic Geology* 97:23-42
- Fraley C, Raftery AE (2007) Bayesian regularization for normal mixture estimation and model-based clustering. *Journal of Classification* 24:155-181
- Garcia A et al. (2007) Fall Chinook Salmon Spawning Ground Surveys in the Snake River Basin Upriver of Lower Granite Dam, 2007.
- Good TP, Waples, R.S., Adams, P. (2005) Updated status of federally listed ESU's of West Coast salmon and steelhead. In: Commerce USDo (ed), vol. Tech. Memo. NOAA, p 598
- Gross M, Coleman R, McDowall R (1988) Aquatic productivity and the evolution of diadromous fish migration. *Science* 239:1291

- Healey M (2009) Resilient salmon, resilient fisheries for British Columbia, Canada. *Ecology and Society* 14:2
- Hilborn R, Quinn T, Schindler D, Rogers D (2003) Biocomplexity and fisheries sustainability. *Proceedings of the National Academy of Sciences* 100:6564
- Hough W (1981) Impact of prescribed fire on understory and forest floor nutrients. *USDA Forest Service Research Notes*:4
- Hutchings J, Myers R (1994) The evolution of alternative mating strategies in variable environments. *Evolutionary Ecology* 8:256-268
- Kennedy B (2011) Personal Communication. In:
- Kennedy B, Blum J, Folt C, Nislow K (2000) Using natural strontium isotopic signatures as fish markers: methodology and application. *Canadian Journal of Fisheries and Aquatic Sciences* 57:2280-2292
- King EM, Beard BL, Valley JW (2007) Strontium and oxygen isotopic evidence for strike/slip movement of accreted terranes in the Idaho Batholith. *Lithos* 96:387-401
- Martin GB, Thorrold SR, Jones CM (2004) Temperature and salinity effects on strontium incorporation in otoliths of larval spot (*Leiostomus xanthurus*). *Canadian Journal of Fisheries and Aquatic Sciences* 61:34-42
- McCullough D (1999) A review and synthesis of effects of alterations to the water temperature regime on freshwater life stages of salmonids, with special reference to chinook salmon. *Water Resources*
- Milá B, Smith TB, Wayne RK (2006) Postglacial Population Expansion Drives The Evolution of Long Distance Migration in a Songbird. *Evolution* 60:2403-2409
- Milks D, Varney M, Schuck M (2009) Lyons Ferry Hatchery Evaluation Fall Chinook Salmon Annual Report: 2006. Washington State Department of Fish and Wildlife
- Outridge P, Chenery S, Babaluk J, Reist J (2002) Analysis of geological Sr isotope markers in fish otoliths with subannual resolution using laser ablation-multicollector-ICP-mass spectrometry. *Environmental Geology* 42:891-899
- Palmer M, Edmond J (1992) Controls over the strontium isotope composition of river water. *Geochimica et Cosmochimica Acta* 56:2099-2111

- Quinn T (2005) The behavior and ecology of Pacific salmon and trout. University of Washington Press
- Quinn TP, Unwin MJ, Kinnison MT (2000) Evolution of temporal isolation in the wild: genetic divergence in timing of migration and breeding by introduced chinook salmon populations. *Evolution* 54:1372-1385
- Raftery AE, Dean N (2006) Variable selection for model-based clustering. *Journal of the American Statistical Association* 101:168-178
- Ruttenberg B, Hamilton S, Hickford M, Paradis G, Sheehy M, Standish J (2005) Elevated levels of trace elements in cores of otoliths and their potential for use as natural tags. Multi-Campus: Retrieved from: <http://www.escholarship.org/uc/item/30h378r1>
- Salewski V, Bruderer B (2007) The evolution of bird migration - a synthesis. *Naturwissenschaften* 94:268-279
- Schmitt R, Steele Jr W, Jones Jr R (1995) Proposed recovery plan for Snake River salmon. US Department of Commerce, NOAA, Washington, DC 347
- Secor D, Dean J, Laban E (1991) Manual for otolith removal and preparation for microstructural examination. Electric Power Research Institute; Belle W. Baruch Institute for Marine Biology and Coastal Research
- Volk E, Blakley A, Schroder S, Kuehner S (2000) Otolith chemistry reflects migratory characteristics of Pacific salmonids: using otolith core chemistry to distinguish maternal associations with sea and freshwaters. *Fisheries Research* 46:251-266
- Waples R, Beechie T, Pess G (2009) Evolutionary History, Habitat Disturbance Regimes, and Anthropogenic Changes: What Do These Mean for Resilience of Pacific Salmon Populations? *Ecology and Society* 14:3
- Waples R, Jones Jr R, Beckman B, Swan G (1991) Status review for Snake River fall chinook salmon. NOAA Technical Memorandum NMFS N/NWC-201, Seattle, Washington
- Waples R, Pess G, Beechie T (2008) Evolutionary history of Pacific salmon in dynamic environments. *Evolutionary Applications* 1:189-206

- Waples R, Teel D, Myers J, Marshall A (2004) Life-history divergence in Chinook salmon: historic contingency and parallel evolution. *Evolution* 58:386-403
- Werner E, Gilliam J (1984) The ontogenetic niche and species interactions in size-structured populations. *Annual review of ecology and systematics* 15:393-425
- Werner EE, Hall DJ (1988) Ontogenetic Habitat Shifts in Bluegill: The Foraging Rate-Predation Risk Trade-off. *Ecology* 69:1352-1366
- Williams J, Zabel R, Waples R, Hutchings J, Connor W (2008) Potential for anthropogenic disturbances to influence evolutionary change in the life history of a threatened salmonid. *Evolutionary Applications* 1:271-285
- Woodhead J, Swearer S, Hergt J, Maas R (2005) In situ Sr-isotope analysis of carbonates by LA-MC-ICP-MS: interference corrections, high spatial resolution and an example from otolith studies. *Journal of Analytical Atomic Spectrometry* 20:22-27
- Zabel R, Chittaro P (2011) Personal communication. In, Seattle, WA
- Zabel R, Williams J (2008) Selective mortality in chinook salmon: What is the role of human disturbance?

CHAPTER 2

DETERMINING SALMON NATAL ORIGINS USING PREDICTIONS FROM BEDROCK GEOLOGIC DIVERSITY AND GEOCHEMICAL SIGNATURES

Abstract

Geochemical fingerprinting methods using stable isotopes or trace elemental signatures have enabled more detailed understanding of migratory behavior across animal taxa, however, the spatial resolution of geochemical fingerprinting methods is limited by the geographic variability of signatures. In particular, isotopes of strontium have been used to reconstruct migration history in salmonids at small spatial scales due to a close relationship between watershed geologic composition and $^{87}\text{Sr}/^{86}\text{Sr}$ signatures. Using fall Chinook salmon in the Snake River of Idaho we present methods for extending the spatial resolution and application of otolith migration studies using a predictive relationship between $^{87}\text{Sr}/^{86}\text{Sr}$ and bedrock geology. Our objectives were to: 1) quantify the relationship between bedrock geology and $^{87}\text{Sr}/^{86}\text{Sr}$ within this region in order to develop a predictive framework for $^{87}\text{Sr}/^{86}\text{Sr}$, 2) to test the ability of this predictive relationship to classify fish to natal origin, and 3) to examine the effects of geologic diversity and scale on the ability of geology to predict spatial $^{87}\text{Sr}/^{86}\text{Sr}$ variation. Our results indicate that that predictions of $^{87}\text{Sr}/^{86}\text{Sr}$ can accurately classify fish to natal origin, indicating the possibility of extending spatial extent or resolution using prediction. Watershed scale as well as geologic diversity place limits on prediction accuracy within our system.

Introduction

Long distance migration represents a novel life history strategy that enables animal populations to cope with large scale spatial or temporal heterogeneity in their environment (Baker 1978). Species adopt this strategy in various ways, with large differences both between and within species in the adoption of this behavior. The distances travelled and energy expended in migration make the allocation of resources involved in migration critically important to survival of the individual. Successful life history strategies, those which best allocate resources during migration, confer selective advantage for those individuals (Alerstam et al. 2003). The selective advantages of migration, however, do not necessarily act at the same scale as the migration itself and local selective pressures can be very important to survival. Understanding migration at both broad and fine scales is necessary to fully understand fitness consequences of varied life history strategies.

Highly localized environmental factors at fine temporal and spatial scales can have significant effects on survival during migration. For example, due to their small body size, migratory neotropical birds often cannot accumulate enough body fat to complete their entire migration from Southern to Northern Latitudes and must stopover to gain the additional energy to complete the journey. This stopover requirement increases the importance of small scale habitat and environmental conditions which determine the foraging potential of potential stopover sites. Thus, birds must successfully integrate these local scale conditions into a larger scale migration path (Moore et al. 1995). Evidence indicates that the environmental conditions and stopover productivity can limit populations in density dependent and independent ways (Newton 2006) Thus it is important to understand migrations not only at their departure and destination points but also at the finer temporal and spatial scales through which individuals migrate. This breadth of scale can be difficult to

capture when studying the effects of life history variation in migratory species inhabiting large geographical extents

Current methods of tracking animals during migration are limited in their ability to quantify migratory movement throughout the lifetime of the individual and across the breadth of spatial scales relevant to migration. The use of Passive Integrated Transponder (PIT) tags has provided a wealth of data on animal migration, however geographic scale is often limited to the location of antenna receivers (Gibbons and Andrews 2004). Acoustic and radio telemetry tags as well as GIS tags allow for excellent spatial resolution but are limited temporally by the battery life of the transponder and geographically by the spatial scale of antenna receivers in the case of radio and acoustic tags (Hebblewhite and Haydon ; Kenward 2001). Further, surgical implantation of tags introduces increased mortality, limiting their utility in small animals and juvenile life stages (Skalski et al. 2009). Tag loss is also an issue for external tags as well as surgically implanted tags. In the case of large scale migrations the logistics of tagging a sufficient sample size and recapturing enough individuals can be difficult (Salewski et al. 2007). In contrast to the limitations of tagging, natural chemical signatures show promise in some species for reconstructing migratory movement at multiple scales.

Over the last decade, geochemical fingerprinting methods using stable isotopes or trace elemental signatures have enabled more detailed understanding of migratory behavior across animal taxa without the need for constant observation or extrinsic marking techniques (Hobson 1999; Hobson et al. 2009; Hogan et al. 2007; Marra et al. 1998; Thorrold et al. 1998). These geochemical techniques generally rely upon geographic isotopic variation that is recorded as chemical signatures in animal tissues. These signatures are later recovered analytically to reconstruct the movement, ontogenetic and trophic behavior of a migratory species.

The spatial resolution of geochemical fingerprinting methods is determined by two factors: the geographic variability of geochemical signatures across the migration path, and the spatial and temporal resolution recorded in the animal tissues in which these signatures are recorded (Hobson et al. 2009). For example, the use of carbon ($\delta^{13}\text{C}$) and Deuterium (δD) to track bird migrations is limited to broad, continental

scale, resolution of breeding grounds due both to the low temporal resolution recorded in feathers and the large scale of isotopic changes with latitude and precipitation across continents (Wassenaar and Hobson 2000). In contrast, Thorrold et al. (1998) were able to determine natal origins of migratory American shad at a finer, regional scale using trace element analysis of otoliths. Similarly, Hogan et al. (2007) used trace element analysis of otoliths to show migration and marine residence in Mekong catfish. These latter studies were made possible by the detailed spatial and temporal records available in fish otoliths and the high spatial variation of trace elements within the study systems. The combination of otoliths with isotopic analysis, however, has allowed the study of migratory fish at much finer spatial and temporal resolution even than trace element analysis.

Because of their unique structure and metabolic stability, otoliths have been shown to record detailed geochemical variations with excellent temporal and spatial resolution throughout the life of the fish and have been used to determine natal location and reconstruct detailed movement in salmon (Barnett-Johnson et al. 2008; Hamann 2010; Kennedy et al. 1997; Kennedy et al. 2002). Otoliths are calcareous structures responsible for balance and hearing in fish. They are made up of biogenic aragonite added in daily accumulated layers whose width varies with daily growth. Elements and isotopes are incorporated into the calcium matrix as the fish grows (Campana and Thorrold 2001) These signatures can be accurately recovered using laser ablation inductively coupled plasma mass spectroscopy (LA-ICP-MS) (Barnett-Johnson et al. 2005). The ratio of radiogenic ^{87}Sr to ^{86}Sr ($^{87}\text{Sr}/^{86}\text{Sr}$) is an excellent tracer of fish movement due to the unique chemistry of strontium and the potential for high geographic variability in many systems. Strontium also remains unfractionated in otoliths, making comparisons across watersheds more straightforward and its similarity to calcium and high environmental concentrations makes it available in high enough abundances in otoliths for high precision analysis.

Spatial variations in $^{87}\text{Sr}/^{86}\text{Sr}$ ratio are based on differences in rock chemistry and age. During the differentiation of the Earth into its primary layers, rubidium (Rb) preferentially segregated in the crust due to its affinity to form lighter for the formation

of less dense, silicate minerals while Sr remained in the mantle due to its affinity for more metallic elements. ^{87}Rb , the only radiogenic isotope of Rb, decays to ^{87}Sr with a half-life of 49 Ga. The resulting evolution of Sr in the crust, made up primarily of felsic rocks such as granite, leads to higher $^{87}\text{Sr}/^{86}\text{Sr}$ ratios than mafic rocks such as basalt which are derived from the mantle. It is the uneven distribution of rocks derived from mafic and felsic sources, as well as variation in rock age, that results in spatial variability of $^{87}\text{Sr}/^{86}\text{Sr}$ across the earth's Earth's surface. (Faure and Mensing 2004) Because these geologic processes are well understood they present an opportunity to predict the spatial variation of $^{87}\text{Sr}/^{86}\text{Sr}$ based on the mafic or felsic nature of rocks.

Sr occurs in freshwater systems through the weathering of underlying bedrock and varies geographically due to variations in the composition of these rocks as well as the relative rates of rock decay (Bain and Bacon 1994; Faure 1977; Stewart et al. 1998). $^{87}\text{Sr}/^{86}\text{Sr}$ signatures of individual watersheds have been shown to be relatively invariant over time and qualitatively related to spatial variation in underlying geology (Bacon et al. 2004; Kennedy et al. 2000). Attempts have been made to quantify the relationship between watershed geologic variability and $^{87}\text{Sr}/^{86}\text{Sr}$ but the predictive ability of this relationship has not been utilized to improve or expand the resolution of otoliths studies (Barnett-Johnson et al. 2008; Humston et al. 2006).

It may be possible to extend current isotopic methods of migration reconstruction, and better account for spatial variation in $^{87}\text{Sr}/^{86}\text{Sr}$, using predictions based on the known relationship between bedrock geology and $^{87}\text{Sr}/^{86}\text{Sr}$. The use of isoscapes, spatially continuous maps of isotope variation, are a promising geospatial tool for studying animal migration (Hobson et al. 2009). The relationship between variation in bedrock geology and $^{87}\text{Sr}/^{86}\text{Sr}$ signature allows for the creation of strontium isoscapes, using GIS to interpolate strontium variability from bedrock geology. These spatially explicit predictions of isotopic variation might then be used to improve migration studies. They can be used to anticipate important areas of $^{87}\text{Sr}/^{86}\text{Sr}$ variation and design experiments to better capture spatial isotopic variation within a study system before effort and funds are expended to collect baseline isotopic samples. Similarly, isoscapes could be used to extend the effective spatial resolution of otolith

based studies of migration or natal origin if isotopic variation could be predicted with high enough precision. Also, If geochemical variation can be predicted *a priori*, experimental effort can be limited only to study areas which exhibit sufficient variability to produce results.

Applying isoscapes to improve migration reconstruction studies requires an understanding of how geologic heterogeneity affects geochemical fingerprints. If the geochemical signature of a watershed is directly related to the rock types present within the watershed, differences in signature between watersheds are the result of variation in rock types between basins. When considering geologic variation, both the number of geologic types present as well as the representation of each rock type may be important. For example, the number of rock types present may be uniform across watersheds, however, the amount of each rock type may differ between basins. In this case we would expect trace element concentrations to be higher in basins containing relatively larger representation of rocks containing these elements. Watershed scale may also play a role. Since geologic structures often occur on large scales, smaller watersheds may be more likely to be made up of homogenous rock types than larger basins whose size may allow them to encompass multiple large geologic elements. Past attempts to quantify the relationship between geochemical signatures and geology have implicitly recognized the importance of these relationships (Barnett-Johnson et al. 2008; Humston et al. 2006) but there is little understanding of the explicit interactions between scale and geologic diversity within and between watersheds. Predictions of geochemical signatures are likely constrained by these scale and diversity relationships. Thus, explicit understanding of these relationships may be important in creating, applying and interpreting geochemical predictions in migration studies.

fall Chinook Salmon in the Snake River of Idaho provide an excellent population in which to test improvements in otolith based migration reconstruction. Snake River fall Chinook salmon, a federally listed threatened species, inhabit a large and geologically diverse basin and their juvenile migration patterns have been previously characterized using otoliths microchemistry (Hegg et al, in review). Recent changes in the outmigration timing of this population have made determination of the spawning

origin of juvenile fish an important conservation question (Connor et al. 2005). The geologic diversity across spatial scales within the basin also allows for examining the scale at which geology may be capable of predicting geochemical variation, and further, the scale at which migratory movements of salmon can be distinguished.

In this study we explore the relationship between surface water $^{87}\text{Sr}/^{86}\text{Sr}$ and bedrock geologic variation in the Snake River Basin of Idaho. Our intent was to explore the broader utility of this relationship in improving and expanding the use of $^{87}\text{Sr}/^{86}\text{Sr}$ system as an ecological tracer in migratory species. Our emphasis is on creating a predictive framework for determining the natal origins of juvenile Snake River fall Chinook Salmon, a species listed as threatened in the Snake River under the Endangered Species Act, using $^{87}\text{Sr}/^{86}\text{Sr}$ fingerprints recovered from otoliths. Our specific objectives were to: 1) quantify the relationship between bedrock geology and $^{87}\text{Sr}/^{86}\text{Sr}$ within this region in order to develop a predictive framework for $^{87}\text{Sr}/^{86}\text{Sr}$ variation within the basin, 2) to test the ability of this predictive relationship to classify fish to natal origin compared to standard methods, and 3) to examine the effects of geologic diversity and scale on the ability of geology to predict spatial $^{87}\text{Sr}/^{86}\text{Sr}$ variation.

Methods

Our goal was to create a regression model of $^{87}\text{Sr}/^{86}\text{Sr}$ variation with which to quantitatively predict the natal origins of fall Chinook salmon directly from the geologic variability of watersheds within the Snake River basin. This predictive framework was then examined for its potential to extend the scale and resolution of natal origin determination based upon otolith microchemistry. Geologic variability was quantified using GIS techniques and available geologic maps. Isotopic and trace element results from water analysis throughout the Snake River Basin, as well as natal origin $^{87}\text{Sr}/^{86}\text{Sr}$ signatures for 134 returning adult spawners from Hegg et al. (in review) comprised the

data for this study. Stream water $^{87}\text{Sr}/^{86}\text{Sr}$ values were used to create a model to predict stream water $^{87}\text{Sr}/^{86}\text{Sr}$. Predictions from this model were then used to create a discriminate function to classify natal signatures of fish to their origin in the basin. The results of classification using prediction from bedrock geology were then compared to the classifications from Hegg et (in review) developed using water samples.

All statistical analyses were conducted in R statistical package (version 2.10.1, <http://www.r-project.org/>)

Study site

The Snake River, the largest tributary to the Columbia River, drains an area of 280,000km² encompassing six states. The river originates in Wyoming and flows 1,670 km to its confluence with the Columbia River in western Washington State with the majority of the basin located in the state of Idaho (Figure 2.1). The Snake River is inhabited by three ESA listed salmonid species, Spring-Summer Chinook salmon, Steelhead and fall Chinook salmon. fall Chinook salmon, which spawn in the lower reaches of the major tributaries in the basin, are the subject of our study.

fall Chinook salmon in the Snake River inhabit a river system which has been significantly altered by hydropower construction. Upstream access to the majority of fall Chinook salmon spawning grounds was blocked by the construction of the Hells Canyon dam complex in 1959. Four downstream dams on the Snake have impounded the river from Ice Harbor Dam near the confluence to the port of Lewiston, ID. Dworshak dam, an impassable dam on the North Fork Clearwater River, blocks salmon migration and supplies cold, hypolimnetic water that cools the lower portion of the Clearwater river during hatching and rearing seasons. Outflows from Dworshak reservoir are also used to adjust temperature and flow as a part of the Columbia and Snake River salmon management plan. Based primarily on aerial redd surveys, the majority of fall Chinook spawning is thought to occur in Hells Canyon reach of the Snake

River and the Clearwater river (Garcia et al. 2005) with smaller runs occurring in the Salmon, Grande Ronde, Tucannon and Imnaha rivers.

Within the Snake River basin five major geologic provinces may broadly influence the $^{87}\text{Sr}/^{86}\text{Sr}$ variability of river water in the basin (Figure 2.1): (1) Teton Range - a heterogeneous mixture of Precambrian to Paleozoic era rocks including marine origin metamorphic rock metamorphosed sedimentary rocks and intrusive granites (Love et al. 1978), forms the headwaters of the Snake River. (2) Idaho Batholith - a felsic granite intrusion dating to the Cretaceous associated with much older Precambrian metamorphic rocks containing high $^{87}\text{Sr}/^{86}\text{Sr}$ (Foster and Fanning 1997). (3) Columbia River Basalts - these basalts date to the Neogene period (16-6Ma) and extend throughout the basin in Western Washington, Eastern Oregon and Western Idaho abutting the Idaho Batholith (Hooper et al. 2007). These basalt flows and are lower in $^{87}\text{Sr}/^{86}\text{Sr}$. (4) Snake River Plain -. This area is dominated by Quaternary basalts but is more geologically diverse than the Columbia River Basalts because of the presence of rhyolitic flows and Paleozoic and Mesozoic sedimentary rock (Leeman 1982). This region influences the $^{87}\text{Sr}/^{86}\text{Sr}$ chemistry of the Snake River but lies outside the current spawning area of Snake River fall Chinook Salmon. (5) Wallowa Terrane - a Mesozoic and Jurassic accreted terrane containing oceanic lithology associated with a large granitic pluton which likely caused uplift of the Wallowa Mountains in Northeastern Oregon 10-15mya, after the completion of the Columbia River Basalt flows (Hales et al. 2005). The Snake River basin encompasses a broad diversity of geologic ages and rock types, both of which contribute to a spatial diversity of geochemical signatures within the tributaries of the basin.

The Snake River tributaries can be grouped broadly by the geology over which they flow. The Clearwater and Salmon rivers flow over the older, felsic rocks of the Idaho batholith, with the Clearwater being influenced most heavily by the older metamorphic rocks of this region. The Tucannon, Grande Ronde and Imnaha rivers flow primarily over the Columbia River Basalts, with the Grande Ronde and Imnaha being influenced in their headwaters by the more diverse Wallowa terrane. The Palouse river has its headwaters in the higher strontium regions near the Idaho batholith but the

majority of its reach flows over the Columbia River basalts. The unique geologic conditions through which each group of rivers flows leads to detectable differences in geochemical fingerprints between rivers in the basin.

Geochemical variation between basin tributaries is high enough to allow classification of tributaries based upon geochemical signature. Hegg et al. (in review) classified the main tributaries and Upper and Lower Snake River into four groups based upon $^{87}\text{Sr}/^{86}\text{Sr}$ ratio. Elemental variation within the basin appears to vary, at least in part, with general geologic makeup of basins (Table 1.1). For instance, rubidium (Rb) appears to vary with potassium (K) which would be expected as K, a fellow incompatible element, is highest in felsic rocks such as granite. The highest calcium (Ca) concentrations occur in the Imnaha River, potentially due to weathering of marine origin sedimentary rocks. The Snake River also shows elevated Ca concentrations, expected due to the much larger drainage basin. The Clearwater River contains low concentrations of most elements, likely reflecting the low weathering rate of the granitic geology it drains. $^{87}\text{Sr}/^{86}\text{Sr}$ generally increases with increasing areas of felsic composition as expected with the Clearwater having the highest $^{87}\text{Sr}/^{86}\text{Sr}$ and the rivers flowing over the Columbia River Basalts having the lowest ratios. The variation of geochemical signature with rock composition within the basin shows the potential for prediction of geochemical signatures if the variation in geology within the basin can be quantified.

Quantification of Geologic Diversity

While quantifying geologic variability within our study area we chose to focus on abundance of rock types within a basin rather than rock age. Rock age has an effect on $^{87}\text{Sr}/^{86}\text{Sr}$ due to the evolution of radiogenic ^{87}Sr from ^{87}Rb over time, however quantifying this relationship is complicated in this study for two reasons. The first is the correlation of rock age with rock type within the Snake River basin. For example, the Idaho Batholith, a granitic structure that would be expected to have high $^{87}\text{Sr}/^{86}\text{Sr}$, is

also generally older and associated with extremely old, high $^{87}\text{Sr}/^{86}\text{Sr}$, metasedimentary deposits. In the opposite case, the Columbia River basalts are relatively young, but would also be expected to have low $^{87}\text{Sr}/^{86}\text{Sr}$ based upon their mafic composition. Secondly, translating geologic ages to continuous data points can be problematic because rock types often contain a large range of ages within each map polygon. In our preliminary work the addition of age did not significantly improve our predictive ability, likely due to the factors mentioned above. For this reason geologic type, rather than age was the focus of our predictive models.

All geological analyses were based upon current bedrock geologic maps from the Preliminary Integrated Geologic Map Database of the United States for the states encompassing the extent of the Snake River (Ludington et al. 2006). These maps detail the bedrock geology of the Snake River basin at 1:500,000 scale with consistent lithology between states. The primary rock type within each map polygon is recorded in the attribute table of the map shapefile according to LithClass 6.1 standard (<http://www.nadm-geo.org>).

Seasonal water samples from 13 sites throughout the Snake River basin (Hegg et al. in review) (Table 2.2) were used to create a multiple linear regression with geologic type as the independent variables and $^{87}\text{Sr}/^{86}\text{Sr}$ as the dependent variable. Using the Arc Hydro extension for ArcMap (ESRI, www.esri.com) the watershed area above each sampling point was delineated. In ArcMap, The intersection between the watershed boundaries and the geologic map layer was used to calculate the map area of each rock type within the watershed above each sample point. The percentage area of each rock type was then calculated from the attribute table of the intersected map.

Our aim in reclassifying rock types was to capture the geologic variation relevant to $^{87}\text{Sr}/^{86}\text{Sr}$ differences in stream water. Since mafic and felsic rocks typically display very different strontium isotopic chemistry based upon the composition of their magma source our rock type classification was primarily based upon distinguishing between mafic and felsic rock types. Thus, all igneous rocks were classified by their mafic or felsic rock type. We distinguished all non-igneous rocks by their protolithic rock type, either mafic or felsic, when the protolith was obvious from the map entry. Many non-

igneous rock types have no obvious protolith composition, however. For instance, metamorphic or sedimentary rocks may consist of a mixture of both felsic and mafic influences. When no obvious protolith could be determined the rock types were then classified into categories of metamorphic, carbonate, or sedimentary/other.

Carbonate rocks tend to have relatively high Sr concentrations. The potentially high rates of weathering in carbonate rocks can also have large impacts on $^{87}\text{Sr}/^{86}\text{Sr}$ ratios within a watershed, hence they were classified separately. We designated a metamorphic rock category since both their chemical makeup and age (such as within very old metamorphic rocks associated with the Idaho batholith) could exert a large impact on $^{87}\text{Sr}/^{86}\text{Sr}$ in our study area even in the absence of a distinguishable protolith. The final category, sedimentary/other, included rocks and unconsolidated sedimentary deposits of indeterminate origin as well as chemical and biogenic deposits other than carbonates. Water bodies shown on the geologic maps were also given their own category. The details of rock reclassification are listed in Table 2.3.

Quantifying Rock Type Variability

The variability of rock types represented within and between watersheds was expected to have an effect on the $^{87}\text{Sr}/^{86}\text{Sr}$ ratio within the basin. To examine this relationship we calculated the Shannon index of diversity (Shannon and Weaver 1949) of rock types within each sampled watershed. The Shannon index (H'), used in this case closer to its information-theoretic roots than its conventional application to biodiversity, takes into account the relative abundance (P_i) of an individual rock type and the number of rock types (S) to calculate the relative evenness and diversity of rock types within a basin.

$$H' = - \sum_{i=1}^S (p_i \ln p_i)$$

This index of rock type diversity and evenness was then used to compare the variation of rock types within and between watersheds in light of the variation of $^{87}\text{Sr}/^{86}\text{Sr}$ between watersheds and at varying scales.

Surface Area Calculation

Surface area may be important when calculating the relative contributions of geologic types. Differential weathering and the propensity for more resistant rock types to form vertical faces may bias the flat map area towards the least resistant rock types. We included 3-dimensional surface area within the basin, alongside conventional 2D map area, as a variable in subsequent regression model selection to determine whether 3D area might be a better predictor of $^{87}\text{Sr}/^{86}\text{Sr}$.

Surface area was calculated using 90 meter elevation rasters available from the National Elevation Dataset (USGS, www.nationalmap.gov) using the Surface Area and Ratio extension from Jenness Enterprises (<http://www.jennessent.com>). The surface area of each rock type within each sample watershed was calculated using the Zonal Statistics tool available in the Spatial Analyst toolbox in ArcMap.

Model Selection

Multiple linear regression was used to create a predictive model of $^{87}\text{Sr}/^{86}\text{Sr}$ using percent geologic area within sampled watersheds in the Snake River as the predictor, similar to Barnett-Johnson et al. (2008) and Humston et al. (2006). Mafic rock area followed an exponential relationship with geographic area and was log transformed to meet normality assumptions.

The most likely candidate models were compared using AICc, a version of Akaike's Information Criterion modified for small datasets (Burnham and Anderson

2002). This statistical technique selects the model that best explains variation in the data while rewarding parsimony by penalizing over-parameterization.

Candidate models were constructed using rock types that were well represented in the basin, and rock types which were expected to have a significant influence on dissolved $^{87}\text{Sr}/^{86}\text{Sr}$ values within the study area. Based upon the large areas of Mafic and Felsic rock within the basin these rock types were considered good candidate variables. Similarly, the $^{87}\text{Sr}/^{86}\text{Sr}$ composition of metamorphic rock in the study area indicated that it might be an important variable. All other rock types were considered to have a representation that was either of minor significance, or too variable in composition, to be effective predictors of $^{87}\text{Sr}/^{86}\text{Sr}$.

Natal Origins Prediction

The linear single factor discriminate function, developed by Hegg et al (in review) to classify fish natal origin from a training set of water $^{87}\text{Sr}/^{86}\text{Sr}$ values, was used as a baseline for comparison with predictions. This discriminate function grouped watershed into four distinguishable groups; the Clearwater and Salmon Rivers (CWS); Tucannon, Grande Ronde, Imnaha Rivers (TGI), Upper Snake River (USK) and Lower Snake River (LSK). Adult fall Chinook salmon were then classified to one of the four natal origins based on the otolith chemistry between 100 μm and 250 μm from the otoliths core.

To test the predictive ability of geologic variation, discriminate functions were developed using $^{87}\text{Sr}/^{86}\text{Sr}$ training sets made up of predicted values output from our geological multiple regression. To develop these predicted values, points were digitized in ArcGIS at equal intervals along the stream courses within the basin. The watershed area above each point was delineated using ArcHydro and the percent area of each rock type within these new watersheds was calculated in ArcMap. These geologic results were then input as independent variables in the multiple regression equation to predict the $^{87}\text{Sr}/^{86}\text{Sr}$ value at each point. These prediction points were then grouped according

to the source river groupings from Hegg et al. (in review) and used as training sets to create new discriminate functions.

Prediction points were drawn in two ways to test the predictive ability of the regression model. In the most conservative case we assumed that $^{87}\text{Sr}/^{86}\text{Sr}$ ratio would be best predicted by points nearby the original water sampling points from Hegg et al. (in review) (Table 2.2). In this case five points were drawn at 5 river kilometer (5-rkm) intervals such that each set of five points was roughly centered around a water sampling location used to create the regression (Figure 2.2). We expected that this method would yield results that were the most similar to the original classifications.

The second method of creating prediction points tested our ability to prediction $^{87}\text{Sr}/^{86}\text{Sr}$ without regard to sampling location. In this method points were drawn at 10rkm intervals over the entire river course within the spawning area of fall Chinook salmon (Figure 2.2). The spawning area was defined as the furthest upstream occurrence of a redd in aerial spawning surveys of the basin (Garcia et al. 2007).

Finally, the $^{87}\text{Sr}/^{86}\text{Sr}$ natal signatures of 134 otoliths from Hegg et al. (in review) were classified using the discriminate functions produced from both prediction methods. Individual natal origin classifications for the 5-rkm and 10-rkm discriminate functions were compared to the classification produced in Hegg et al. (in review) using the water sample training set. The percentage of individual fish classifications matching those from Chapter 1 were calculated for both the 5-rkm and 10-rkm prediction datasets. The proportion of fish classified to each source river group was tested using a monte carlo chi-square test with the null hypothesis that all classification methods maintained equal representation of fish in each basin.

The Effects of Scale

To discern the effect of watershed scale on $^{87}\text{Sr}/^{86}\text{Sr}$ variability we used our regression model to predict the $^{87}\text{Sr}/^{86}\text{Sr}$ ratios of much smaller basins within the Snake River with varying geologic heterogeneity. $^{87}\text{Sr}/^{86}\text{Sr}$ water sample values were obtained

for three watersheds, two in the Middle Fork Salmon river drainage and one in the Lower Clearwater drainage. All $^{87}\text{Sr}/^{86}\text{Sr}$ values were determined using Thermal Ionization Mass Spectrometry (TIMS) except Lapwai Creek, which was analyzed using Multi-Collector Inductively Coupled Plasma Mass spectrometry (MC-ICPMS).

The Big Creek watershed (1545.06 km²), a tributary of the Middle Fork Salmon River in Central Idaho, is characterized by large areas of felsic and metamorphic bedrock geology. (Figure 2.3) GPS locations and $^{87}\text{Sr}/^{86}\text{Sr}$ values for nineteen samples from Big Creek and the mouth of the major tributaries in the Big Creek watershed were obtained from Hamann (2010). (Table 2.2)

Lapwai Creek (722.36 km²) is a small tributary watershed joining the Clearwater river just before it's confluence with the Snake river. Lapwai creek's bedrock geology is made up primarily of mafic rocks from the Columbia River basalt formation. (Figure 2.4) Six water samples and GPS locations were taken from Lapwai Creek and its major tributaries and analyzed for $^{87}\text{Sr}/^{86}\text{Sr}$ using MC-ICPMS. (Table 2.2)

Bear Valley Creek (496.16 km²), a small headwater tributary of the Middle Fork Salmon River, drains felsic bedrock of the Idaho Batholith. (Figure 2.5) Twelve $^{87}\text{Sr}/^{86}\text{Sr}$ water samples and GPS coordinates were taken as part of a prior feasibility study in cooperation with the US Forest Service (Kennedy, personal communication). (Table 2.2)

Using ArcMap the percent area of each geologic classification upstream of each water sampling point within the Lapwai, Big Creek and Bear Valley Creek watersheds was calculated. The predicted $^{87}\text{Sr}/^{86}\text{Sr}$ value for each sample point was calculated using the regression equation developed above.

We hypothesized that as watershed area decreased the distance between observed and predicted $^{87}\text{Sr}/^{86}\text{Sr}$ (ΔSr) would increase. We expected that as watershed area decreased below the range of watershed areas used to create the regression, the relationship between geologic area and Sr ratio would begin to fall apart.

If the geologic regression is useful for predicting $^{87}\text{Sr}/^{86}\text{Sr}$ at smaller scales we would expect additional data to fit the model well. The fit of new data can be evaluated based upon the error between observed values and predicted values from the regression. Errors from new data predicted by the model should have the same mean

and variance as the original data. Thus, ΔSr for new datasets should have the same mean and variance as ΔSr the original data. We tested this assumption using Kolmogorov-Smirnov tests comparing ΔSr of each new watershed to the ΔSr of the Snake River data used to create the regression model. Kolmogorov-Smirnov is an omnibus test which tests for differences in location and scale between two samples. Type I error was controlled using Bonferroni adjustment.

A regression model was also fit to the combined data for all water samples in the original Snake River dataset as well as Big, Lapwai and Bear Valley Creeks to test the ability to build a predictive model which encompassed a larger range of watershed scales. Candidate models were constructed using the same independent variable combinations of Mafic, Felsic and Metamorphic rock using only conventional map area. The model with the highest AICc weight was selected.

Results

Quantification of Geologic Diversity

The percent area of each rock type as well as Shannon diversity of each watershed in the study is listed in (Table 2.2). Shannon diversity was greatest for the Snake River watershed with the largest watersheds also displaying the highest overall diversity (1.37). Average diversity of the sub-watersheds within the Snake River watershed was 1.02 (St. Dev. = 0.32). The Snake River watershed was dominated by sedimentary rock (34%) followed by mafic rock (30%) and felsic rock (26%).

Of the three small watersheds used to test the effects of scale, Lapwai Creek contained the highest overall diversity (0.87) while showing very little variation in observed $^{87}Sr/^{86}Sr$. Average diversity of the sub-watersheds within the Lapwai Creek drainage was 0.56 (St. Dev. = 0.18). Lapwai Creek was dominated by mafic rock.

Bear Valley Creek was made up predominantly of Felsic rock types. Shannon diversity for the entire watershed was 0.75, with the average diversity of the sub-watersheds being 0.66 (St. Dev. = 0.22). Big Creek had the lowest overall Shannon diversity (0.60) with average sub-watershed diversity being 0.56 (St. Dev. = 0.18).

Surface area results were very close to those determined using conventional map area. In the Snake River the percent area of rock types within all sub-watersheds differed by a maximum of 1.4%, with the majority of rock types differing by less than 1% (mean = 0.26%).

Model Selection

Model fit for multiple linear regression of the Snake River water samples was assessed based upon AICc weights as shown in Table 2.4. Independent variables were restricted to Mafic, Felsic and Metamorphic rock as these were thought to be the best predictors based on representation within the basin and prior knowledge of the general trends in $^{87}\text{Sr}/^{86}\text{Sr}$ for these rock types. Model fit was very good for all models with all models being significant ($p > 0.05$) and accounting for greater than 70% of the variation in the data.

Models containing three dimensional surface area rather than conventional map area appeared to be favored, with three of the top four models being constructed using surface area. The difference between the top two models was slight, however, with both models containing mafic and metamorphic rock as independent variables. The equations for both models are shown below.

Three Dimensional Area:

$$y = 0.7069197 + 0.0135009(\text{Metamorphic}) - 0.0011872(\log(\text{Mafic})) + \varepsilon$$

Conventional Map Area:

$$y = 0.7069302 + 0.0136641(\text{Metamorphic}) - 0.0011946(\log(\text{Mafic})) + \varepsilon$$

The model with the highest AICc weight was constructed using three-dimensional surface area. The model was significant ($p < 0.001$, $\alpha = 0.05$) and fit the data very well (R^2 adjusted = 0.96). The next candidate model had an AICc score less than one point lower than the top model. This model contained the same variables as the top model, but produced using conventional flat map area rather than three dimensional surface area. This model was also significant ($p < 0.001$, $\alpha = 0.05$) and fit the data nearly as well (R^2 adjusted = 0.95).

Both models predicted $^{87}\text{Sr}/^{86}\text{Sr}$ for the Snake River sample sites with excellent accuracy. The three dimensional surface area model performed only marginally better in predicting the known water samples used to create the regression (mean |observed-predicted| = 0.000394) than the model using conventional map area (mean |observed-predicted| = 0.000406).

Although the model created using three-dimensional surface area was ranked highest by AICc we chose to select the model created using flat map area. This model was chosen based upon the intent of the study to create a useful predictive tool for future studies in the basin. It is commonly accepted that for a model to be considered significantly superior it should be at least two AICc points greater than competing models. Because the models performed essentially identically there seems to be no reason to rely on extra computation of three-dimensional surface area when the results are not significantly different.

Natal Origins Prediction

The 5-rkm prediction method produced the highest natal origins classification accuracy, with 94% of individuals being classified to the same source river as Hegg et al.

(in review). (Figure 2.6) The less conservative 10-rkm prediction method correctly classified 89% of fish as compared to the results of Chapter 1. (Figure 2.7)

The proportion of fish classified to each source river group was not significantly different between classification methods using water samples, five-kilometer or ten-kilometer predictions (Monte Carlo Chi-Square, $p=0.75$, $\alpha=0.05$) (Table 2.5)

Effects of Scale

The error of $^{87}\text{Sr}/^{86}\text{Sr}$ prediction increased significantly when predicting values within the three smallest watersheds. While ΔSr for the large Snake River watershed samples was quite low ($0.000406\pm 81\%$) the grand mean of ΔSr for the three small watersheds was much higher ($0.001983\pm 91\%$). Of the small watersheds Lapwai Creek had the lowest ΔSr ($0.001088\pm 56\%$) followed by Bear Valley Creek ($0.001294\pm 115\%$) and Big Creek ($0.002700\pm 74\%$).

The results of Kolmogorov-Smirnov multiple comparisons of ΔSr for small watersheds to ΔSr of the larger watersheds of the Snake River indicate significant differences between small watersheds and the watersheds used to create the regression. Bonferroni correction based on an α of 0.05 and three comparisons results in a significance level of 0.017, very conservative given that the probability of Type I error is approximately 14%. Still, Big Creek ($p<0.001$) and Lapwai Creek ($p=0.009$) appear to have significantly different error distributions than the samples used to create the geologic regression. Bear Valley Creek is marginally significant as well ($p=0.018$).

Prediction accuracy of $^{87}\text{Sr}/^{86}\text{Sr}$ appears to decrease with decreasing watershed area (Figure 2.8). Prediction accuracy also appears to decrease with decreasing Shannon diversity. (Figure 2.9)

To test our ability to predict $^{87}\text{Sr}/^{86}\text{Sr}$ across large differences in watershed scale a multiple linear regression was created using the combined large and small watershed sample data. The regression model with the highest AICc weight using combined data

was the global model including Mafic, Felsic and Metamorphic rock. AICc score was -474.03 (Table 2.6). The model was significant ($p < 0.001$, $\alpha = 0.05$), however variance explained by the model ($R^2 = 0.65$) was less than the original model using the 13 Snake River sample points.

Discussion

Geologic Prediction

The data indicate that simplified geologic classifications based upon protolithic rock type may be a useful predictor of $^{87}\text{Sr}/^{86}\text{Sr}$ in watersheds. Although the LithClass 6.1 standard is a mix of rock classifications based upon texture, origin and chemical makeup of rock types, the majority of important rock types within the Snake River basin can be grouped into broad categories of mafic and felsic origin rocks without prior knowledge of the geology of the basin.

The prediction accuracy of the top models suggests that geology can be a very accurate predictor of $^{87}\text{Sr}/^{86}\text{Sr}$. Significant differences in $^{87}\text{Sr}/^{86}\text{Sr}$ between tributaries in the basin are apparent in the parts per hundred range (± 0.005) while the prediction accuracy was generally less than parts per thousand (< 0.0001). Furthermore, nearly all the variation in the data was explained by the model. Thus, we would expect that within the spatial constraints of the observations used to create the model $^{87}\text{Sr}/^{86}\text{Sr}$ predictions would be an accurate method for assessing $^{87}\text{Sr}/^{86}\text{Sr}$ variation of unsampled areas within the study area.

Using three dimensional surface area of watersheds to calculate geologic makeup of watersheds seemed to provide a very slight improvement in prediction of $^{87}\text{Sr}/^{86}\text{Sr}$ over models using conventional flat map area. Within the Snake River basin this improvement was negligible and any improvement in accuracy would be below the analytical error of otoliths analysis. Calculation of 3D surface area requires specialized

extensions to ArcMap and more complex analysis while providing limited benefit. Increased time and complexity of analysis may limit the utility of this method for improving otoliths microchemistry studies in the basin, or the application of the method to other systems. For these reasons we chose to select a predictive regression which used conventional flat map area for prediction.

Fish Classification

Geologic prediction has great potential as a method for improving our ability to determine location and movement patterns of fish from their otoliths. By accurately predicting $^{87}\text{Sr}/^{86}\text{Sr}$ variation within a basin it may be possible to increase the spatial resolution of baseline samples, thus increasing our ability to correctly predict the location of fish during important life history time points. Geologic prediction may also allow researchers to determine the location of fish with unknown signatures or to determine *a priori* the areas within a basin which will allow analysis movement patterns or natal origin. These possibilities hinge on our ability to successfully classify fish to known origin using predicted $^{87}\text{Sr}/^{86}\text{Sr}$.

Our results show that fish can be successfully classified to location using $^{87}\text{Sr}/^{86}\text{Sr}$ predicted directly from watershed geology. Individual fish classified to natal source using the more conservative 5-rkm prediction method were classified with high accuracy (94%) to the same natal source using conventional baseline water sampling. Less conservative 10-rkm prediction methods maintained high prediction accuracy (89%) however they did not perform as well as the more conservative approach.

Declining prediction accuracy with the 10-rkm method may be due in part to increased spatial resolution not accounted for using traditional water samples. Using traditional water sampling provides a snapshot of the $^{87}\text{Sr}/^{86}\text{Sr}$ signature at only a few points within the basin. Prediction of $^{87}\text{Sr}/^{86}\text{Sr}$ at 10-rkm intervals throughout the reach can estimate the entire spectrum of $^{87}\text{Sr}/^{86}\text{Sr}$ variation within the reach, thus possibly

allowing the discriminate function to include fish which otherwise might be misclassified simply due to the low spatial resolution of baseline samples.

Alternately, the accuracy of predictions may simply decline as predictions are made further from sample sites used to create the regression. Values of $^{87}\text{Sr}/^{86}\text{Sr}$ below the confluence of two streams are a function of the relative concentration of dissolved strontium in each stream, the discharge of each stream, as well as the $^{87}\text{Sr}/^{86}\text{Sr}$ ratio of both streams. Our predictions did not take into account variability in stream discharge or relative strontium concentrations and thus may under or over predict $^{87}\text{Sr}/^{86}\text{Sr}$ values based on these factors. Similarly, the effect of variations in groundwater inputs on $^{87}\text{Sr}/^{86}\text{Sr}$ values within the Snake River basin is unknown and may create additional error in predictions.

Despite these potential sources of error, accuracy of fish classifications in this study remained high. This indicates that prediction of $^{87}\text{Sr}/^{86}\text{Sr}$ may be a relatively simple method of extending the spatial resolution of future otoliths studies, especially in study systems where large numbers of baseline water samples are not feasible or where predictions from unknowns is required.

Scale and Diversity

Our results point to a significant effect of scale and geologic diversity in the accuracy of $^{87}\text{Sr}/^{86}\text{Sr}$ predictions from bedrock geology. Watershed area appears to have a major effect on prediction accuracy, with watersheds larger than $\sim 10,000 \text{ km}^2$ having much less error than smaller watersheds. (Figure 2.8) Similarly, watersheds with geologic diversity greater than ~ 1.0 have markedly lower error than those watersheds with lower geologic diversity. (Figure 2.9).

Geologic formations can be large scale (e.g. $> 10,000$'s of km^2) structures. In the Snake River the Idaho Batholith and Columbia River basalts cover large areas of the basin in a fairly homogenous fashion. Thus, we would expect that as watershed size decreases the chances of a watershed containing more than one rock type would

decrease as well. Thus, below a certain size, most watersheds would contain fairly homogenous geology. Homogenous watersheds would be expected to have higher error using a multiple regression approach since all other explanatory variables would fall to zero. Thus, it is important to determine at what watershed size geologic diversity is too low to calculate accurate predictions.

Figure 2.10 shows the relationship between geologic diversity and watershed size for all water samples in the study. Interestingly, Watershed area begins to increase exponentially in watersheds with a Shannon diversity of ~ 1 . All watersheds with a Shannon score below 1 have areas below 8901.76 (The Grande Ronde River sample point). All Shannon scores greater than 1 occur in watersheds larger than 13,733.19 km². Incidentally, ⁸⁷Sr/⁸⁶Sr prediction accuracy increases when Shannon diversity of watershed geology is greater than ~ 1 as shown in Figure 2.9.

The interaction of watershed size and geologic diversity appear to create a lower spatial limit on prediction accuracy within the Snake River basin. Our predictive multiple regression is likely to be accurate only in watersheds of the Snake River with areas 8,400 km² or larger and geologic Shannon diversity scores >1 using our reclassification method for rock types. This lower limit does not constrain attempts at prediction at lower spatial scales however. In any given basin it may be possible to predict ⁸⁷Sr/⁸⁶Sr based upon geologic makeup of sub-watersheds, however predictions are not likely to be generalized outside of the target watershed.

Future Applications

This study provides the first quantitative evidence that predictions based on bedrock geology can be used to accurately expand the spatial resolution of studies using ⁸⁷Sr/⁸⁶Sr to reconstruct the location of migratory fish. Our methods provide a robust and repeatable method for classifying lithology that accounts for the major geologic drivers of ⁸⁷Sr/⁸⁶Sr variation and is generally applicable to any geologic setting. We

hope application of these tools will allow researchers to improve the accuracy and spatial resolution of future otoliths microchemical studies.

The mechanistic processes underlying $^{87}\text{Sr}/^{86}\text{Sr}$ variation in streamwater are not well understood. Past work has shown the ability to quantify the relationship between geological diversity and $^{87}\text{Sr}/^{86}\text{Sr}$ for the purpose of predicting fish natal origin (Barnett-Johnson et al. 2008). Other studies have attempted to create a scale-independent method of predicting microchemical variation to guide study design (Humston et al. 2006). Our results provide evidence that scale is an important consideration when creating predictive models of $^{87}\text{Sr}/^{86}\text{Sr}$ variation using bedrock lithology, and provide initial guidelines for determining spatial limits for further studies.

Predicting $^{87}\text{Sr}/^{86}\text{Sr}$ may allow us to extend studies into large and difficult to sample watersheds, while providing spatial resolution beyond what is feasible using standard techniques. Still, our data shows that prediction of $^{87}\text{Sr}/^{86}\text{Sr}$ is dependent on the scale and geologic diversity within the watersheds of interest. Our methods are best suited for extension of conventional studies, planning of additional water sampling, and limited prediction of unsampled watersheds that fall within the spatial and diversity limits of the basin.

These results provide a starting point for the development of more rigorous assessment of watersheds for $^{87}\text{Sr}/^{86}\text{Sr}$ studies. Humston (2006) provides a preliminary *a priori* framework for assessing candidate watersheds for the feasibility of microchemical studies, however a tendency to cluster discontinuous stream segments without regard to spatial location limits this approach. We believe that our data provides valuable information which can be used to create more general, easily applied and accurate methods for developing $^{87}\text{Sr}/^{86}\text{Sr}$ isotopic tracer studies in fish or other lotic organisms.

Tables

Table 2.1

Elemental and isotopic variation across major watersheds of the Snake River basin from Hegg et al. (in review) show elemental variation throughout the basin which roughly corresponds to geologic differences, including a strong correlation between Rubidium (Rb) and Potassium (K). Internal precision was measured with repeated measurement of a standard over the course of three sampling days. Coefficient of variation expressed as a percentage (%CV) for each element is listed. Limits of Detection (LOD) were calculated as three times the standard deviation of a blank. External Precision was measured throughout the study through comparison to a known standard, NIST 1640. The percent deviation from the expected value is listed for each element (%Dev NIST 1640).

Sample Name	n	Sr		Ca		Mg		K		Rb	
		(ppm)	%SE	(ppt)	%SE	(ppt)	%SE	(ppm)	%SE	(ppm)	%SE
Clearwater											
(Below Dworshak)	2	0.0264	9%	0.0035	7%	0.6496	6%	0.5336	1%	0.7314	14%
Clearwater											
(Lewiston)	4	0.0259	6%	0.0034	7%	0.7021	9%	0.5101	5%	0.6065	6%
Clearwater											
(Orofino)	3	0.0376	6%	0.0042	8%	0.8134	10%	0.6096	4%	0.6292	2%
Grande Ronde	3	0.0856	8%	0.0157	7%	2.9106	7%	2.0245	4%	2.1896	2%
Imnaha (Cow											
Creek)	1	0.2767	*	0.0236	*	3.4508	*	1.7045	*	1.5970	*
Imnaha (Imnaha,											
OR)	1	0.4917	*	0.0345	*	3.5408	*	0.9733	*	0.9859	*
Palouse River	4	0.1412	5%	0.0245	3%	8.0778	4%	2.9241	2%	2.3859	8%
Salmon River	4	0.1054	2%	0.0148	1%	2.9237	16%	1.0315	7%	0.9367	11%
Snake											
(Below Lewiston)	4	0.1305	8%	0.0212	8%	6.3873	10%	2.2774	8%	2.4888	7%
Hells Canyon											
(Pittsburg											
Landing)	4	0.2037	4%	0.0349	4%	12.0129	6%	3.9215	6%	4.2576	4%
Snake (Lyons											
Ferry)	2	0.1695	4%	0.0268	6%	8.9764	7%	3.0806	4%	3.0470	8%
Snake											
(Above Lewiston)	2	0.1892	6%	0.0317	5%	10.6649	3%	3.2975	2%	3.5067	2%

Tucannon	4	0.0439	5%	0.0116	6%	4.2051	6%	2.5988	4%	3.2492	5%
LOD		0.0010		0.0002		0.0410		0.0206		0.0787	
%CV (internal)		2.35%		1.87%		3.27%		4.59%		2.95%	
%Dev NIST 1640		2.7%		2.3%		7.9%		7.2%		4.4%	

Table 2.2

Details of the makeup of water sampling points within the basin. The percent of each rock type upstream of the sample point was calculated using arcGIS. Predicted $^{87}\text{Sr}/^{86}\text{Sr}$ is the output of a multiple regression model using percent rock type as the independent variable. Shannon Diversity of watershed geology as well as total area (km^2) is listed for each sampled watershed. Numbers on Snake River Basin samples correspond to numbers in Figure 2.1. Observed $^{87}\text{Sr}/^{86}\text{Sr}$ values of the Snake River Basin are from Hegg et al. (in review). Big Creek watershed $^{87}\text{Sr}/^{86}\text{Sr}$ values are from Hamann (2010). Bear Valley Creek data are from Kennedy (personal communication).

Sample Site	Rock Type						Observed $^{87}\text{Sr}/^{86}\text{Sr}$	Predicted $^{87}\text{Sr}/^{86}\text{Sr}$	Shannon Diversity Index	Total Area (km^2)
	Carbonates	Felsic	Mafic	Meta- morphic	Sedimentary / Other	Water				
Snake River Basin	3.6%	25.7%	30.2%	5.9%	34.0%	0.7%	-	-	1.37	279062.04
1. U. Snake (Pittsburg Landing)	4.5%	22.0%	32.5%	0.9%	39.3%	0.7%	0.708685	0.708401	1.25	187960.15
2. Salmon River	3.9%	52.3%	3.6%	19.2%	20.9%	0.1%	0.713048	0.713529	1.23	34692.91
3. L. Clearwater	0.0%	51.4%	10.1%	33.5%	4.5%	0.5%	0.714254	0.714245	1.08	20541.79
4. L. Clearwater	0.1%	45.5%	15.2%	30.3%	8.6%	0.4%	0.713586	0.713318	1.23	24074.30
5. U. Clearwater	0.0%	59.5%	13.1%	24.3%	3.1%	0.0%	0.712292	0.712677	1.03	13733.19
6. L. Snake (Lewiston)	4.2%	25.2%	31.5%	3.6%	35.0%	0.6%	0.709677	0.708797	1.33	238334.22
7. L. Snake (Chief Timothy)	3.8%	26.9%	30.1%	6.0%	32.7%	0.6%	0.709781	0.709182	1.37	263583.01
9. L. Snake (Lyons Ferry)	3.6%	25.9%	30.3%	5.9%	33.7%	0.6%	0.709576	0.709162	1.37	275645.71
10. Palouse	0.0%	4.1%	32.7%	5.9%	56.9%	0.4%	0.709225	0.709078	0.99	8434.43
11. Grand Ronde	0.0%	6.5%	74.2%	0.1%	19.1%	0.2%	0.706488	0.707304	0.72	8901.76

12. Imnaha (Cow Creek)	0.0%	0.5%	72.8%	0.1%	26.5%	0.1%	0.707340	0.707323	0.62	717.96
13. Imnaha (Imnaha, OR)	0.0%	0.7%	88.3%	0.3%	10.7%	0.0%	0.707136	0.707117	0.40	2092.01
14. Tucannon	0.0%	0.1%	52.0%	0.0%	47.9%	0.0%	0.706756	0.707711	0.70	1294.78
Big Creek Watershed	0.0%	73.3%	0.0%	26.3%	0.4%	0.0%	-	-	0.60	1545.06
Beaver Creek	0.0%	62.3%	0.0%	37.7%	0.0%	0.0%	0.713606	0.712082	0.66	113.68
Big (downstream of Beaver)	0.0%	58.8%	0.0%	39.4%	1.8%	0.0%	0.713726	0.712310	0.75	363.41
Big (downstream of Cabin)	0.0%	72.3%	0.0%	27.2%	0.6%	0.0%	0.714152	0.710641	0.62	1153.80
Big (downstream of Crooked)	0.0%	65.0%	0.0%	33.9%	1.1%	0.0%	0.713875	0.711566	0.70	595.63
Big (downstream of Logan)	0.0%	85.3%	0.0%	11.4%	3.4%	0.0%	0.710600	0.708482	0.50	131.26
Big (downstream of Monumental)	0.0%	69.1%	0.0%	30.2%	0.7%	0.0%	0.713574	0.711054	0.65	920.67
Big Ramey Creek	0.0%	76.0%	0.0%	24.0%	0.0%	0.0%	0.708361	0.710208	0.55	87.24
Big (upstream of Beaver)	0.0%	57.4%	0.0%	39.9%	2.7%	0.0%	0.714780	0.712388	0.78	248.92
Big(upstream of Cabin)	0.0%	71.7%	0.0%	27.7%	0.6%	0.0%	0.714791	0.710716	0.63	1089.48
Big (upstream of Crooked)	0.0%	59.1%	0.0%	39.6%	1.4%	0.0%	0.714331	0.712341	0.74	493.41
Big (upstream Rush Cabin Creek)	0.0%	72.2%	0.0%	27.3%	0.6%	0.0%	0.714375	0.710659	0.62	1186.56
Crooked Creek	0.0%	82.7%	0.0%	17.4%	0.0%	0.0%	0.708462	0.709301	0.46	63.97
Crooked Creek	0.0%	93.4%	0.0%	6.6%	0.0%	0.0%	0.706769	0.707829	0.24	101.99
Lower Big Creek	0.0%	75.1%	0.0%	24.4%	0.5%	0.0%	0.713762	0.710264	0.58	1432.06

Logan Creek	0.0%	83.9%	0.0%	15.7%	0.4%	0.0%	0.711463	0.709078	0.46	56.29
Monumental Creek	0.0%	76.7%	0.0%	23.3%	0.0%	0.0%	0.720223	0.710115	0.54	324.92
Rush Creek	0.0%	89.8%	0.0%	10.2%	0.0%	0.0%	0.710239	0.708329	0.33	244.92
Smith Creek	0.0%	37.0%	0.0%	63.0%	0.0%	0.0%	0.717113	0.715540	0.66	52.10
Upper Big Creek	0.0%	98.4%	0.0%	0.0%	1.6%	0.0%	0.709448	0.706930	0.08	55.74
Bear Valley Creek										
Watershed	0.0%	67.5%	0.0%	3.9%	28.6%	0.0%	-	-	0.75	496.16
Bear Valley Creek #4	0.0%	66.3%	0.0%	4.9%	28.9%	0.0%	0.708239	0.707596	0.78	385.03
Bear Valley Creek #5	0.0%	67.7%	0.0%	5.0%	27.3%	0.0%	0.708230	0.707612	0.77	376.02
Bear Valley Creek #6	0.0%	68.2%	0.0%	1.6%	30.2%	0.0%	0.708195	0.707142	0.69	170.71
Bear Valley Creek #7	0.0%	69.5%	0.0%	0.0%	30.5%	0.0%	0.708204	0.706930	0.61	153.76
Bearskin Creek	0.0%	70.9%	0.0%	0.0%	29.1%	0.0%	0.708260	0.706930	0.60	45.06
Cook Creek	0.0%	84.3%	0.0%	8.7%	7.0%	0.0%	0.708015	0.708123	0.54	16.43
East Fork Elk Creek	0.0%	98.0%	0.0%	0.0%	2.0%	0.0%	0.708349	0.706930	0.10	16.86
Elk Creek #11	0.0%	66.7%	0.0%	7.5%	25.8%	0.0%	0.708289	0.707955	0.81	186.02
Elk Creek #13	0.0%	65.9%	0.0%	12.3%	21.7%	0.0%	0.708294	0.708616	0.86	105.03
Elk Creek #15	0.0%	69.7%	0.0%	0.0%	30.4%	0.0%	0.708263	0.706930	0.61	57.23
Elk Creek #16	0.0%	76.5%	0.0%	0.0%	23.5%	0.0%	0.708245	0.706930	0.55	75.52
Porter Creek	0.0%	27.2%	0.0%	55.1%	17.7%	0.0%	0.708669	0.714454	0.99	19.03
Lapwai Creek										
Watershed	4.1%	2.7%	64.1%	0.0%	28.9%	0.2%	-	-	0.87	722.36
Mission Creek	9.9%	5.7%	84.4%	0.0%	0.0%	0.0%	0.706233	0.707132	0.53	91.15
Sweetwater Creek	7.8%	0.0%	63.6%	0.0%	28.2%	0.4%	0.706387	0.707472	0.84	214.65
Tom Beall Creek	0.0%	0.0%	21.9%	0.0%	78.1%	0.0%	0.706657	0.708747	0.53	45.13
Upper Lapwai Creek	0.0%	16.4%	83.0%	0.0%	0.0%	0.6%	0.706758	0.707152	0.45	73.97
Upper Sweetwater Creek	7.4%	0.0%	56.9%	0.0%	35.5%	0.2%	0.706398	0.707604	0.88	119.03
Webb Creek	10.4%	0.0%	78.5%	0.0%	10.3%	0.9%	0.706368	0.707220	0.66	77.05

Table 2.3

Reclassification of rock types from the LithClass 6.1 standard. Reclassified rock types were used to create predictive multiple regression models of $^{87}\text{Sr}/^{86}\text{Sr}$ within watersheds of the Snake River. Rocks were reclassified primarily by protolith mafic or felsic composition. When protolith could not be determined from the listed rock type they were classified into the remaining categories. Metamorphic rocks with unknown protolith were classified separately due to the presence of very old, high $^{87}\text{Sr}/^{86}\text{Sr}$ metasedimentary rocks in the basin and their potential to influence $^{87}\text{Sr}/^{86}\text{Sr}$. Carbonate rocks were also separately classified due to their potential to influence $^{87}\text{Sr}/^{86}\text{Sr}$ signatures. Sedimentary/Other was a bucket category for rocks of unknown composition.

Carbonates	Felsic	Mafic	Metamorphic	Sedimentary/Other
carbonate	alkali rhyolite	alkalic volcanic rock	augen gneiss	chemical
dolostone (dolomite)	alkali syenite	alkaline basalt	biotite gneiss	coal
limestone	alkali trachyte	amphibole schist	blueschist	evaporite
marble	alkalic intrusive rock	amphibolite	calc-silicate rock	exhalite
mixed clastic/carbonate	anorthosite	basalt	calc-silicate schist	iron formation
	aplite	diabase	cataclasite	mixed clastic/coal
	ash-flow tuff	dunite	eclogite	phosphorite
	dacite	gabbro	flaser gneiss	alluvial fan
	diorite	gabbroid	gneiss	alluvial terrace
	felsic gneiss	greenschist	granofels	alluvium
	felsic			
	metavolcanic rock	greenstone	granulite	andesite
	felsic volcanic rock	hawaiite	greisen	arenite
	granite	hornblendite	hornfels	argillite
	granitic gneiss	keratophyre	intermediate metavolcanic rock	arkose
	granitoid	kimberlite	meta-argillite	beach sand
	granodiorite	mafic gneiss	meta-conglomerate	bentonite
		mafic		
	ignimbrite	metavolcanic rock	metamorphic rock	bimodal suite

lamprophyre	mafic volcanic rock	metasedimentary rock	biogenic sediment
meta-rhyolite	meta-basalt	metavolcanic rock	black shale
metaluminous granite	monzogabbro	mica schist	calcarenite
monzodiorite	norite	migmatite	chert
monzonite	peridotite	mylonite	clastic
obsidian	phonolite	paragneiss	clay or mud
orthogneiss	pyroxenite	pelitic schist	claystone
pegmatite	quartz gabbro	phyllite	coarse-grained mixed clastic
peralkaline granite	quartz monzogabbro	phyllonite	colluvium
peraluminous granite	spilite	quartz-feldspar schist	conglomerate
plutonic rock (phaneritic)	tephrite (basinite)	quartzite	coral
porphyry	tholeite	schist	debris flow
pumice	trachybasalt	serpentinite	delta
quartz diorite	troctolite	skarn (tactite)	dune sand
quartz latite	ultramafic intrusive rock	slate	eolian
quartz monzodiorite	ultramafite (komatiite)	tectonic breccia	fine-grained mixed clastic
quartz monzonite		tectonic melange	flood plain
quartz syenite		tectonic rock	glacial drift
rhyodacite		tectonite	glacial-marine
rhyolite			glaciolacustrine
subaluminous granite			glassy volcanic rock
syenite			gravel
tonalite			graywacke
trachyte			intermediate volcanic rock
trondhjemite			intrusive carbonatite
alkali granite (alaskite)			lahar
			lake or marine deposit
			landslide
			latite

lava flow
levee
loess
mass wasting
medium-grained mixed
clastic
melange
mixed clastic/volcanic
moraine
mud flat
mudflow
mudstone
nepheline syenite
novaculite
oil shale
olistostrome
orthoquartzite
outwash
peat
playa
pyroclastic
residuum
sand
sand sheet
sandstone
sedimentary breccia
sedimentary rock
shale
silt
siltstone
stratified glacial sediment
sub- and supra-glacial
sediment
talus
terrace
till
trachyandesite
tuff
unconsolidated

				vitrophyre
				volcanic ash
				volcanic breccia (agglomerate)
				volcanic carbonatite
				volcanic rock (aphanitic)
				wacke
				welded tuff

Table 2.4

Candidate models used for AIC model selection. The independent variables included in each model and whether variables were calculated using three-dimensional surface area or conventional map area is shown. Models with higher AICc weights are favored. A difference in AICc of >2 indicates a significant difference between models.

Independent Variables			Calculation Method		AICc	Δ AICc	AICc Weight
ln(Mafic)	Felsic	Metamorphic	3D Surface Area	Map Area			
●	○	●	●	○	-147.99	0	0.52
●	○	●	○	●	-147.01	0.98	0.32
●	●	●	●	○	-143.41	4.58	0.05
○	●	●	●	○	-142.81	5.18	0.04
●	●	●	○	●	-142.64	5.35	0.04
○	●	●	○	●	-142.37	5.62	0.03
○	●	○	○	●	-135.23	12.76	0
○	●	○	●	○	-135	12.99	0
●	●	○	●	○	-133.87	14.11	0
●	●	○	○	●	-133.77	14.22	0
●	○	○	●	○	-132.17	15.82	0
●	○	○	○	●	-131.31	16.67	0

Table 2.5

Comparison of classification accuracy using two methods of predicting $^{87}\text{Sr}/^{86}\text{Sr}$, 5-rkm and 10-rkm, to classifications using water samples from Hegg et al (in review). Classifications were completed using discriminate functions with predicted values or water sample values as the training set. Proportions of fish classified to each source group are not significantly different between methods (Monte Carlo Chi-Square, $\alpha=0.05$) indicating that predictions of $^{87}\text{Sr}/^{86}\text{Sr}$ are capable of predicting fall Chinook Natal origins.

Natal Source Group	Classification Method		
	10-rkm	5-rkm	Water Samples
Tucannon, Grande Ronde,			
Imnaha	2 (1%)	2 (1%)	2 (1%)
Clearwater/Salmon	53 (40%)	49 (37%)	45 (34%)
Lower Snake	53 (40%)	60 (45%)	68 (51%)
Upper Snake	26 (19%)	23 (17%)	19 (14%)
Total	134	134	134
Classification Accuracy			
Compared to Water Sample Method	89%	94%	

Table 2.6

List of candidate models generated using combined water sampling data from large and small scale watersheds in the Snake River basin. While the global model was the most parsimonious, the addition of small scale watersheds decreased the overall prediction accuracy of $^{87}\text{Sr}/^{86}\text{Sr}$.

Independent Variables

			AICc	ΔAICc	AICc Weight
ln(Mafic)	Felsic	Metamorphic	AICc	ΔAICc	Weight
●	●	●	-474.03	0	0.52
○	●	●	-472.08	1.96	0.27
●	○	●	-467.69	6.34	0.03
●	●	○	-431.63	42.40	0
●	○	○	-431.16	42.87	0
●	○	○	-423.75	50.28	0

Figures

Figure 2.1

Lithology of the Snake River watershed showing rock type categories with strong impacts on $^{87}\text{Sr}/^{86}\text{Sr}$ based primarily on protolith composition (Table 2.3). Rock types of unknown protolith were categorized into Carbonate, Metamorphic or Sedimentary/Other based on their original classification. The Snake River basin shows large variation in the geology between river basins with rivers being influenced by both felsic and mafic geologies.

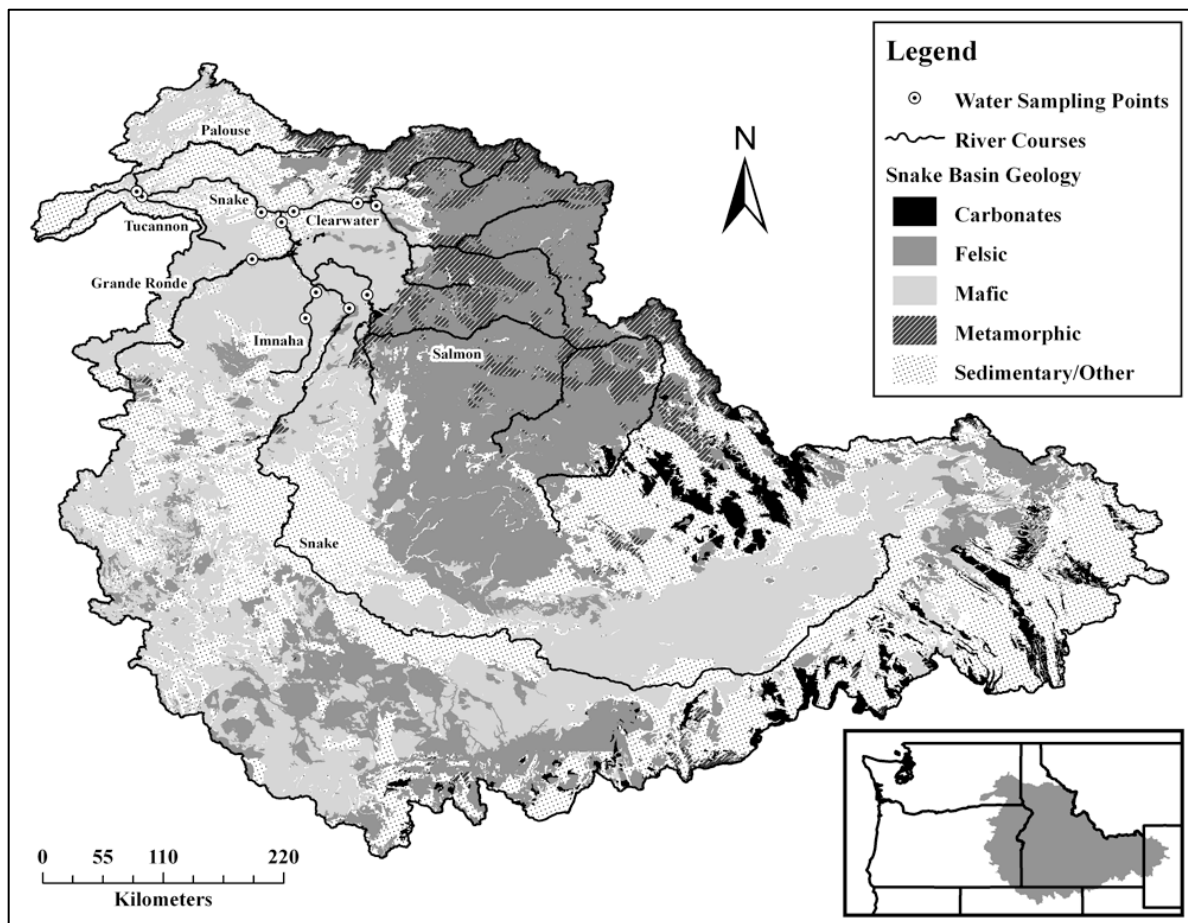


Figure 2.2

Map showing the location of measured and predicted $^{87}\text{Sr}/^{86}\text{Sr}$ within the Snake River basin. Each point represents the outlet of a watershed. The geologic makeup of the watershed upriver of each point was used to predict $^{87}\text{Sr}/^{86}\text{Sr}$ for that point. Numbered points represent water sampling points within the basin. Filled circles (●) represent points predicted at 5-rkm intervals upstream and downstream of water sampling locations. Open circles (○) represent points predicted ever 10-rkm throughout the basin. Split circles represent points included in both groups.

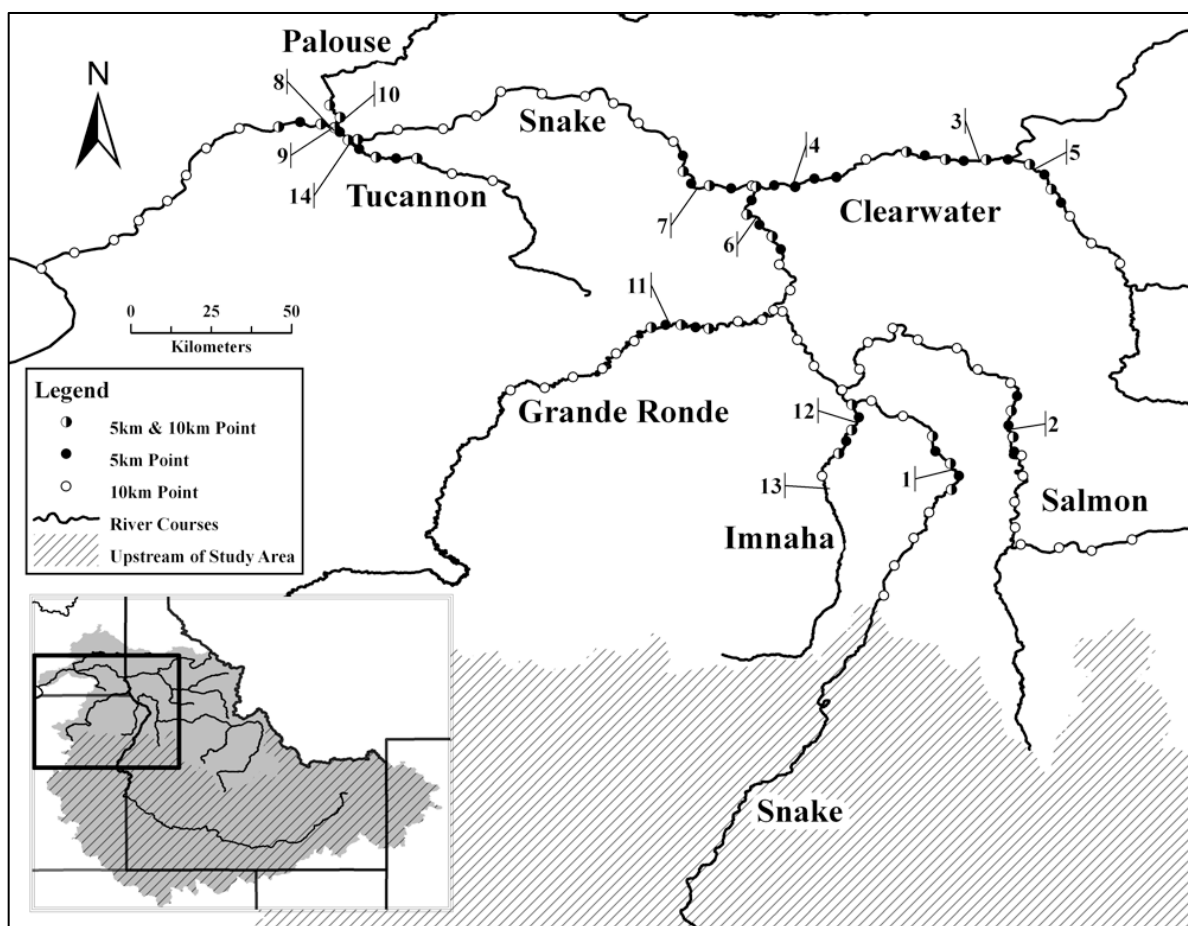


Figure 2.3

Map showing basic lithology of Big Creek, a tributary of the Middle Fork Salmon River. Rock types based on reclassified geology (Table 2.3). Big Creek is dominated by Felsic and Metamorphic rocks.

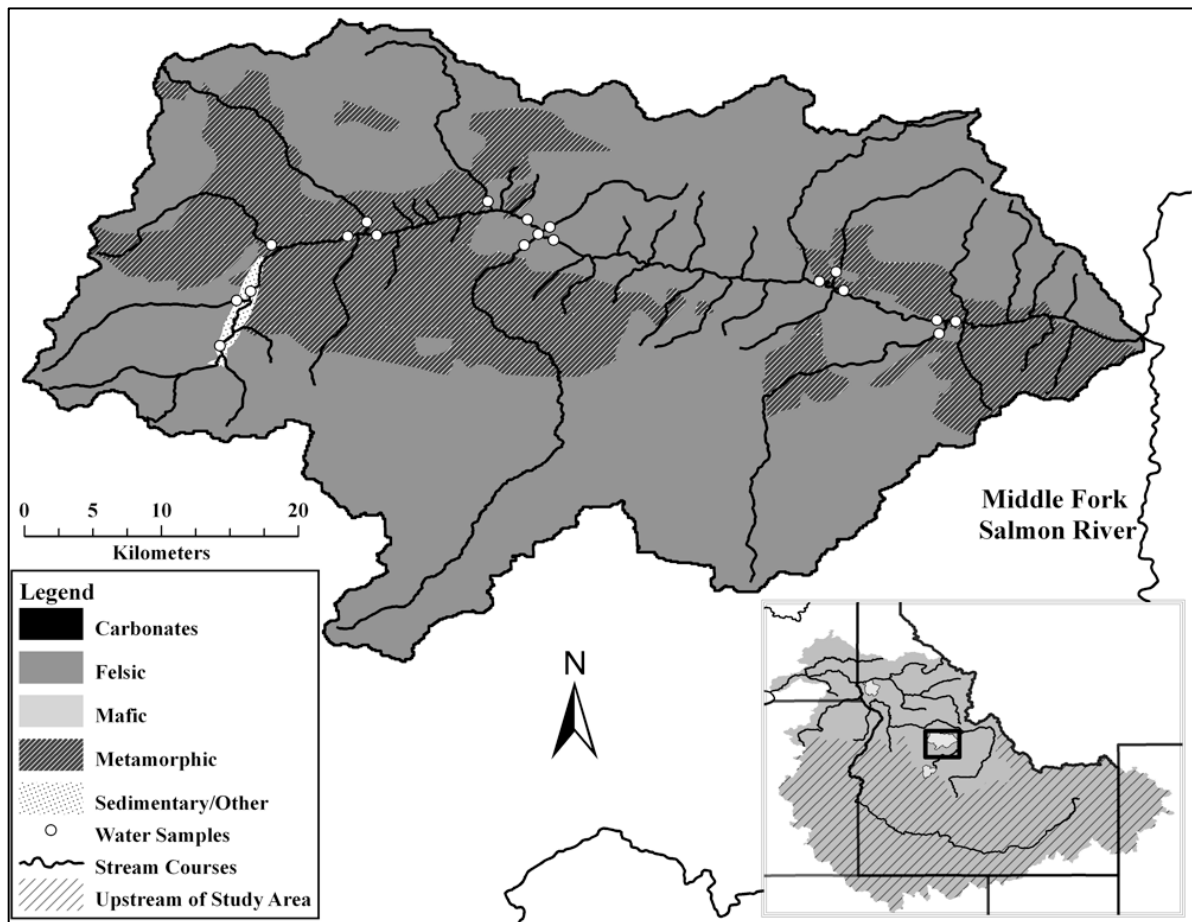


Figure 2.4

Map showing basic lithology of Bear Valley Creek, a tributary of the Middle Fork Salmon River. Rock types based on reclassified geology (Table 2.3). Bear Valley Creek is dominated by Felsic and Sedimentary rocks.

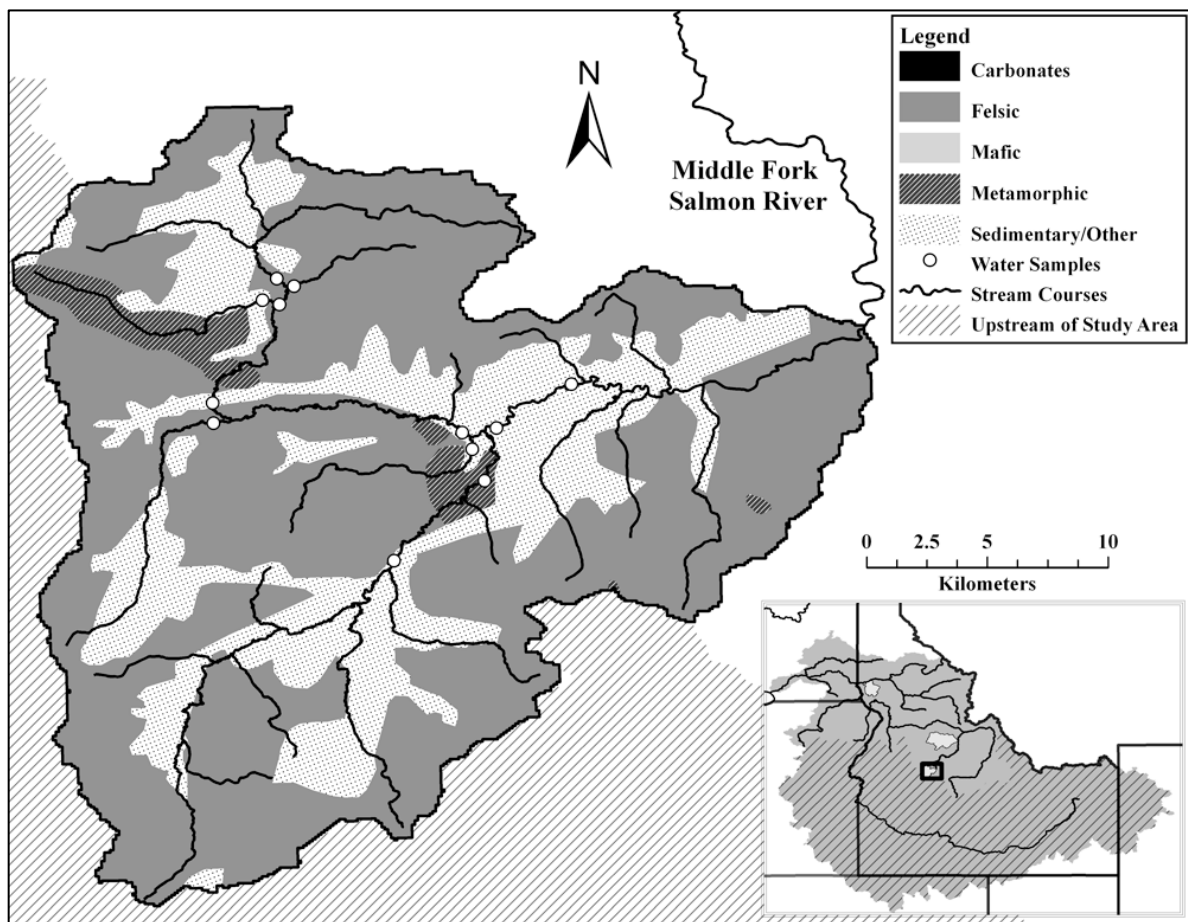


Figure 2.5

Map showing basic lithology of Lapwai Creek, a tributary of the Middle Fork Salmon River. Rock types based on reclassified geology (Table 2.3). Bear Valley Creek is dominated by Mafic and Sedimentary rocks.

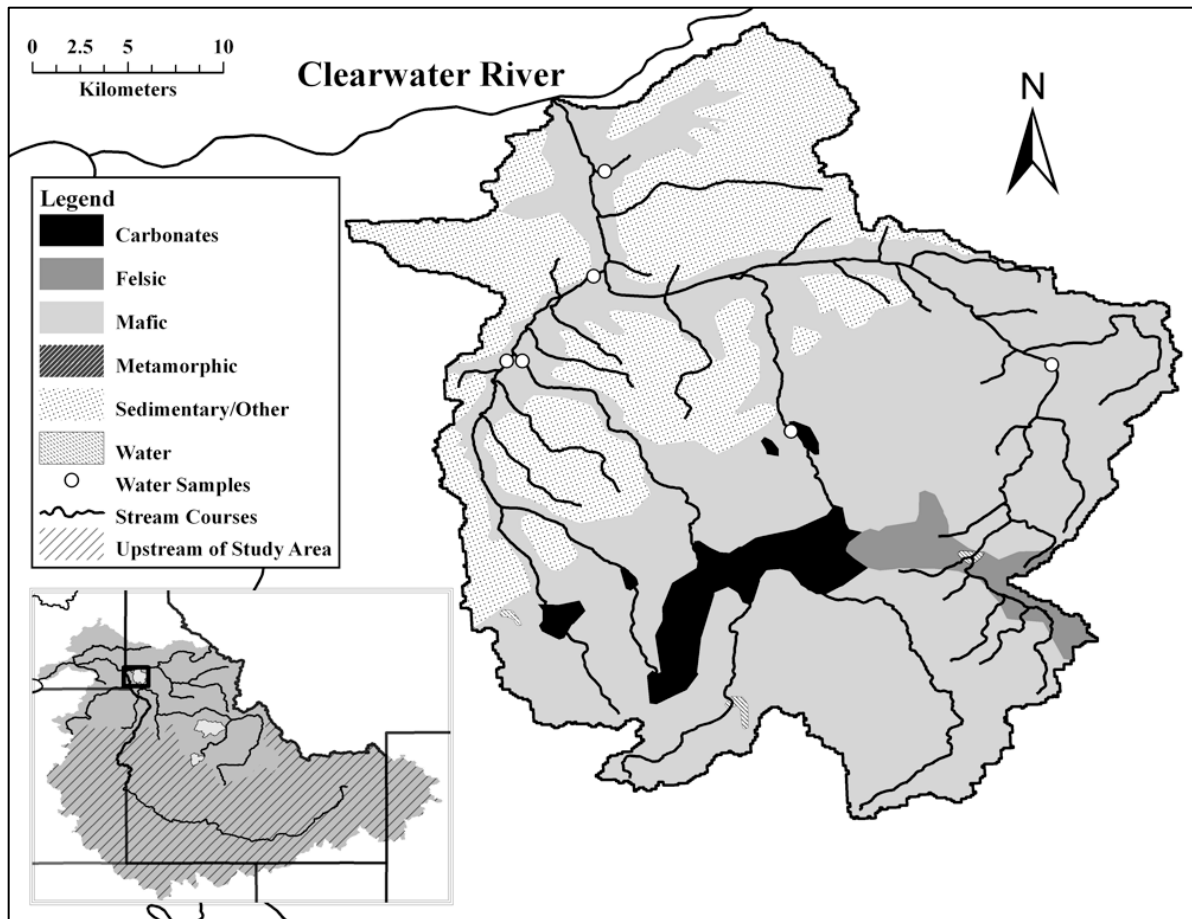


Figure 2.6

Classification to natal source location of 134 fall Chinook salmon using a discriminate function constructed using $^{87}\text{Sr}/^{86}\text{Sr}$ values predicted from geology at 5-rkm intervals. Shape indicates classification from Hegg et al. (in review) while plot location indicates where a fish was classified using the 5-rkm prediction method. Fish misclassified using the 5-rkm prediction method do not match the shape of the group in which they are located. Open shapes indicate fish of known origin.

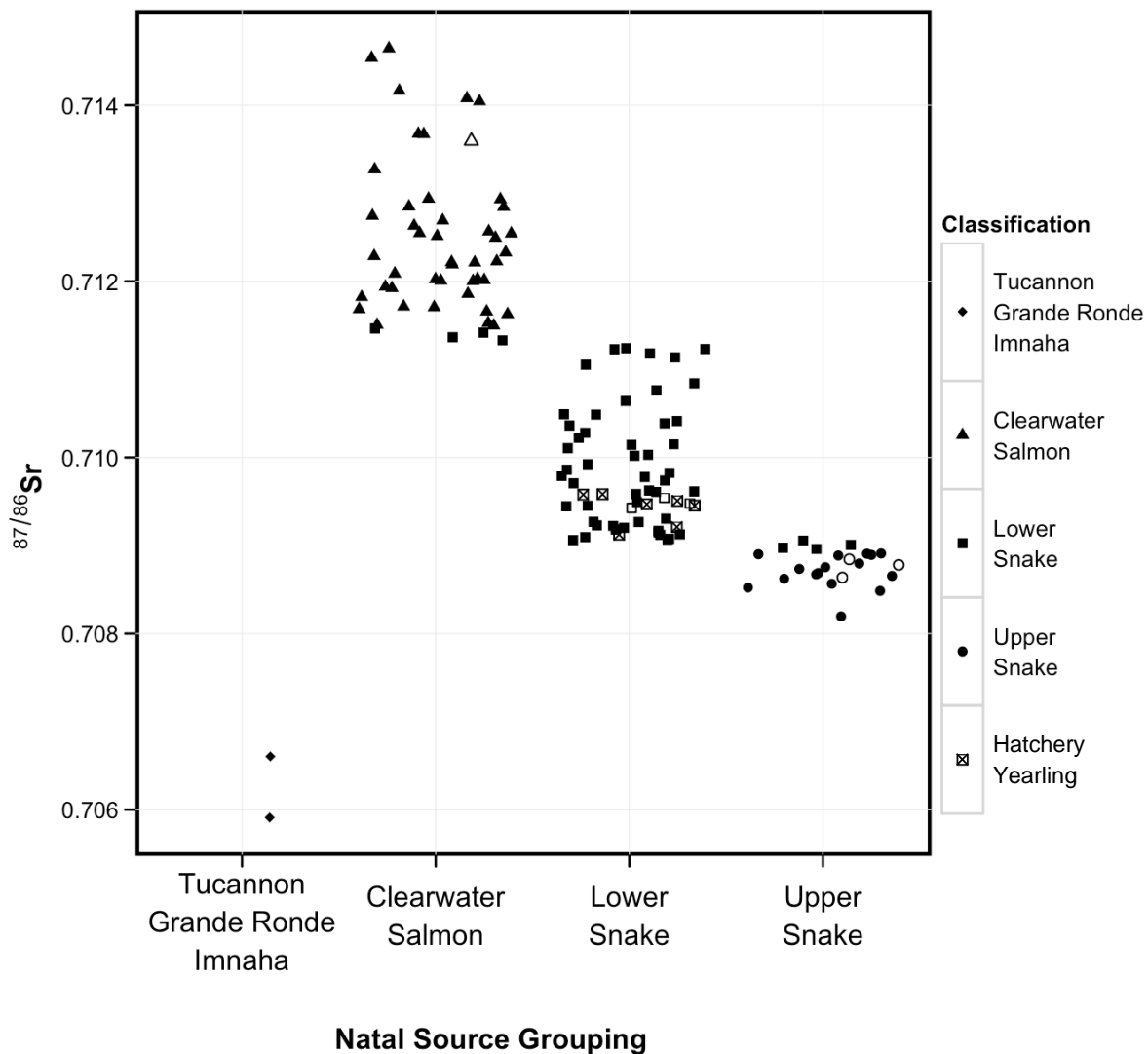


Figure 2.7

Classification to natal source location of 134 fall Chinook salmon using a discriminate function constructed using $^{87}\text{Sr}/^{86}\text{Sr}$ values predicted from geology at 10-rkm intervals. Shape indicates classification using traditional method while plot location indicates where a fish was classified using the 10-rkm method. Fish misclassified using the 10-rkm prediction method do not match the shape of the group in which they are located. Open shapes indicate fish of known origin.

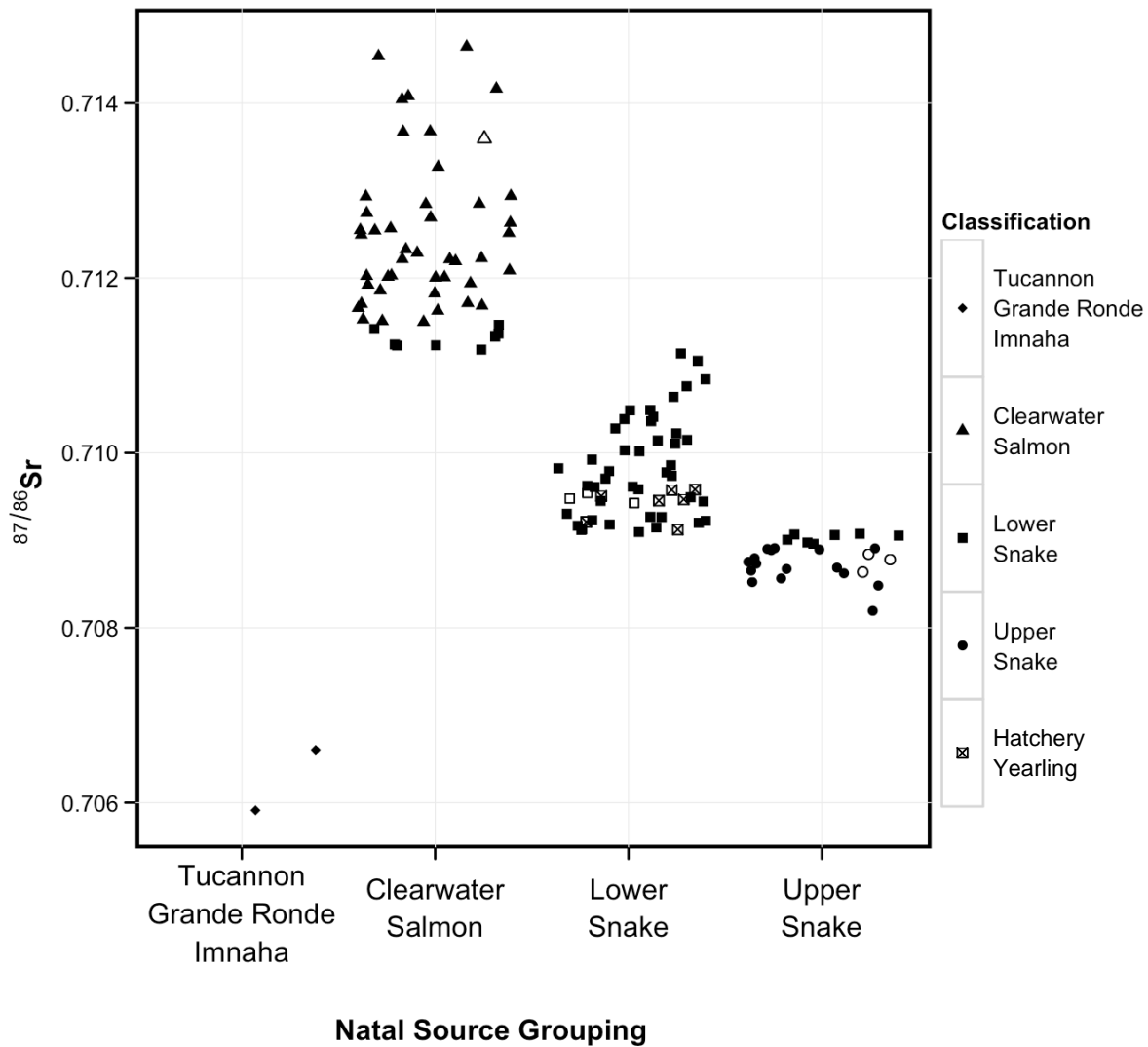


Figure 2.9

Accuracy of $^{87}\text{Sr}/^{86}\text{Sr}$ predictions using watershed geologic makeup increases with increasing diversity of watershed geology. The Shannon index of diversity takes into account both the richness of rock types within a basin (# of unique rock types) and the relative representation (% watershed area) of rock types in calculating the diversity index. Our results indicate that watersheds in the Snake River basin with rock type diversity below ~ 1.0 may have higher prediction error.

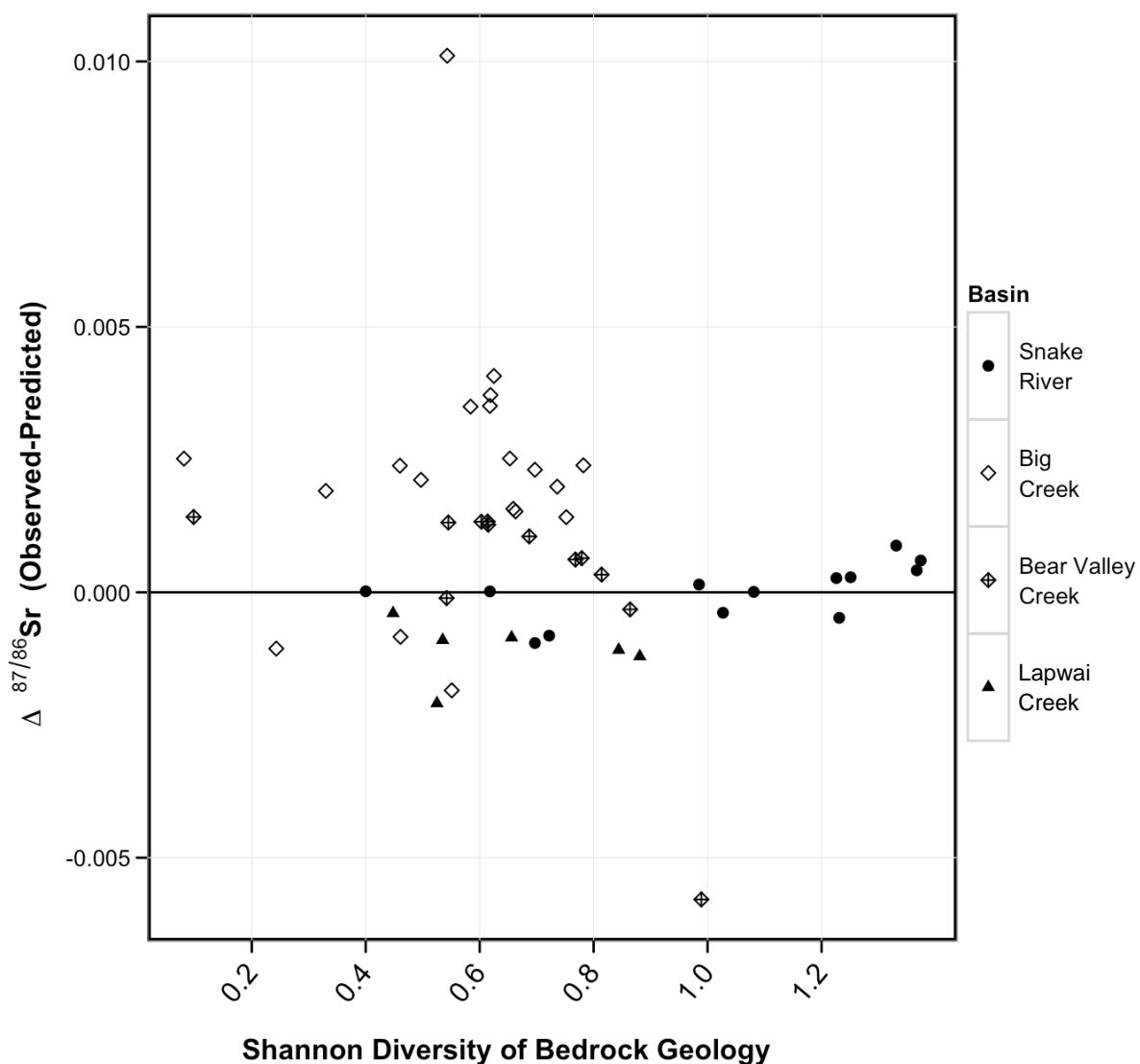
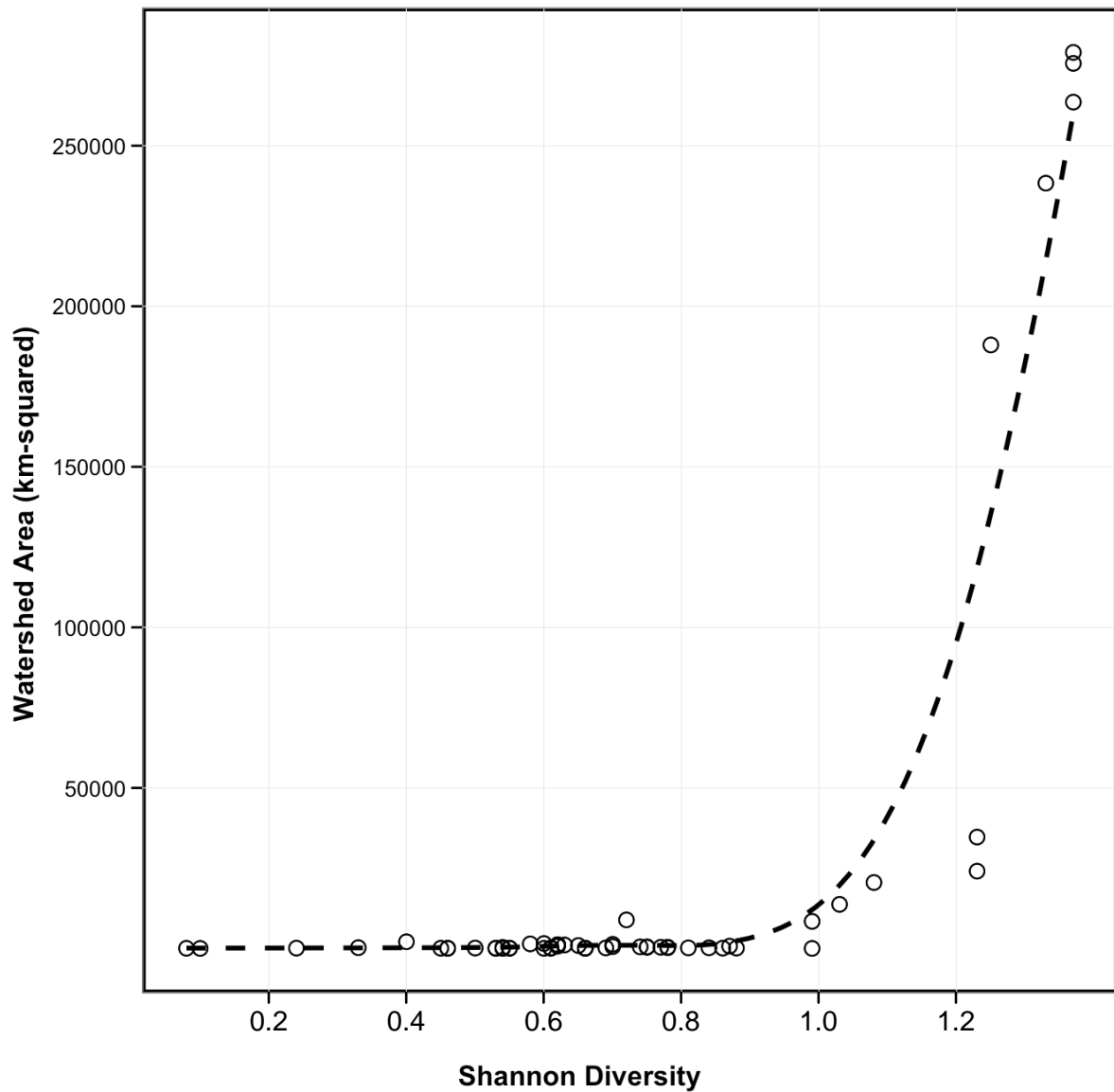


Figure 2.10

Watershed geologic diversity increases exponentially with increases in watershed area within the Snake River basin. The interaction of watershed area and geologic diversity indicates a lower spatial limit on prediction accuracy within the Snake River Basin. Watersheds below 8400km² or Shannon diversity index scores of <1 show lower ⁸⁷Sr/⁸⁶Sr prediction accuracy.



References Cited (Chapter 2)

- Alerstam T, Hedenström A, Åkesson S (2003) Long distance migration: evolution and determinants. *Oikos* 103:247-260
- Bacon C, Weber P, Larsen K, Reisenbichler R, Fitzpatrick J, Wooden J (2004) Migration and rearing histories of chinook salmon (*Oncorhynchus tshawytscha*) determined by ion microprobe Sr isotope and Sr/Ca transects of otoliths. *Canadian Journal of Fisheries and Aquatic Sciences* 61:2425-2439
- Bain D, Bacon J (1994) Strontium isotopes as indicators of mineral weathering in catchments. *Catena* 22:201-214
- Baker RR (1978) The evolutionary ecology of animal migration
- Barnett-Johnson R, Pearson T, Ramos F, Grimes C, MacFarlane R (2008) Tracking natal origins of salmon using isotopes, otoliths, and landscape geology. *Limnology and Oceanography* 53:1633-1642
- Barnett-Johnson R, Ramos F, Grimes C, MacFarlane R (2005) Validation of Sr isotopes in otoliths by laser ablation multicollector inductively coupled plasma mass spectrometry (LA-MC-ICPMS): opening avenues in fisheries science applications. *Canadian Journal of Fisheries and Aquatic Sciences* 62:2425-2430
- Burnham K, Anderson D (2002) Model selection and multimodel inference: a practical information-theoretic approach. Springer Verlag
- Campana S, Thorrold S (2001) Otoliths, increments, and elements: keys to a comprehensive understanding of fish populations? *Canadian Journal of Fisheries and Aquatic Sciences* 58:30-38
- Connor W, Sneva J, Tiffan K, Steinhorst R, Ross D (2005) Two alternative juvenile life history types for fall Chinook salmon in the Snake River basin. *Transactions of the American Fisheries Society* 134:291-304
- Faure G (1977) Principles of isotope geology
- Faure G, Mensing T (2004) Isotopes: principles and applications. John Wiley & Sons Inc

- Foster D, Fanning M (1997) Geochronology of the northern Idaho batholith and the Bitterroot metamorphic core complex: Magmatism preceding and contemporaneous with extension. *Geological Society of America Bulletin* 109:379
- Garcia A et al. (2007) Fall Chinook Salmon Spawning Ground Surveys in the Snake River Basin Upriver of Lower Granite Dam, 2007.
- Garcia A, Bradbury S, Arnsberg B, Rocklage S, Groves P (2005) Fall Chinook salmon spawning ground surveys in the Snake River basin upriver of Lower Granite Dam, 2004. 2004 Annual Report to Bonneville Power Administration. Project:03
- Gibbons JW, Andrews KM (2004) PIT tagging: simple technology at its best. *BioScience* 54:447-454
- Hales TC, Abt D, Humphreys E, Roering JJ (2005) A lithospheric instability origin for Columbia River flood basalts and Wallowa Mountains uplift in northeast Oregon. *Nature* 438:842-845
- Hamann E (2010) Assessing spawning habitat selection and quantifying straying rates of wild Chinook salmon (*Oncorhynchus tshawytscha*) in a wilderness basin.82
- Hebblewhite M, Haydon DT Distinguishing technology from biology: a critical review of the use of GPS telemetry data in ecology. *Philosophical Transactions of the Royal Society B: Biological Sciences* 365:2303
- Hobson K (1999) Tracing origins and migration of wildlife using stable isotopes: a review. *Oecologia* 120:314-326
- Hobson K, Barnett-Johnson R, Cerling T (2009) Isoscapes
- Hogan Z, Baird IG, Radtke R, Vander Zanden MJ (2007) Long distance migration and marine habitation in the tropical Asian catfish, *Pangasius krempfi*. *Journal of Fish Biology* 71:818-832
- Hooper PR, Camp VE, Reidel SP, Ross ME (2007) The origin of the Columbia River flood basalt province: Plume versus nonplume models. *Geological Society of America Special Papers* 430:635

- Humston R, Harbor D, Eversole A, Wong K, Miller D, Galvez J (2006) Geologic Analyses for Evaluating Watershed Heterogeneity: Implications for Otolith Chemistry Studies. In. Southeastern Association of Fish and Wildlife Agencies, 7221 Covey Trace Tallahassee FL 32308 USA
- Kennedy B, Blum J, Folt C, Nislow K (2000) Using natural strontium isotopic signatures as fish markers: methodology and application. *Canadian Journal of Fisheries and Aquatic Sciences* 57:2280-2292
- Kennedy B, Folt C, Blum J, Chamberlain C (1997) Natural isotope markers in salmon. *Nature* 387:766-767
- Kennedy B, Klaue A, Blum J, Folt C, Nislow K (2002) Reconstructing the lives of fish using Sr isotopes in otoliths. *Canadian Journal of Fisheries and Aquatic Sciences* 59:925-929
- Kenward R (2001) A manual for wildlife radio tagging. Academic Pr
- Leeman W (1982) Development of the Snake River Plain-Yellowstone Plateau province, Idaho and Wyoming: an overview and petrologic model. *Cenozoic Geology of Idaho* 26:155-177
- Love JD, Leopold EB, Love D (1978) Eocene rocks, fossils, and geologic history, Teton Range, northwestern Wyoming. US Govt. Print. Off.
- Ludington S et al. (2006) Open-File Report (2005-1305) Preliminary integrated geologic map databases for the United States. USGS
- Marra P, Hobson K, Holmes R (1998) Linking winter and summer events in a migratory bird by using stable-carbon isotopes. *Science* 282:1884
- Moore FR, Gauthreaux Jr SA, Kerlinger P, Simons TR (1995) Habitat requirements during migration: important link in conservation. *B* 144:121
- Newton I (2006) Can conditions experienced during migration limit the population levels of birds? *Journal of Ornithology* 147:146-166
- Salewski V, Thoma M, Schaub M (2007) Stopover of migrating birds: simultaneous analysis of different marking methods enhances the power of capture-recapture analyses. *Journal of Ornithology* 148:29-37

- Shannon CE, Weaver W (1949) The mathematical theory of communication. University of Illinois Press, Urbana
- Skalski JR, Buchanan RA, Griswold J (2009) Review of Marking Methods and Release-Recapture Designs for Estimating the Survival of Very Small Fish: Examples from the Assessment of Salmonid Fry Survival. *Reviews in Fisheries Science* 17:391-401
- Stewart B, Capo R, Chadwick O (1998) Quantitative strontium isotope models for weathering, pedogenesis and biogeochemical cycling. *Geoderma* 82:173-195
- Thorrold S, Jones C, Campana S, McLaren J, Lam J (1998) Trace element signatures in otoliths record natal river of juvenile American shad (*Alosa sapidissima*). *Limnology and Oceanography*:1826-1835
- Wassenaar LI, Hobson KA (2000) Stable-carbon and hydrogen isotope ratios reveal breeding origins of red-winged blackbirds. *Ecological Applications* 10:911-916